MAPPING A GENE RESPONSIBLE FOR NATURAL RESISTANCE TO RIFT VALLEY FEVER VIRUS IN INBRED RATS

A Dissertation

by

CATHERINE MICHELLE BUSCH

Submitted to the Office of Graduate and Professional Studies of
Texas A&M University
in partial fulfillment of the requirements for the degree of

DOCTOR OF PHILOSOPHY

Chair of Committee,	James E. Womack
Committee Members,	Duane C. Kraemer
	Loren C. Skow
	C. Jane Welsh
Intercollegiate Faculty Chair,	Craig J. Coates

August 2015

Major Subject: Genetics

ABSTRACT

The Rift Valley Fever virus (RVFV) presents an epidemic and epizootic threat in sub-Saharan Africa, Egypt, and the Arabian Peninsula, and has recently gained attention as a potential weapon of bioterrorism due to its ability to infect both livestock and humans. Inbred rat strains show similar characteristic responses to the disease as humans and livestock, making them a suitable model species. Previous studies had shown differences among various inbred rat strains in susceptibility to RVFV hepatic disease, including a higher susceptibility of Wistar-Furth (WF) rats compared to a more resistant Lewis (LEW) strain. Further study revealed that this resistance trait follows the pattern of a dominant gene inherited in Mendelian fashion. A congenic WF.LEW strain resistant to infection with RVFV was derived from the susceptible WF and resistant LEW strains, and a subsequent genome scan revealed two prospective regions for the location of the gene, one on chromosome 3 and the other on chromosome 9. Subsequently, this study employed the methods of backcrossing, genotyping, viral challenges, gene expression studies, and sequencing to define a practicable region of interest and to further identify a viable candidate gene and prospective mechanism by which resistance is conferred.

A program of backcrossing WF.LEW rats to WF rats, genotyping offspring using SNPs and microsatellites, and subsequently challenging N1 litters with RVFV was used to determine that the ~2Mb region on the distal end of chromosome 3 contains the gene conferring resistance. The use of genetic markers to detect recombination in further backcross generations resulted in the identification of two recombinants in this newly

established region of interest. Through RVFV challenges, the recombinants narrowed the prospective region of chromosome 3 to ~500Kb containing 20 genes. Comparative qPCR analysis of all 20 genes combined with comparative sequencing studies of the entire region between susceptible WF/NHsd rats and resistant WF.LEW rats facilitated the identification of candidate gene Rtel1 and a proposed mechanism by which resistance is conferred, which will potentially become the basis for developing new preventive measures against the virus.

ACKNOWLEDGEMENTS

The author would like to thank her committee chair, Dr. James Womack, and her committee members, Dr. Duane Kraemer, Dr. Loren Skow, and Dr. Jane Welsh, for their guidance and support throughout the course of this research.

Thanks also go to Dr. Erin Gillenwaters Flores, Dr. Brittany Jones, Junfeng Chen, Jan Elliott, Elaine Owens, Christie Fickey, Dr. John Morrill, Dr. C.J. Peters, Dr. Ralph Callicott, Dr. Christopher Seabury, Dr. Sarah Black, and Dr. Jessica Nerren for their invaluable assistance, advice, training, and reflection during the course of this study.

Finally, thanks to the author's family and friends for their patience, love, encouragement, and prayers throughout this process.

NOMENCLATURE

CNV	Copy-number variation
DIP	Deletion / insertion polymorphism
IFN	Interferon
LEW	Lewis
N1	First backcross generation
NSs	Non-structural protein of the S segment
qPCR	Quantitative polymerase chain reaction
Q.S.	Quantity sufficient
R1	First recombinant generation
ROI	Region of interest
RNO3	Rat chromosome 3
RNO9	Rat chromosome 9
RVFV	Rift Valley Fever virus
SNP	Single nucleotide polymorphism
SSLP	Simple sequence length polymorphism
UTR	Untranslated region
VHF	Viral hemorrhagic fever
WF	Wistar Furth
WF.LEW	Wistar Furth / Lewis congenic strain

TABLE OF CONTENTS

Page

LIST OF FIGURES

LIST OF TABLES

CHAPTER I

INTRODUCTION: RIFT VALLEY FEVER VIRUS AND INBRED RAT STRAINS

Introduction to Rift Valley Fever Virus

Rift Valley Fever (RVF) virus is an arthropod-borne phlebovirus of the family *Bunyaviridae* that can cause severe epizootic disease in both human and animal hosts, mainly infecting domesticated livestock such as sheep, cattle, and goats, but also infecting camels, buffalo, monkeys, and gray squirrels as well as other rodents [1-3]. It was first identified in a 1930 outbreak in sheep in the greater Rift Valley of Kenya [4,5], and while originally endemic to sub-Saharan Africa, the disease has demonstrated ecologic flexibility by spreading across the continent from Egypt in the north [6,7] to South Africa in the south [8,9], from Kenya in the east [4,10] to Senegal and Mauritania in the west [11-15], and even extending its reach outside of the African continent to the island of Madagascar [16] and into Saudi Arabia and Yemen in the Arabian Peninsula [17-19]. The disease has not only displayed the ability to emerge in new regions but also to re-emerge after long periods of silence in endemic regions, as seen in Somalia, Kenya, and Tanzania in 2006 [20,21] and in South Africa in 2010 [22]. This viral competency combined with the presence of potential vectors in currently RVF-free regions such as Europe [23] and the USA [24,25], an increase in international trade in live animals, and the uncertain effects of climate change, have all led to concerns about the introduction of

RVF into RVF-free countries, prompting preparations, preventive measures, and warnings from numerous national and international agencies [20,26-34].

Viral Structure

The Rift Valley Fever virus (RVFV) is an enveloped RNA virus with a negative-sense, single-stranded, tripartite RNA genome. This genome's three segments are identified as L (large), M (medium), and S (small), and they encode a total of seven proteins with various functions [35]. These are the L protein (viral RNA-dependent RNA polymerase) coded for by the L segment, the glycoproteins G_1 (G_c) and G_2 (G_n) along with the two non-structural proteins NSm1 (78 kDa) and NSm2 (14 kDa), all encoded by the M segment, and the nucleoprotein N and non-structural protein NSs encoded by the S segment [20,36-40]. The viral envelope glycoproteins are essential for penetration into host cells; these are also recognized by the host's immune system and induce the production of neutralizing antibodies [20]. NSm2 has anti-apoptotic function and contributes to pathogenesis [41]. NSs, meanwhile, has been identified as a major factor of virulence (primarily as an interferon antagonist), being largely responsible for the ability of the virus to evade the host antiviral response and playing an important role in viral replication and pathogenesis [20,42-45]. NSs is a multifunctional protein, responsible for inhibiting general cellular transcription in addition to suppressing two separate aspects of the interferon response [44,45]. Within the first 3-4 hours of RVFV infection, NSs works to block IFN-β production by transcriptional repression via interaction with the host protein SAP30 [20,45,46]; it appears that the virulence of a

particular RVFV strain does not depend on its interferon sensitivity but rather on its ability to block the production of IFN-α/β [43]. Next, it interferes with basal transcription factor TFIIH: although the virus replicates in the host cell cytoplasm, NSs forms a ribbon-like filamentous structure in the host cell nucleus which sequesters the p44 subunit of the TFIIH complex. This then prevents assembly and action of the TFIIH complex in the cell. By this mechanism, NSs begins to inhibit general transcription in infected cells by 8 hours post-infection [20,45,47-51]. Finally, NSs targets and specifically triggers degradation of the antiviral, IFN-induced, dsRNA-dependent protein kinase R (PKR), a serine-threonine kinase activated by viral RNAs which mediates translational suppression by preventing the phosphorylation of eukaryotic initiation factor 2 alpha (eIF2α) [20,52-55]. Mice expressing PKR are capable of clearing infection of attenuated RVF virus Clone 13, which has a defective NSs gene due to a large in-frame deletion, but knockout mice lacking PKR (thereby mimicking the conditions of infection with a functional NSs protein) are unable to do so [52]. Thus, NSs has multiple functions to counteract the host interferon response and to prevent the production of antiviral proteins at both transcriptional and translational levels. Interestingly, NSs also targets and interacts with specific DNA regions of the host genome, an action which is correlated with the induction of chromosome cohesion and segregation defects in RVFV-infected murine and ovine cells. It has been postulated that an accumulation of such defects during embryonic development might be partly responsible for the fetal deformities and abortions observed in RVFV-infected animals [56].

Pathogenesis and Host Immune Response

The pathogenesis of RVFV after natural transmission is likely similar to that of other arboviruses and thus involves the virus being transported from the initial infection site to lymph nodes via the lymphatic system. Early viral replication occurs in the lymph nodes, and the virus then spreads through the bloodstream, resulting in primary viremia and subsequent infection of target organs. Major sites of viral replication include the liver, spleen, and, in animals that succumb to encephalitis, the brain [57,58]. The principal site of RVF-induced lesions is the liver in both human and animal hosts; this organ is clearly an early and dominant target of the virus. However, during severe infections, virus can be found in virtually all tissues and cell types, indicating a likely ubiquitous cellular receptor for the virus [20,59].

Infection with RVFV is regulated by interferons and terminated by neutralizing antibodies (NA). The lytic virus-cell interaction observed with RVFV suggests that its major effects are due to direct, virus-induced necrosis, particularly in the liver, by the destruction of infected cells [60]. Virus maturation typically occurs within Golgi vesicles with subsequent exocytosis; therefore, it was originally proposed that cells infected with phleboviruses such as RVFV did not express cell-surface antigens [61]. According to further studies, however, in certain virus-cell combinations, morphogenesis of RVFV progresses by budding from the plasma membrane, thus resulting in the cell membrane bearing viral antigens [62]. Regardless, RVFV infection usually does not result in significant expression of cell-surface viral antigens, and as such, infected cells are not targeted for elimination by cytotoxic T lymphocytes. Thus, the organism is not rescued

from RVFV infection by the processes of cell-mediated immunity. Rather, neutralizing antibodies appear to be the primary host response involved in recovery; therefore, humoral adaptive immunity is responsible for survival of infection with RVFV [60]. A strong innate immune response to restrain initial virus replication and dissemination is crucial for survival of the host and must be followed by a robust adaptive immune response. Detectable levels of NA are produced within 4-8 days after infection and are primarily directed against the viral glycoproteins G_n and G_c; these are followed by IgM and IgG antibodies targeting the nucleoprotein N and the non-structural protein NSs [20,63-67]. In studies with rhesus macaques, which present clinical disease symptoms similar to humans in response to RVFV infection, significant viremia (as well as abnormal liver function) was observed in all subjects, both survivors and mortalities, and the severity of the disease corresponded to the extent and persistence of viremia. The appearance of NA in surviving monkeys coincided with termination of viremia [68]; furthermore, passive immunization had previously proven highly effective as a means of prophylaxis [69]. The high viral titers observed in lymphoid tissues may explain the inability of the majority of fatally infected macaques to mount a serum antibody response [60,69]. Rodent models support the concept that antibodies play a dominant role in recovery from RVFV, as fatal disease can be prevented in immunosuppressed rats by the administration of sufficient quantities of antibody to mimic the titers of serum NA that naturally develop in intact, infected animals [70]. Disease can similarly be prevented or treated with antibody in mice [71,72], implicating neutralizing antibodies as the decisive component in the primary and continuing protection of infected animals and

also therefore as an appropriate measure of the level of protection conferred by vaccines [20,68,73].

Interferon (IFN) has also proven extremely important in determining the fate of infected rodents and monkeys. A type of cytokine made and released by lymphocytes and other interferon-producing cells (IPCs), also known as plasmacytoid dendritic cells, as part of the innate immune system, interferon interrupts viral replication within host cells and also induces transcription of certain genes, creating an antiviral state in target cells. In the previously cited studies in rhesus macaques, there was a noticeable correlation observed between a delayed interferon response and death. Serum interferon appeared significantly earlier in surviving monkeys, while those that died had transient and low-level serum interferon, indicating a failure to limit virus replication and to establish an effective antiviral state. This suggests that the early appearance of serum IFN (within the first 24 hours of infection) is critical for limiting the severity of disease [68]. Additionally, the therapeutic administration of IFN-α in rhesus monkeys beginning 24 hours before RVFV inoculation either prevents or greatly diminishes viremia and clinical disease [74]. The virus also has proven sensitive to IFN-α *in vitro*, and multiple studies indicate the importance of interferon along with serum antibody in determining the outcome of both simian and rodent infections with RVFV *in vivo* [68,72-76]. In particular, RVFV has been shown to be sensitive to murine interferon *in vitro*, and in various *in vivo* studies, administration of interferon inducer poly(ICLC) within 24 hours of virus infection has resulted in virtually complete protection of RVFV-infected mice and hamsters [72,77]. Additionally, knockout mice lacking the β-subunit of the IFN-α/β

receptor are highly susceptible to attenuated strains of RVFV [78]. Multiple studies also indicate that interferon plays a crucial role in resistance to RVFV in rats. Sensitivity of the particular RVFV strain to interferon has been found to be a major determining factor in the recovery of infected rats [79]. Stimulation with IFN type I *in vitro* prior to infection inhibits RVFV replication in otherwise permissive peritoneal macrophages obtained from RVFV-resistant LEW/NHsdBR rats; however, the same effect cannot be achieved by interferon stimulation in the macrophages of RVFV-susceptible WF/HsdBR rats [80,81]. Additionally, injection of anti-IFN type I antibodies into RVFV-resistant LEW/Mai rats produces a marked increase in sensitivity to RVFV, while treatment of susceptible WF/Mai rats with interferon increases the likelihood of surviving infection with the virus [82]. Furthermore, studies involving cytoplasmic Mx proteins in humans and in rats have produced evidence of RVFV sensitivity to these IFN-induced antiviral GTPases. Specifically, the human MxA protein has been shown to inhibit early RVFV viral replication [83], and the Mx2 protein exhibited similar inhibition of RVFV in cotton rats [84] and laboratory rats [85]. Thus, a strong and immediate innate immune system interferon response to restrict initial viral replication and dissemination, accompanied by a prompt and robust adaptive immune response with the production of neutralizing antibodies, is critical for host survival of RVFV infection. However, it is acknowledged that further detailed study of the host innate, humoral, and cell-mediated immune pathways is necessary to attain a comprehensive knowledge of RVFV immunology [20].

Virus Transmission

RVF virus is primarily transmitted between animals by a wide array of arthropod vectors, including ticks, biting midges, hematophagous flies, and especially mosquitoes [2,3]. The accepted transmission method involves transovarial transmission of RVFV in certain *Aedes* species (spp.) of mosquitoes via their eggs, which can withstand desiccation and serve as reservoirs during periods of drought [86,87]. After rainfall and flooding, biological transmission occurs near water sources from vectors to bovid hosts via infected mosquito saliva. If flooding remains for 2-3 weeks, *Culex* spp. mosquitoes succeed the *Aedes* spp. in a population explosion [88] and become infected from feeding on nearby viremic bovids. *Culex* spp. are more likely to disperse in search of vertebrate hosts than *Aedes* spp., leading to dissemination of the virus and potentially resulting in epidemics [20,89]. For this reason, outbreaks of RVF tend to coincide with an increase in mosquito breeding grounds due to events such as the building of dams or to periods of heavy rainfall and flooding [58]. RVFV can also be transmitted transcutaneously through direct contact with infected animals, tissues, carcasses, or bodily fluids, and by aerosolization and inhalation; these methods are the greatest concern for human infection [2,90].

RVF Disease, Threat Risk, and Current Countermeasures

Of the numerous significant outbreaks of RVF over the years, the extensive epidemic that occurred in the Nile Delta of Egypt in 1977 is particularly noteworthy as it was when the four distinct manifestations of the disease in humans were first recorded.

The vast majority of infected humans suffer only mild, flu-like symptoms which last 4-7 days, but in a small percentage of cases, the disease becomes more severe. Ocular disease, taking the form of retinal lesions which appear 1-3 weeks after initial symptoms, occurs in 0.5-2% of cases and may result in permanent loss of vision. Meningoencephalitis occurs in less than 1% of cases; within 1-4 weeks after initial symptoms comes the onset of headache, memory loss, confusion, hallucinations, and possibly coma. Sufferers of this form of disease may have lasting neurological complications. The final and most deadly form of the disease is hemorrhagic fever. Occurring in less than 1% of cases, about 2-4 days after initial symptoms, jaundice and signs of hemorrhaging begin to appear. The case-fatality ratio for this form is approximately 50% and usually occurs within 3-6 days of the onset of symptoms [2,91,92].

The severity of RVF is strongly age-dependent, with resistance increasing with age. General symptoms include fever, loss of appetite, jaundice, and weakness; the disease often causes fulminant hepatitis with high mortality rates and nearly 100% abortion rates (termed “abortion storms”) in domestic ruminant herds, especially those of European origin, which are more susceptible than native African stock [2,20,35,93]. This makes RVF a disease of great economic and agricultural concern to the USA as it presents a frighteningly devastating potential weapon of bioterrorism, particularly due to its ability to infect humans as well as livestock. This threat has been recognized by the Centers for Disease Control and Prevention, the United States Department of Health and Human Services, and the United States Department of Agriculture, who have classified

the virus as a select agent [94]. Additionally, it is one of the three primary animal diseases being focused on by the Department of Homeland Security's Institute for Infectious Animal Diseases (IIAD) due to posing "significant risks to public health or the national economy" [95]. Vaccines exist, in both attenuated [96,97] and inactivated [98] forms, which have been approved for use in both humans and animals but which are not optimally efficacious. The inactivated vaccine is not as effective as the attenuated forms, requiring multiple inoculations and providing only low levels of protection [99]. Two attenuated forms, MP12 and clone 13, have been developed which have mutations in the NSs gene and thus are excellent inducers of early IFN-α/β production [43,96,97,100]. Trials of the attenuated MP12 variant in young lambs, pregnant ewes, fetal and neonatal bovids, and cattle proved promising [63-65,101,102], and additionally, the vaccine induced a good immunity in rhesus macaques and showed potential as a candidate for human vaccination; however, concurrent neurovirulence testing in the macaque trials indicated that the vaccine is not completely innocuous [103]. Additionally, MP12 trials in South Africa resulted in some abortions and teratogenesis during early pregnancy in ewes [104]. The naturally attenuated Clone 13 viral variant, containing a deletion in the S segment coding for the NSs protein and thus incapable of reverting, is another promising prospect. In trials carried out in sheep and cattle, no deleterious effects or abortions were observed in pregnant ewes, and the vaccine elicited a high antibody response resulting in protection against a virulent challenge [20,97]. However, there is currently no real established course of treatment for infection, and it

would be advantageous to develop additional, less conventional options for protection against the potentially disastrous consequences of a threat such as RVF.

RVF and Inbred Rat Strains

Animal models are a necessity for studying this RVF disease. Current models range from ruminants (sheep, goats, and cattle) to rodent laboratory animals (mice, rats, hamsters, and gerbils) to non-human primates such as rhesus macaques [20,105,106]. The mouse model of RVF disease simulates both the acute-onset hepatitis and the delayed-onset encephalitis seen in human infection, and recognition of the need for a well-characterized small animal model of RVF infection has prompted recent detailed studies examining RVFV in the mouse model [35,107]. As a small animal model species, the laboratory rat (*Rattus norvegicus*) is particularly valuable because it either demonstrates resistance (exhibiting an immunizing infection with no obvious symptoms of illness), develops hepatitis, or develops fatal encephalitis, mimicking characteristic responses of both humans and livestock to the disease [76]. Thus, the rat provides a useful model for study, and it is additionally the only species for which inbred strains exist which are either naturally resistant or susceptible to RVF hepatic disease [70]. This hepatic disease is the focus of this particular study. In a previous report, differential pathogenesis of RVFV was found between the Wistar Furth (WF) and Lewis (LEW) inbred rat strains due to genetic differences between the strains. The disease was found to progress quickly in WF rats, with all subjects dead from fatal liver necrosis by day 2 post-inoculation. LEW rats, on the other hand, showed resistance to liver disease,

resulting in an 84% survival rate, with the other 16% developing fatal necrotizing encephalitis 2-3 weeks post-inoculation. Further examination showed that viral replication progressed rapidly in WF, causing extensive organ damage before the body could mount an effective immune response. By contrast, LEW rats were better able to restrict initial virus growth and replication, thus allowing the body time to mount an antibody response able to control and terminate the infection [70]. Classical genetic studies showed that the LEW resistant phenotype was controlled by a single dominant gene (or possibly a closely linked gene complex) inherited in classic Mendelian fashion [79]. Subsequently, a WF.LEW congenic strain was developed by backcrossing the resistant LEW genome (using the LEW/Mai substrain as the donor strain) onto the susceptible WF background (using the WF/Mai substrain as the recipient strain) with selection at each generation for resistance to RVF [108]. However, studies later appeared reporting results which conflicted with those that formed the basis for the creation of this congenic strain. These studies found that, conversely, WF rats of the WF/Mol substrain were resistant to RVFV infection and that LEW rats of the LEW/Mol substrain were susceptible. Additionally, while the resistance of the WF/Mol rats also segregated as a single dominant gene, it did not appear to depend on an interferon response [109] as had been previously described in rat models [79-82,85]. Subsequently, a complete genome comparison of the LEW/Ztm and LEW/Mol substrains using SSLP markers with a minimum of three markers per chromosome revealed the introduction of approximately 37% non-LEW genome into the LEW/Mol substrain [110]. These conflicting data were further reconciled by a comprehensive genomic comparison of five commercially

available LEW and WF substrains using microsatellite markers [111]. According to 159 SSLPs spanning the entire rat genome with a minimum of four markers per chromosome, the LEW/MolTac substrain showed approximately 37% difference from the LEW/SsNHsd substrain and approximately 45% difference from the LEW/Crl substrain while the LEW/SsNHsd and LEW/Crl substrains demonstrated only an approximately 8% difference from each other. The two WF substrains examined, WF/NHsd and WF/CrCrl, similarly demonstrated an approximately 8% difference between them. This study not only offered an explanation for the striking differences in resistance and susceptibility seen in the LEW/Mol rat substrain when compared to other substrains [109,110] but also served as a reminder of the importance of utilizing inbred strains from a single source when possible [111].

Efforts were then initiated to further investigate the source of the natural resistance exhibited by the WF.LEW strain. As the original LEW/Mai and WF/Mai parental substrains were extinct, an initial genome scan of 137 SSLP markers was performed and compared to the five WF and LEW substrains previously investigated [111] in order to characterize the genome of the congenic strain. LEW markers were identified on *Rattus norvegicus* chromosomes 3 (RNO3) and 9 (RNO9). Those regions were then further characterized in the congenic strain and the five other substrains by an additional 15 SSLP markers and 24 SNP markers on RNO3 and an additional 7 SSLP markers and 8 SNP markers on RNO9 [112]. In total, 5 SNP markers and 3 SSLP markers defined an approximately 1.8Mb LEW region on RNO3 while only 1 SSLP LEW marker was discovered on RNO9. Clearly, further study was required to determine

the responsible gene, discover the mechanism by which it confers resistance to RVF, and investigate beneficial future applications of that knowledge.

CHAPTER II

CHARACTERIZATION AND IDENTIFICATION OF THE CHROMOSOME OF INTEREST

Introduction

The first objective to be accomplished was to determine whether RNO3 or RNO9 contained the location of the primary agent of resistance, or alternatively, if the regions on both chromosomes were required to achieve the effect. In order to reach this conclusion, the first step taken was to test an additional 13 SNP markers and 5 SSLP markers from the distal end of RNO3 and compare them across 6 different rat substrains: LEW/SsNHsd, LEW/Crl, WF.LEW, LEW/MolTac, WF/NHsd, and WF/Crl. (Appendices A and B contain the list of the specific RNO3 SSLP and SNP markers, respectively, and their corresponding alleles for each strain.) This resulted in the identification of 6 supplementary differential SNP markers, more precisely defining the region of interest (ROI) on that chromosome and increasing the total number of differential markers for the RNO3 region to 14, consisting of 11 SNPs and 3 SSLPs (Fig. 1 and Fig. 2).

Meanwhile, a breeding plan was organized to generate N1 offspring from the WF.LEW rats which could be used to contrast the RNO3 and RNO9 regions via viral challenge. To produce the N1 offspring, a susceptible inbred strain was needed to backcross with the resistant WF.LEW. Unfortunately, the colonies of WF/Mai and

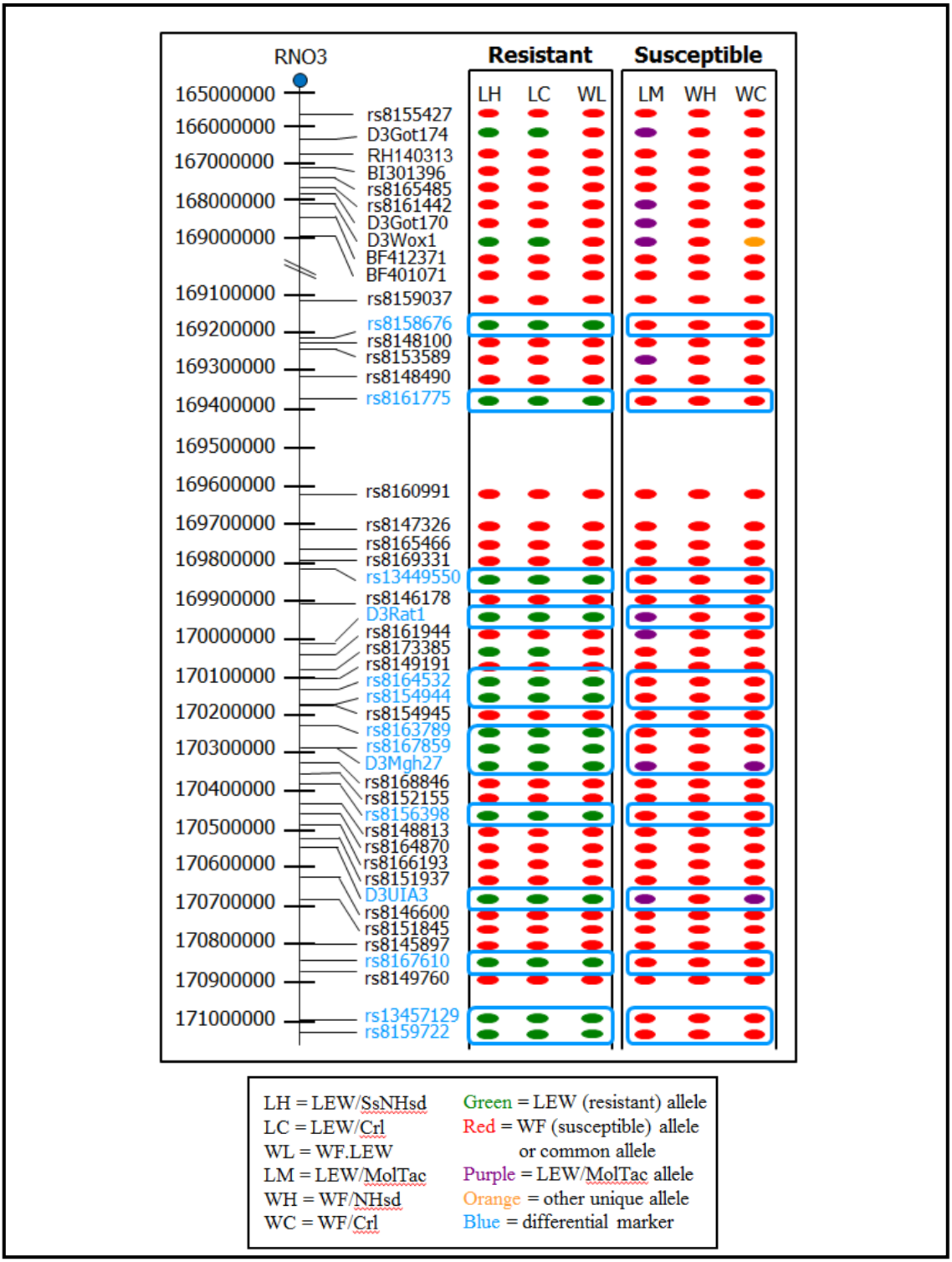

Fig. 1 RNO3 SSLP and SNP marker locations and alleles for six substrains.

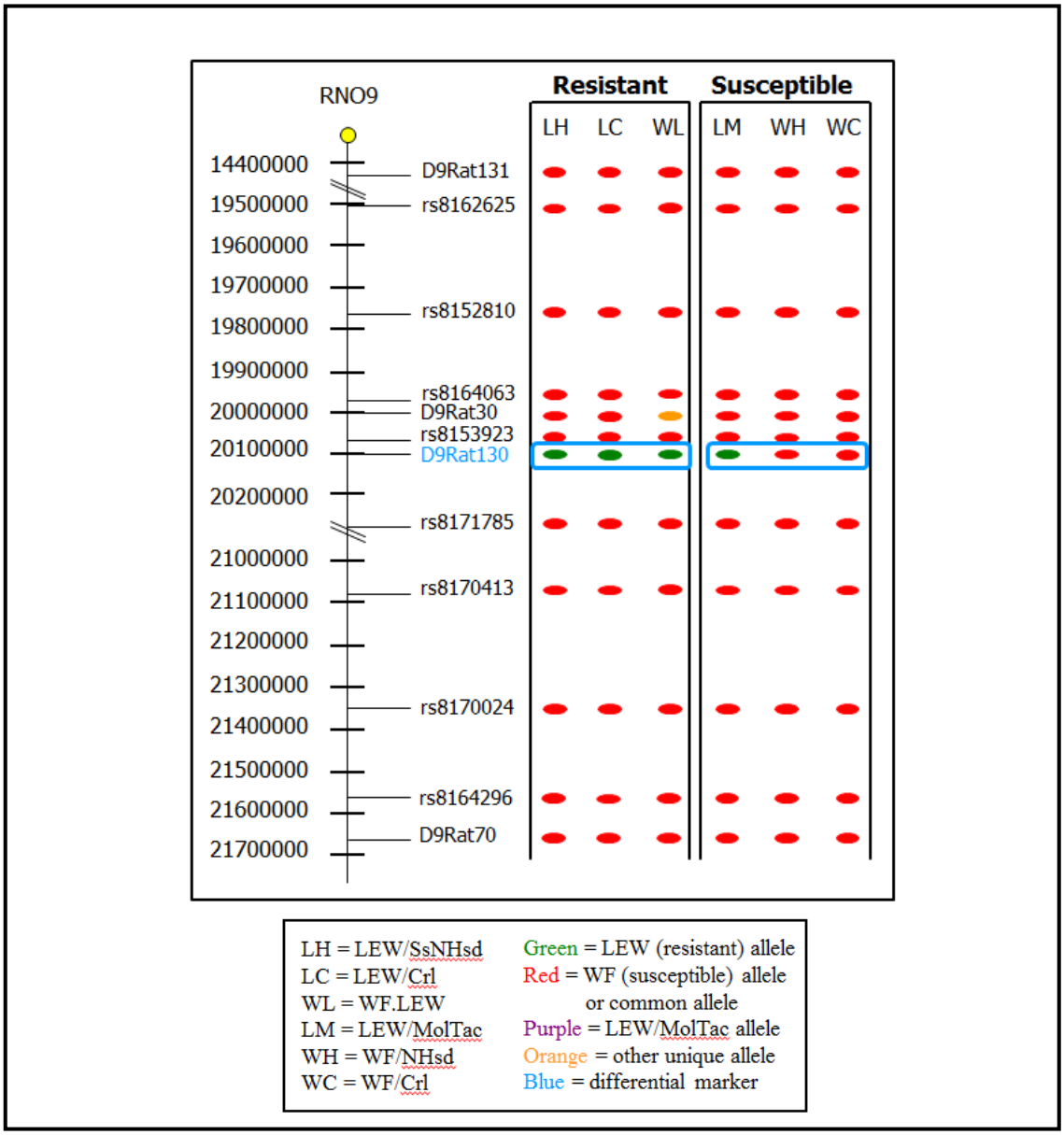

Fig. 2 RNO9 SSLP and SNP marker locations and alleles for six substrains.

LEW/Mai rats, the original substrains used to create the congenic strain, had been discontinued, and thus those substrains were extinct. However, the LEW/SsNHsd and WF/NHsd rat substrains may have been derived from similar source colonies as the

LEW/Mai and WF/Mai rats, respectively, and are postulated to be the most closely related extant substrains to the defunct LEW/Mai and WF/Mai substrains [111]. Results of the previous investigation comparing the DNA of WF.LEW rats to that of five inbred substrains using 137 SSLP markers supported this claim, as the Harlan substrains shared the most markers in common with the congenic strain [112]. As such, for all breeding and challenge purposes, the LEW/SsNHsd and WF/NHsd rat substrains were utilized in conjunction with the WF.LEW rats in lieu of the original founding LEW/Mai and WF/Mai substrains. Accordingly, to generate N1 rats, resistant WF.LEW rats were crossed with susceptible WF/NHsd rats, resulting in F1 hybrids which were then backcrossed to WF/NHsd rats to produce the N1 generation. Once a sufficient number of N1 offspring had been generated, each one was characterized by the previously established differential markers (14 on RNO3 and 1 on RNO9) in order to segregate them into four genotypic groups: those showing no LEW markers; those showing LEW markers on RNO3 only; those showing LEW markers on RNO9 only; and those showing LEW markers on both RNO3 and RNO9 (Fig. 3). Eventually, 25 N1 rats collected from three separate litters, along with positive and negative control rats of various inbred strains, were challenged with RVFV to establish and verify the phenotype corresponding to each genotype.

Materials and Methods

Previously, live WF.LEW rats were re-derived by the Rat Resource and Research Center (RRRC) at the University of Missouri (Columbia, MO) from frozen embryos that

had been maintained at the National Institutes of Health (NIH), and breeding pairs were sent to Texas A&M University (College Station, TX) to found a colony. Once established, WF.LEW female rats were mated with WF/NHsd male rats purchased from Harlan (Indianapolis, IN) to produce (WF.LEW x WF/NHsd)F1s. Female F1s were then

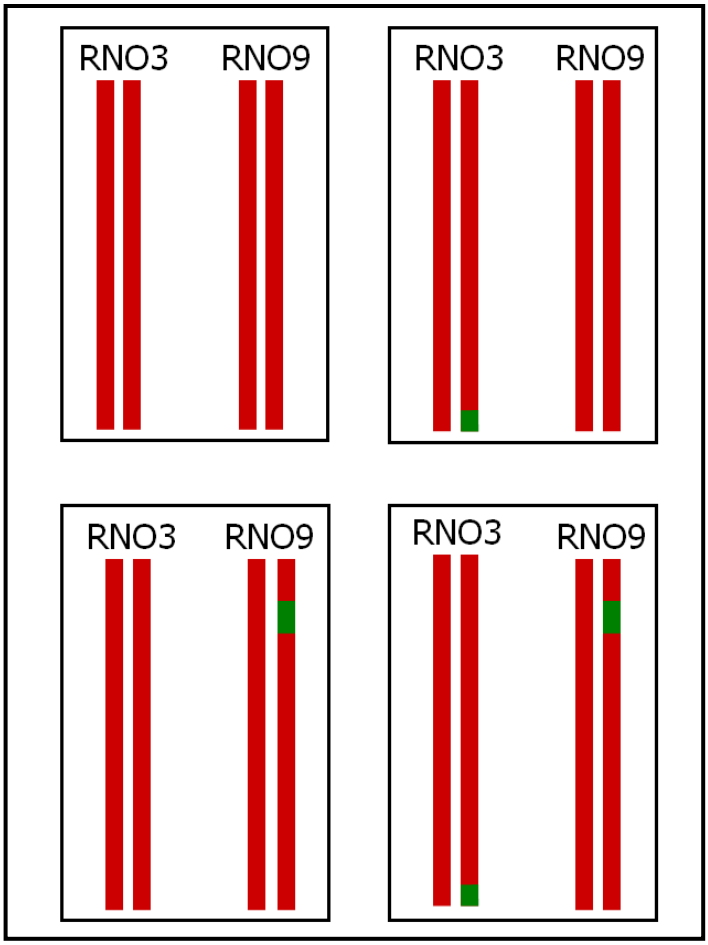

Fig. 3 Representation of RNO3 and RNO9 chromosome pairs of the four N1 genotypic groups. Red denotes WF genome (from WF/NHsd or WF/Mai recipient strain of WF.LEW); green denotes LEW genome (from LEW/Mai donor strain of WF.LEW).

backcrossed to WF/NHsd males to produce an N1 generation of (WF.LEW x WF/NHsd)F1 x WF/NHsd rats. Rats were housed on Texas A&M University campus in the Laboratory Animal Resources and Research Facility (LARR), accredited by the Association for the Assessment and Accreditation of Laboratory Animal Care, International (AAALAC). Animals were maintained according to the Animal Use Protocol (AUP) filed with the TAMU Office of Research Compliance under the Animal Welfare Assurance Program (AWAP) and approved by the Institutional Animal Care and Use Committees (IACUC).

Genomic DNA for initial SSLP and SNP marker testing of the six strains had previously been extracted from rat spleen tissue by phenol extraction with ethanol precipitation [113]. Genomic DNA of N1 rats was extracted from 0.2cm tail snips, collected humanely from neonates, by a previously described HotSHOT protocol [114], using a 30min heating time in a TC-512 (Techne, Minneapolis, MN) thermal cycler.

SSLPs and SNPs were selected using the Genome Browser of the Rat Genome Database (RGD) v3.4 Assembly [115]. Established primers cited on RGD were used for SSLPs; SNP forward and reverse primers were designed using Primer3 (v. 0.4.0) [116]. Each specific SNaPshot primer consisted of the 30 bases immediately 5' to the SNP location according to RGD v3.4. A previously described method utilizing M13-tailed primers was used to streamline genotyping by SSLP markers [117]. Each forward SSLP primer was created with a 5'-tail of the M13 sequence. Additionally, M13 sequence primers were synthesized with a 5' label of either 6-FAM, HEX, or NED (Applied Biosystems, Foster City, CA). For the forward primer component of each reaction, a

mixture of the M13-tailed forward SSLP primer with a fluorescent-labeled M13 primer in a 1:15 ratio was used. Each SSLP was amplified by standard polymerase chain reaction (PCR) [118]. Each reaction consisted of 1µl 10x PCR Buffer with 15mM $MgCl_2$ (Applied Biosystems), 0.5U AmpliTaq Gold® DNA Polymerase (Applied Biosystems), 200µM each dNTP, 250nM each forward and reverse primer, 100ng genomic DNA, and Q.S. of double-distilled water to produce a 10µl reaction. Thermal cycling parameters were set as follows: initialization at 94ºC for 10min, followed by 35 cycles of denaturation at 94ºC for 30s, annealing at 58ºC for 30s, and extension at 72ºC for 30s, and ending with a final extension at 72ºC for 5min. SNPs were genotyped utilizing the SNaPshot® Multiplex Kit (Applied Biosystems). The initial PCR reaction contained 1µl 10x PCR Buffer with 15mM $MgCl_2$ (Applied Biosystems), 0.5U AmpliTaq Gold DNA Polymerase (Applied Biosystems), 200µM each dNTP, 250nM each forward and reverse primer, 100ng genomic DNA, and Q.S. of double-distilled water to produce a 10µl reaction. Thermal cycling conditions were set as follows: initialization at 94ºC for 10min, followed by 35 cycles of denaturation at 94ºC for 30s, annealing at 60ºC for 30s, and extension at 72ºC for 30s, and ending with a final extension at 72ºC for 5min. Postreaction products were subsequently purified using the QIAquick® PCR Purification Kit (Qiagen, Valencia, CA) according to the manufacturer's recommended protocol, adding 20µl of double-distilled water to elute in the final step. The ensuing SNaPshot reactions consisted of 3µl of purified PCR product, 2µl of SNaPshot Multiplex Ready Reaction Mix, 500nM SNaPshot primer, and the necessary amount of double-distilled water to yield a 10µl reaction. Thermal cycling parameters for the

SNaPshot reaction and following post-extension treatment with 1.0 Unit of Shrimp Alkaline Phosphatase (SAP) were set according to the manufacturer's instructions. All PCR and SNaPshot reactions were performed using either a TC-512 (Techne) or a GeneAmp PCR System 9700 (Applied Biosystems) thermal cycler. Final reaction products of both SSLP and SNaPshot reactions were analyzed using a 3130*xl* Genetic Analyzer (Applied Biosystems), and genotypes were visualized using GeneMapper® version 4.0 (Applied Biosystems) and exported to a spreadsheet for organization and comparison (Excel, Microsoft, Redmond, WA).

All viral challenge work was performed in ABSL-4 containment at the University of Texas Medical Branch in Galveston, Texas. Groups of adult rats 10 weeks of age or older were inoculated subcutaneously with 0.1ml of $5x10^5$ ZH501 strain of RVFV for the experimental groups or with 0.1ml Hank's Balanced Salt Solution (HBSS) diluent for control animals. Commercially available inbred strains tested included LEW/SsNHsd and WF/NHsd, purchased from Harlan (Indianapolis, IN), LEW/MolTac, purchased from Taconic (Germantown, NY), and LEW/Crl and WF/CrCrl, purchased from Charles River Laboratories (Boston, MA). Additionally, WF.LEW rats, (WF.LEW x WF/NHsd)F1 hybrids, and their (WF.LEW x WF/NHSd)F1 x WF/NHsd N1 backcross offspring, obtained and produced by the previously described methods, were also challenged. All animals were properly transported and handled in accordance with the guidelines of the Animal Use Protocol (AUP) referenced above. Survival was compared by the log-rank test, and all statistical analyses were conducted using the GraphPad

Prism 6.0 software (GraphPad, La Jolla, CA). Differences in survival were considered to be significant at $P < 0.05$.

Results and Discussion

The results of the challenge showed a statistically significant difference ($P < 0.0001$) in survival among the four groups and clearly implicated the approximately 1.8Mb LEW region on the distal end of RNO3 as containing the major gene responsible for resistance to RVFV, with N1 rats possessing only the region on RNO9 surviving only slightly longer than susceptible rats lacking both regions (Table 1, Fig. 4). Interestingly, rats containing the LEW region of both RNO3 and RNO9 had a 100% survival rate, compared to a 75% survival rate for rats containing the LEW region on RNO3 only. However, these results were reasonably congruous with previous findings of a LEW survival rate of 84% with death delayed until the second week post-infection [70]. Thus, while possible contributions of the LEW region of RNO9 to resistance in a supporting capacity could not be ruled out, it was the LEW region on RNO3 which was discovered to merit further investigation.

Table 1 Viral challenge survival: N1s, plus assorted inbred strains

Strain / Group Identification	Inoculated	Survived	Percent Survival
WF/NHsd	5	0	0%
WF/CrCrl	5	0	0%
LEW/MolTac	5	0	0%
LEW/SsNHsd	5	2	40%
LEW/Crl	5	4	80%
WF.LEW	5	4	80%
(WF.LEWxWF/NHsd)F1	5	4	80%
N1: No LEW genome	6	0	0%
N1: LEW genome RNO3 only	8	6	75%
N1: LEW genome RNO9 only	6	0	0%
N1: LEW genome RNO3 and RNO9	5	5	100%

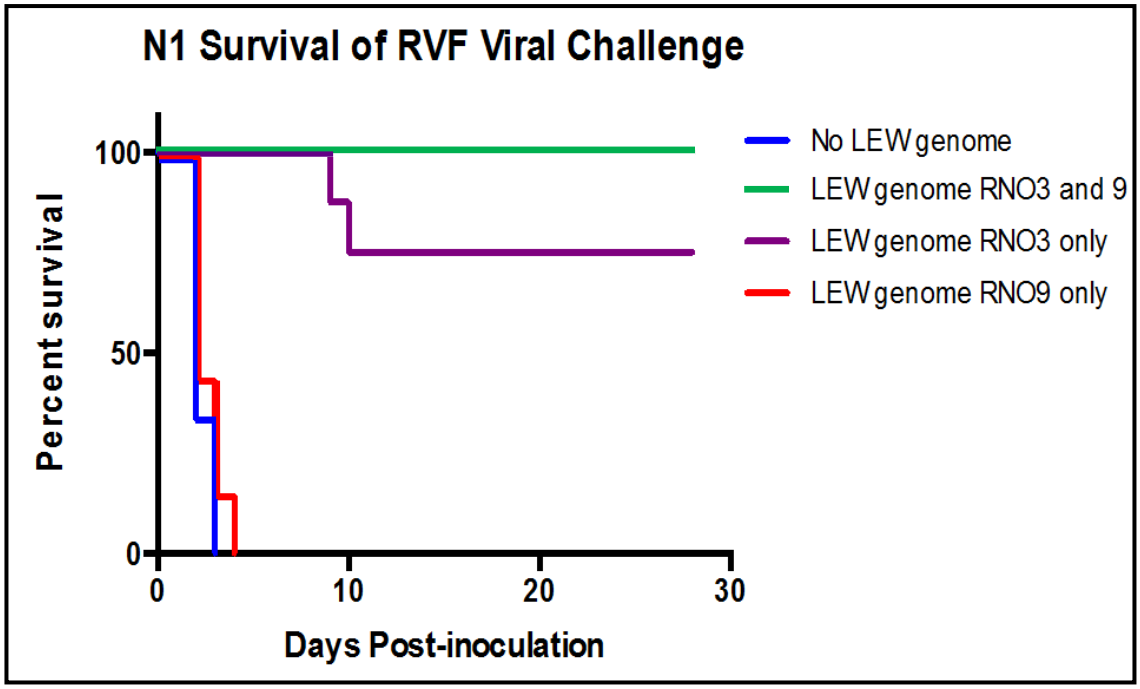

Fig. 4 N1 survival of RVF viral challenge. From a minimum of five rats from each group challenged with 0.1ml of $5x10^5$ ZH501 strain of RVFV. $P < 0.0001$. All surviving rats were humanely euthanized on day 28.

CHAPTER III

ISOLATION AND DEFINITION OF THE CHROMOSOMAL REGION OF INTEREST

Introduction

With the LEW region on RNO3 having been established as the primary region of interest for conferring resistance to RVFV, the next step in seeking out the responsible gene was to narrow this ~1.8Mb region to a more practicable size for further investigation. This was proposed to be accomplished mainly through continued backcrossing of F1 hybrids of WF.LEW rats and WF/NHsd rats to WF/NHsd rats, with subsequent genotyping of the N1 offspring using the 14 previously established differential markers in order to identify any recombination within the LEW region. With a reported recombination rate of 0.55cM/Mb for RNO3 [119], the expectation was that approximately 1 in 100 N1 rats produced would exhibit recombination within the ~1.8Mb region. The first recombinant rat generated happened to be an offspring from a unique pairing of two N1 rats previously produced and genotyped as containing the LEW region on RNO3 only but not used for the earlier referenced RVFV challenges. This male offspring showed recombination between microsatellite D3Rat1 and SNP marker rs8164532, thus retaining the LEW genome only in the approximate upper half of the ROI (~0.9Mb) (Fig. 5). The recombinant rat furthermore showed from genotyping to have received the entire ~1.8Mb RNO3 LEW region from one parent and the recombined approximate half of the RNO3 LEW region from the other parent; thus, this

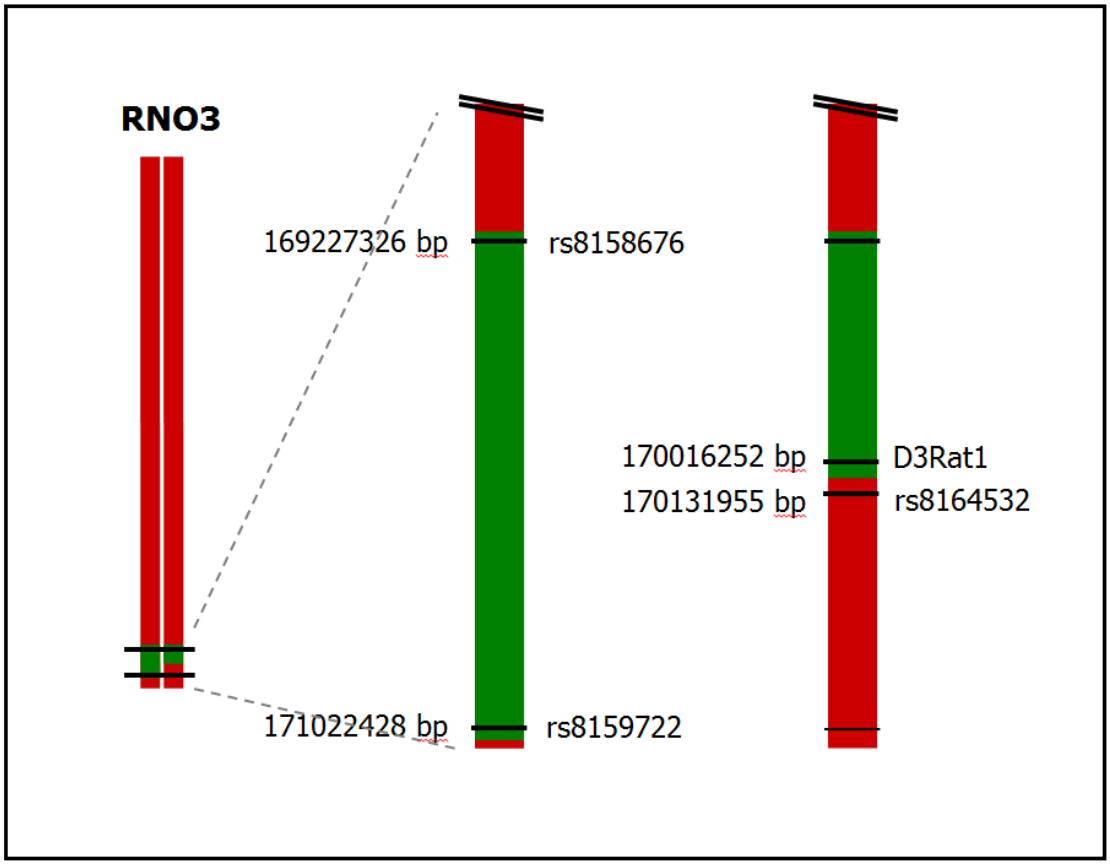

Fig. 5 Genotype of first recombinant rat for RNO3.

male recombinant was backcrossed to WF/NHsd females, and the R1 (first recombinant generation) offspring were genotyped to determine which approximate half of the offspring exhibited the full ~1.8Mb LEW region and which contained the smaller, recombined ~0.9Mb LEW region. Those with the recombined LEW region were considered of interest and were subsequently challenged with RVFV. Incidentally, one of these R1 offspring indicated the occurrence of a second recombination event between SNP marker rs8156398 and microsatellite D3UIA3, thus gaining back an additional

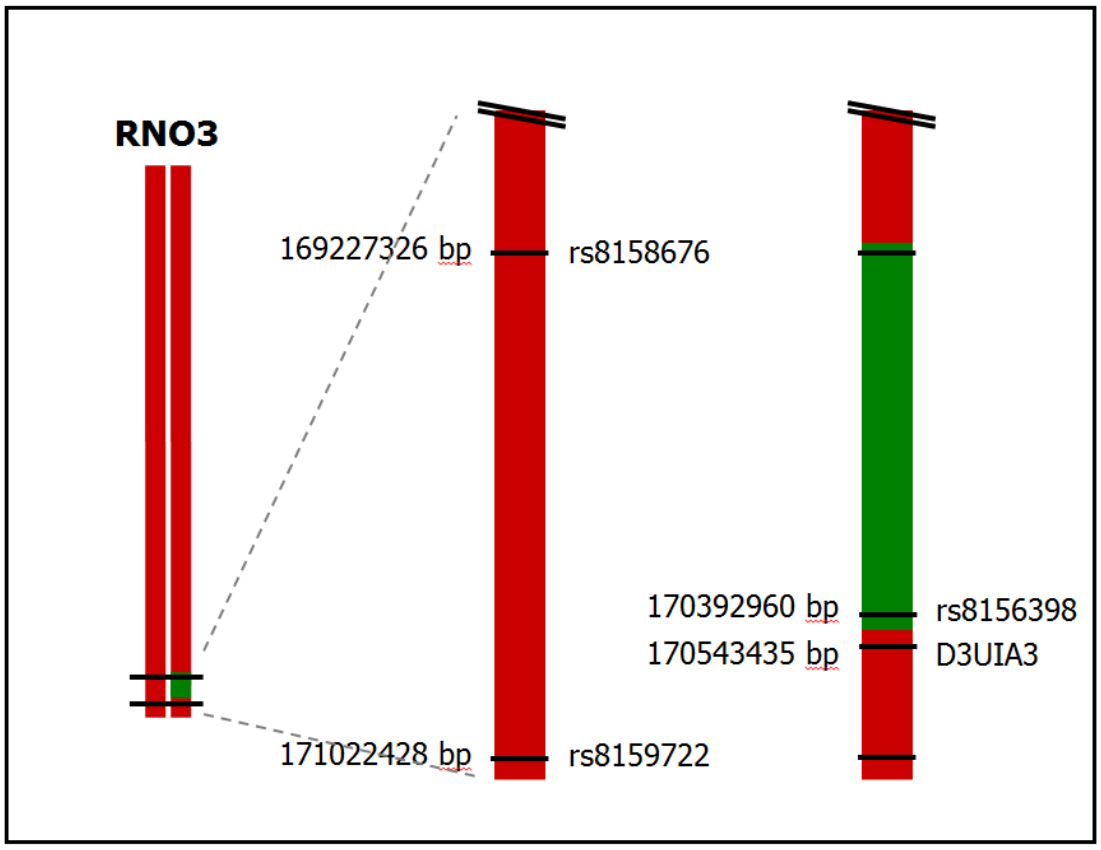

Fig. 6 Genotype of second recombinant rat for RNO3.

~0.5Mb of LEW region as compared to the original recombinant (Fig. 6). This second male recombinant was accordingly bred to female WF/NHsd rats, the offspring were genotyped to determine which contained the second recombination event, and appropriate representatives were then challenged with RVFV in order to further isolate and define a smaller region of interest on RNO3.

Materials and Methods

Previously established (WF.LEW x WF/NHsd)F1 rats were mated with WF/NHsd rats purchased from Harlan to produce additional (WF.LEW x WF/NHSd)F1 x WF/NHsd N1 backcross offspring. One N2 litter from a N1 x N1 cross was also produced. Rats were housed at LARR and maintained in accordance with the AUP previously referenced.

As before, 0.2cm tail snips, collected humanely from neonates, were used to obtain genomic DNA from N1 and N2 rats by extraction according to the previously referenced HotSHOT protocol [114] with a 30min heating time in a TC-512 (Techne) thermal cycler. The previously established SSLPs were amplified by standard PCR [118] using M13-tailed primers [117] as previously described. Each reaction consisted of 1µl 10x PCR Buffer with 15mM $MgCl_2$ (Applied Biosystems), 0.5U AmpliTaq Gold DNA Polymerase (Applied Biosystems), 200µM each dNTP, 250nM each forward and reverse primer, 100ng genomic DNA, and Q.S. of double-distilled water to produce a 10µl reaction. Thermal cycling parameters were set as follows: initialization at 94ºC for 10min, followed by 35 cycles of denaturation at 94ºC for 30s, annealing at 58ºC for 30s, and extension at 72ºC for 30s, and ending with a final extension at 72ºC for 5min. As before, the previously established SNPs were genotyped utilizing the SNaPshot Multiplex Kit (Applied Biosystems). The initial PCR reaction contained 1µl 10x PCR Buffer with 15mM $MgCl_2$ (Applied Biosystems), 0.5U AmpliTaq Gold DNA Polymerase (Applied Biosystems), 200µM each dNTP, 250nM each forward and reverse primer, 100ng genomic DNA, and Q.S. of double-distilled water to produce a 10µl

reaction. Thermal cycling conditions were set as follows: initialization at 94ºC for 10min, followed by 35 cycles of denaturation at 94ºC for 30s, annealing at 60ºC for 30s, and extension at 72ºC for 30s, and ending with a final extension at 72ºC for 5min. Postreaction products were subsequently purified using the QIAquick PCR Purification Kit (Qiagen) according to the manufacturer's recommended protocol, adding 20µl of double-distilled water to elute in the final step. The ensuing SNaPshot reactions consisted of 3µl of purified PCR product, 2µl of SNaPshot Multiplex Ready Reaction Mix, 500nM SNaPshot primer, and the necessary amount of double-distilled water to yield a 10µl reaction. Thermal cycling parameters for the SNaPshot reaction and following post-extension treatment with 1.0 Unit of Shrimp Alkaline Phosphatase (SAP) were set according to the manufacturer's instructions. All PCR and SNaPshot reactions were performed using either a TC-512 (Techne) or a GeneAmp PCR System 9700 (Applied Biosystems) thermal cycler. As previously, final reaction products of both SSLP and SNaPshot reactions were analyzed using a 3130*xl* Genetic Analyzer (Applied Biosystems), and genotypes were visualized using GeneMapper version 4.0 (Applied Biosystems) and exported to a spreadsheet for organization and comparison (Excel, Microsoft).

All viral challenge work was carried out in ABSL-4 containment at the University of Texas Medical Branch in Galveston, Texas. To test the resistance status of the two recombinants, offspring were produced by mating each recombinant male rat with female WF/NHsd rats. Those offspring which retained the respective recombined paternal RNO3 were challenged at a minimum of 10 weeks of age by subcutaneous

inoculation with 0.1ml of $2x10^5$ ZH501 strain of RVFV for the experimental groups of the first recombinant and 0.1ml $1x10^5$ ZH501 strain of RVFV for the experimental groups of the second recombinant, or with 0.1ml Hank's Balanced Salt Solution (HBSS) diluent for control animals. Additionally, WF.LEW rats, WF/NHsd rats, and littermates of the recombinants which were determined to be heterozygous for the full ROI on RNO3 (genetically identical to (WF.LEW x WF/NHsd)F1 hybrids), all of which were obtained, maintained, or produced from the previously explained sources or by the previously described methods, were also challenged under these conditions. All animals were appropriately transported and handled in accordance with the guidelines of the Animal Use Protocol (AUP) referenced above. Survival comparison by the log-rank test was performed using the GraphPad Prism 6.0 software (GraphPad). Differences in survival were considered to be significant at $P < 0.05$.

Results and Discussion

As can be seen in Table 2 and Fig. 7, results for each recombinant were clear and consistent, and furthermore were determined to be statistically significantly different ($P < 0.01$): all rats containing the first recombination event died within 48 hours post-inoculation, in keeping with previous results from susceptible rats, while the group retaining the second recombination event had an 80% survival rate with the single non-surviving subject lasting nearly a week post-inoculation, as has been seen previously in resistant rats [70]. As such, the region of interest was now determined to be limited to the ~0.5Mb area between microsatellites D3Rat1 and D3UIA3. This new ROI,

containing a total of 20 genes (including the two genes containing D3Rat1 and D3UIA3, respectively) was considered to be a reasonable size for further investigation in the form of qPCR experiments and sequencing comparisons between the resistant WF.LEW and the susceptible WF/NHsd strains.

Table 2 Viral challenge survival: Recombinants #1 and #2, plus controls

Strain / Group Identification	Inoculated	Survived	Percent Survival
WF/NHsd	5	0	0%
WF.LEW	7	7	100%
Heterozygote (F1)	3	2	67%
Recombinant #1	3	0	0%
Recombinant #2	5	4	80%

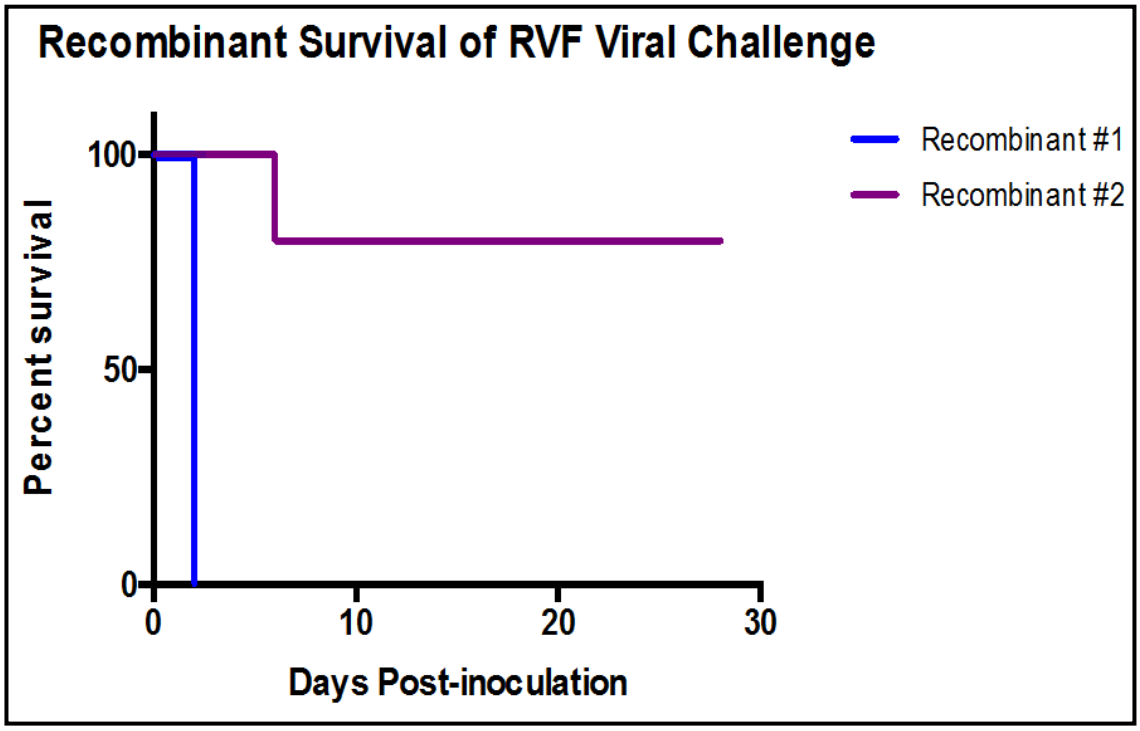

Fig. 7 Recombinant survival of RVF viral challenge. Based on a minimum of three rats per group challenged with 0.1ml of either $2x10^5$ or $1x10^5$ ZH501 strain of RVFV. $P < 0.01$. All surviving rats were humanely euthanized on day 28.

CHAPTER IV

HOMOLOGY OF THE REGION OF INTEREST ACROSS RELEVANT SPECIES

Introduction

Before embarking on the qPCR and sequencing experiments, a brief further exploration and genomic comparison of the newly defined ROI among pertinent species was conducted. The species considered particularly relevant to this RVF study included *Mus musculus* as a model organism closely related to the rat, *Bos taurus* representing susceptible and at-risk agriculturally important livestock species, and *Homo sapiens* due to the zoonotic nature of the virus.

Materials and Methods

Thorough characterization of the ROI in *Rattus norvegicus* was established using the Rat Genome Database (RGD) v3.4 Assembly [115]. Subsequent investigation of the corresponding ROI in each relevant species was carried out using the genome resources of the National Center for Biotechnology Information (NCBI) [120] and the University of California, Santa Cruz (UCSC) Genome Bioinformatics Site [121]. Assemblies used included GRCm38 for *Mus musculus*, BTAU 4.6.1 for *Bos taurus*, and GRCh37 for *Homo sapiens*.

Results and Discussion

The ROI proved to be fairly well conserved across all four species. The corresponding region of RNO3 mapped to the distal end of mouse chromosome MMU2, to the central area of bovine chromosome BTA13, and to the distal end of human chromosome HSA20 (Fig. 8). Based on RGD, the final ROI in the rat contained 20 genes: Ythdf1, Birc7, Nkain4, Arfgap1, Col20a1, Chrna4, Kcnq2, Eef1a2, Ppdpf, Ptk6, Srms, RGD1564340, Helz2, Gmeb2, Stmn3, Rtel1, Arfrp1, Zgpat, Lime1, and Zbtb46. All of these genes, with the exception of RGD1564340, were present in the corresponding ROI of *Mus musculus* and *Homo sapiens*; furthermore, according to the UCSC Genome Browser, the RGD1564340 sequence matched to the expected position (between genes Srms and Helz2) in each of these two genomes as a Non-Mouse or Non-Human RefSeq Gene, respectively. Meanwhile, the *Bos taurus* ROI contained 13 of the 20 genes, with 6 of the remaining 7 genes similarly matching in sequence on the UCSC Genome Browser to the expected position in the genome as Non-Cow RefSeq Genes. The other gene, Helz2, could not be discovered anywhere in the bovine genome. It was also observed that an inversion event involving the ROI seems to have taken place in the bovine genome relative to the other three, as the gene order of the entire ROI in the cow is reversed compared to that of mouse, human, and rat (Fig. 9). Additionally, the overall size of the ROI was smaller in *Bos taurus*, stretching across ~0.35Mb as compared to the approximate 0.55-0.6Mb length of the region in the other three species. While a few interposing predicted genes and pseudogenes were found in the ROI in each species, the overall consensus of the region was maintained. Thus, the homology of the region

appears strong enough for the results of this rat study to prove useful in other species, both for additional model species and for endangered target species of the RVF virus.

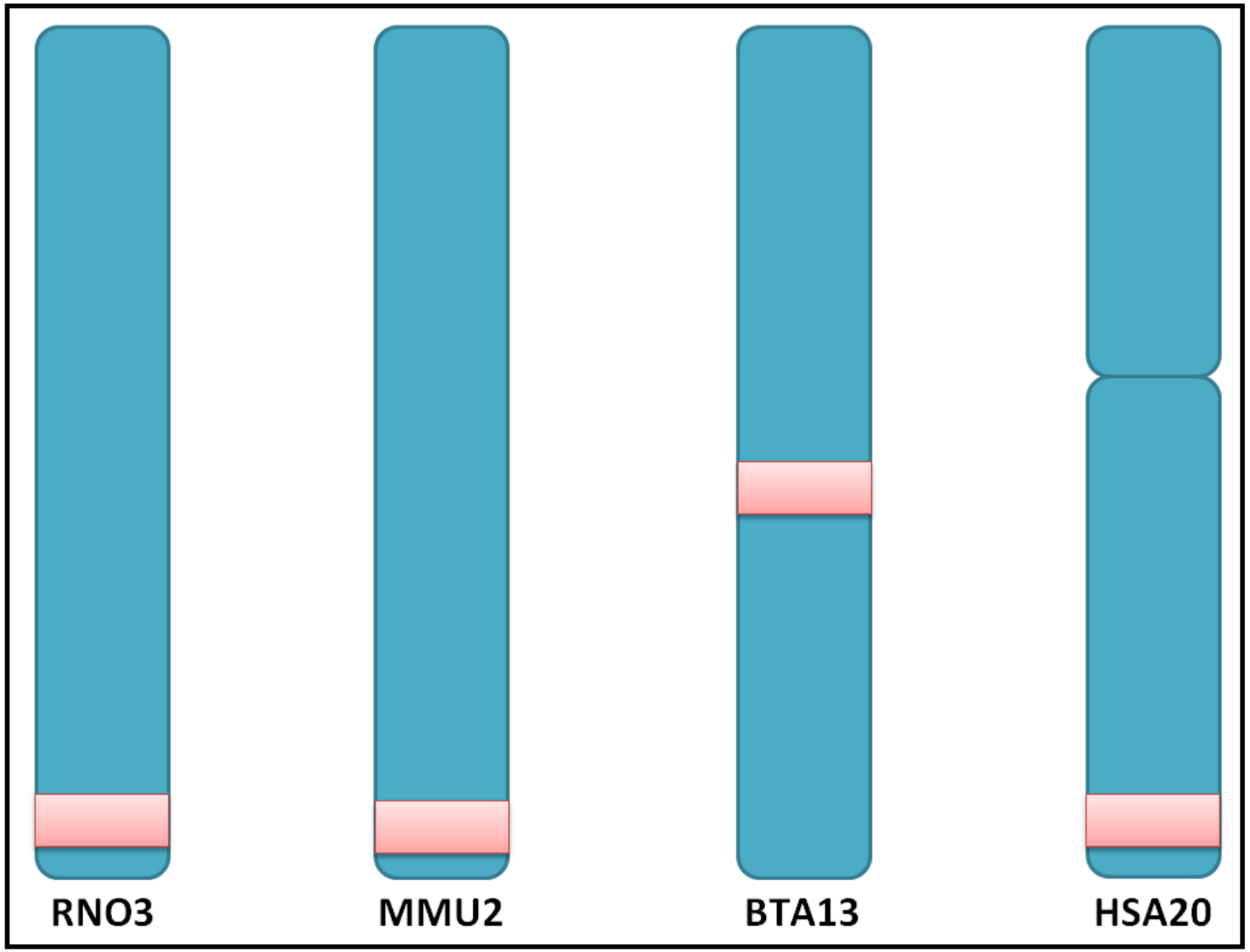

Fig. 8 Relative locations of the homologous ROI among relevant species. Chromosome sizes and region sizes are not to scale.

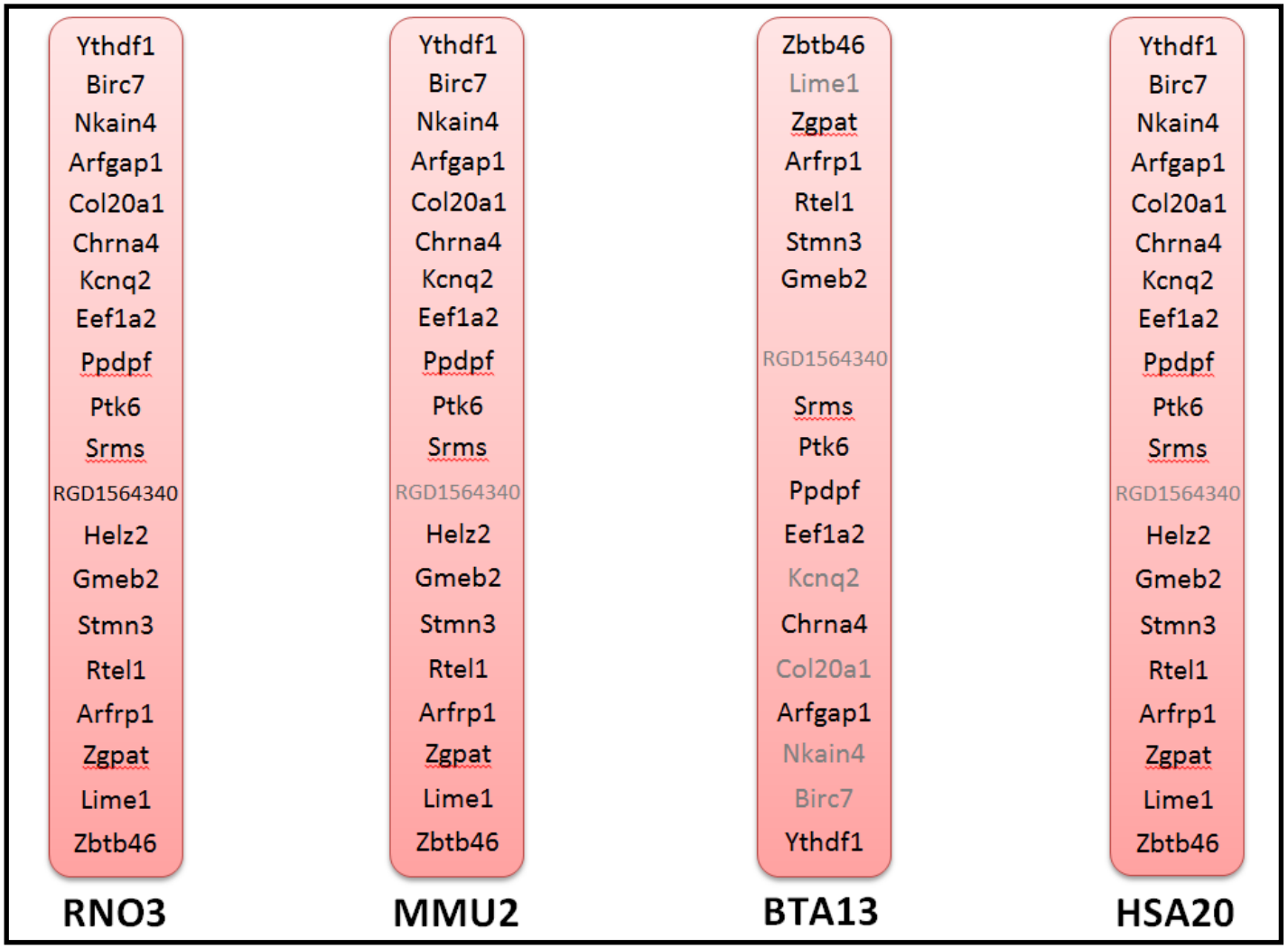

Fig. 9 RNO3 ROI genes present and their arrangement in the corresponding ROI of relevant species. Black type indicates a gene present in the species' genome; gray type indicates the presence of a Non-Species RefSeq Gene on the UCSC Genome Browser. Region sizes are not to scale.

CHAPTER V

ELICITING A PROSPECTIVE GENE AND MECHANISM FOR CONFERRING RESISTANCE TO RVF

Introduction

To further refine this search down to a single proposed responsible gene or mutation, gene expression analysis was carried out by quantitative polymerase chain reaction (qPCR) to examine the relative expression levels of the 20 genes in the ROI between resistant WF.LEW rats and susceptible WF/NHsd rats under varying conditions. Furthermore, in-depth sequencing was performed to compare the resistant WF.LEW strain to the susceptible WF/NHsd substrain at the nucleotide level in the RNO3 ROI and also to search for larger insertion/deletion events, inversions, and copy number variations. The ultimate goal of these experiments was to elucidate a single candidate gene or mutation which, upon further investigation, could provide a possible mechanism of resistance to be confirmed and reproduced through eventual further study.

Materials and Methods

All viral challenge work was carried out in ABSL-4 containment at the University of Texas Medical Branch in Galveston, Texas. In total, 9 resistant WF.LEW rats and 9 susceptible WF/NHsd rats were challenged after 10 weeks of age by subcutaneous inoculation with 0.1ml of $1x10^5$ ZH501 strain of RVFV for infected

animals or with 0.1ml Hank's Balanced Salt Solution (HBSS) diluent for mock-infected animals. Rats were sacrificed and livers harvested at the necessary times and conditions to obtain 3 samples each for the following categories: mock-infected susceptible rats; mock-infected resistant rats; susceptible rats infected for 8hrs; resistant rats infected for 8hrs; susceptible rats infected for 16hrs; and resistant rats infected for 16hrs. All animals were transported and handled in accordance with the guidelines of the Animal Use Protocol (AUP) referenced above.

RNA from rats infected with RVFV was extracted from decontaminated liver tissue using the RNAqueous® Kit (Ambion, Austin, TX) according to the manufacturer instructions. Additionally, RNA was extracted from fresh liver tissue of one each of uninfected WF/NHsd and WF.LEW subjects using the RNeasy® Mini Kit (Qiagen) according to the manufacturer's protocol for "Purification of Total RNA from Animal Tissues" using 30ul of RNase-free water to elute in the final step to maximize final RNA concentration. All RNA samples were treated with the TURBO DNA-*free*™ Kit (Ambion) according to the "Routine DNase Treatment" protocol to eliminate genomic contamination. cDNA synthesis was performed using the SuperScript® III First Strand Synthesis System (Invitrogen, Carlsbad, CA) with oligo(dT) primers according to the manufacturer's instructions. RNA samples were stored at -80ºC, and cDNA samples were stored at -20ºC.

Established TaqMan® Gene Expression Assays (Applied Biosystems) were utilized for the qPCR reactions for the 20 genes in the ROI. Assays used were as

follows: Clone ID Rn00620538_m1 for Ythdf1; Clone ID Rn01412717_g1 for Birc7; Clone ID Rn01754303_m1 for Nkain4; Clone ID Rn00709933_m1 for Arfgap1; Clone ID Rn01415880_m1 for Col20a1; Clone ID Rn00577436_m1 for Chrna4; Clone ID Rn00591249_m1 for Kcnq2; Clone ID Rn00561973_m1 for Eef1a2; Clone ID Rn01416146_g1 for Ppdpf; Clone ID Rn01220413_m1 for Ptk6; Clone ID Rn01754314_m1 for Srms; Clone ID Rn01412535_m1 for RGD1564340; Clone ID Rn01220411_g1 for Helz2; Clone ID Rn00582564_m1 for Gmeb2; Clone ID Rn00456287_m1 for Stmn3; Clone ID Rn01220420_m1 for Rtel1; Clone ID Rn01416050_g1 for Arfrp1; Clone ID Rn01412640_m1 for Zgpat; Clone ID Rn01416098_g1 for Lime1; and Clone ID Rn01220398_m1 for Zbtb46. After analysis of cDNA serial dilutions, a 1:5 dilution was found to be the best across all samples and was subsequently used for all qPCR reactions. Additionally, after preliminary experimentation, ActB (beta-actin) was determined to be a remarkably consistent endogenous control for these experiments and was therefore used for all qPCR runs. Three replicates of each of the 20 samples were tested for each of the 20 genes. 10ul reactions were prepared using 1.0ul template RNA, 0.5ul of the respective TaqMan Gene Expression Assay (20X), 5.0ul TaqMan Gene Expression Master Mix (2X) (Applied Biosystems), and 3.5ul RNase-free water (Qiagen) and were run on the 7900HT Fast Real-Time PCR System (Applied Biosystems) for 40 cycles on standard mode with default settings. Results were exported to a spreadsheet (Excel, Microsoft, Redmond, WA) for analysis. Relative quantitation of qPCR results was performed according to the

$2^{-\Delta\Delta C}{}_T$ method [122] as recommended by Life Technologies (Carlsbad, CA) since their TaqMan assay products meet the assumptions necessary for the appropriate application of the method [123]. Before the three replicates of each individual sample were combined to determine its average ΔC_T, their concordance was examined to identify replicate failures, outliers, or excessive ranges. Individual samples with fewer than two of the three replicates succeeding were considered to have failed and were excluded from the analysis. Average ΔC_T of each successful individual sample, having been normalized to ActB as the endogenous reference, was combined with the other individual samples in its category (uninfected susceptible, uninfected resistant, mock-infected susceptible, mock-infected resistant, 8hr-infected susceptible, 8-hr infected resistant, 16hr-infected susceptible, or 16hr-infected resistant) to obtain a combined average ΔC_T for each category. Before the three separate samples of individuals of one strain were combined for each category, a preliminary check was performed for concurrence of the data across individual samples to ensure no discrepancies or outliers existed and to establish awareness of any inappropriately wide ranges in average ΔC_T values across individual samples. The $\Delta\Delta C_T$ value was calculated using the susceptible WF/NHsd strain as the calibrator, and the resulting $2^{-\Delta\Delta C}{}_T$ value was considered to represent fold change of the resistant strain gene expression as compared to the susceptible strain for each category.

In preparation for sequencing studies, quality of WF.LEW and WF/NHsd genomic DNA previously extracted from rat spleen tissue by phenol extraction with

ethanol precipitation [113] was assessed by a NanoDrop spectrophotometer (Thermo Fisher Scientific, Wilmington, DE) [124] and by gel electrophoresis on a 0.8% agarose gel to determine its suitability for high-throughput genomic sequencing. Qualifying samples were diluted to 50ng/ul using Buffer EB, and accurate concentration was verified using a Qubit® dsDNA BR Assay Kit and a Qubit 2.0 Fluorometer (Invitrogen). 3ug each of WF.LEW and WF.NHsd genomic DNA was submitted to the DNA Core facility of the University of Missouri (Columbia, MO), where sequencing at a minimum depth of 8x coverage was performed on the HiSeq 2000 (Illumina, San Diego, CA). ELAND was used as the alignment algorithm to the rat v5.0 genome (with the Brown Norway (BN/SsNHsdMCW) rat strain as reference), and subsequent SNP, DIP, and CNV detection was performed utilizing CLC Genomics Workbench 5.1 (CLC Bio, Aarhus, Denmark), using stringent parameters to ensure accuracy of the resulting reports.

Results and Discussion: qPCR

The results obtained by qPCR analysis demonstrating determined fold differences in expression of the resistant WF.LEW strain compared to the susceptible WF/NHsd substrain can be seen in Table 3; a label of "Undetermined" indicates that too few replicates or samples succeeded in the qPCR reaction to perform the analysis. Those categories of various genes which showed a twofold or greater increase or decrease in expression in the resistant WF.LEW when compared to the susceptible WF/NHsd were

Table 3 Fold differences in expression of ROI genes in WF.LEW rats as compared to WF/NHsd rats under the conditions of four categories. Expression differences greater than twofold or less than half are highlighted in yellow.

	Uninfected	Mock-infected	8hr	16hr
Ythdf1	2.21209805	0.976390765	0.912556703	0.952286407
Birc7	Undetermined	Undetermined	Undetermined	Undetermined
Nkain4	1.903922824	2.007531094	0.592719507	1.029099714
Arfgap1	1.862742602	1.016163348	0.926155278	1.033185125
Col20a1	1.817068323	0.774492049	1.622360764	0.700592012
Chrna4	Undetermined	2.070657463	0.839517355	1.241481895
Kcnq2	2.180625465	1.467989631	1.050857951	1.04443513
Eef1a2	2.807166559	0.559333702	1.050625051	0.918136426
Ppdpf	1.312620012	1.007890175	0.861313026	1.109024574
Ptk6	Undetermined	0.830787261	Undetermined	1.02532125
Srms	2.019463401	0.526621664	1.61201655	2.982906314
RGD1564340	Undetermined	2.246969824	Undetermined	1.918179118
Helz2	1.410186851	0.979673327	0.84038145	1.372939661
Gmeb2	1.360001271	0.902984072	0.79283909	1.249365368
Stmn3	1.24730994	1.819907202	1.108764266	1.0061281
Rtel1	1.834960491	2.314137269	2.042598522	2.345811175
Arfrp1	1.780930644	0.904472298	0.892017	0.998532453
Zgpat	0.934291081	1.095539962	0.935037343	1.025248366
Lime1	2.117146838	0.932025788	1.040297062	1.052094204
Zbtb46	1.055088001	1.143515651	0.843540489	1.170618964

further examined and are summarized in Fig. 10. Interestingly, the only twofold-or-greater differences in expression were increases in expression of WF.LEW genes over their WF/NHsd counterparts; no underexpression of WF.LEW genes as compared to WF/NHsd genes at this level of significance was observed. Several genes (Ythdf1,

Kcnq2, Eef1a2, and Lime1) presented a fold difference of this magnitude only in uninfected animals; three other genes (Nkain4, Chrna4, and RGD1564340) showed it only in mock-infected specimens. Only two genes, Srms and Rtel1, exhibited a twofold or greater difference in expression in more than one category: Srms in two (both mock-infected and 16-hour infected animals) and Rtel1 in three (mock-infected, 8-hour infected, and 16-hour infected animals.) It should be noted that Kcnq2, Eef1a2, Chrna4, RGD1564340, and Srms for the mock-infected condition were accepted for further consideration with one caveat: that as those particular results had C_T values of around or slightly higher than 35, their reliability was somewhat questionable, as Life Technologies cautions for their TaqMan Gene Expression Assays that such high C_T values approach the sensitivity limits of the qPCR system [123].

One would typically expect a higher basal level of gene expression (i.e., in the "Uninfected" category) to carry through the course of infection, particularly if the gene is connected with or responsible for resistance to the pathogen (provided that resistance is conferred based on expression level and not – or at least not solely – based on sequence, and therefore gene product, differences.) As such, those genes showing a greater-than-twofold difference in expression in the "Uninfected" category only were not considered prime candidates; furthermore, as only one sample of each strain was available for this state, the lack of robustness due to sample size was taken into consideration. Those genes presenting an appreciable difference in expression in the

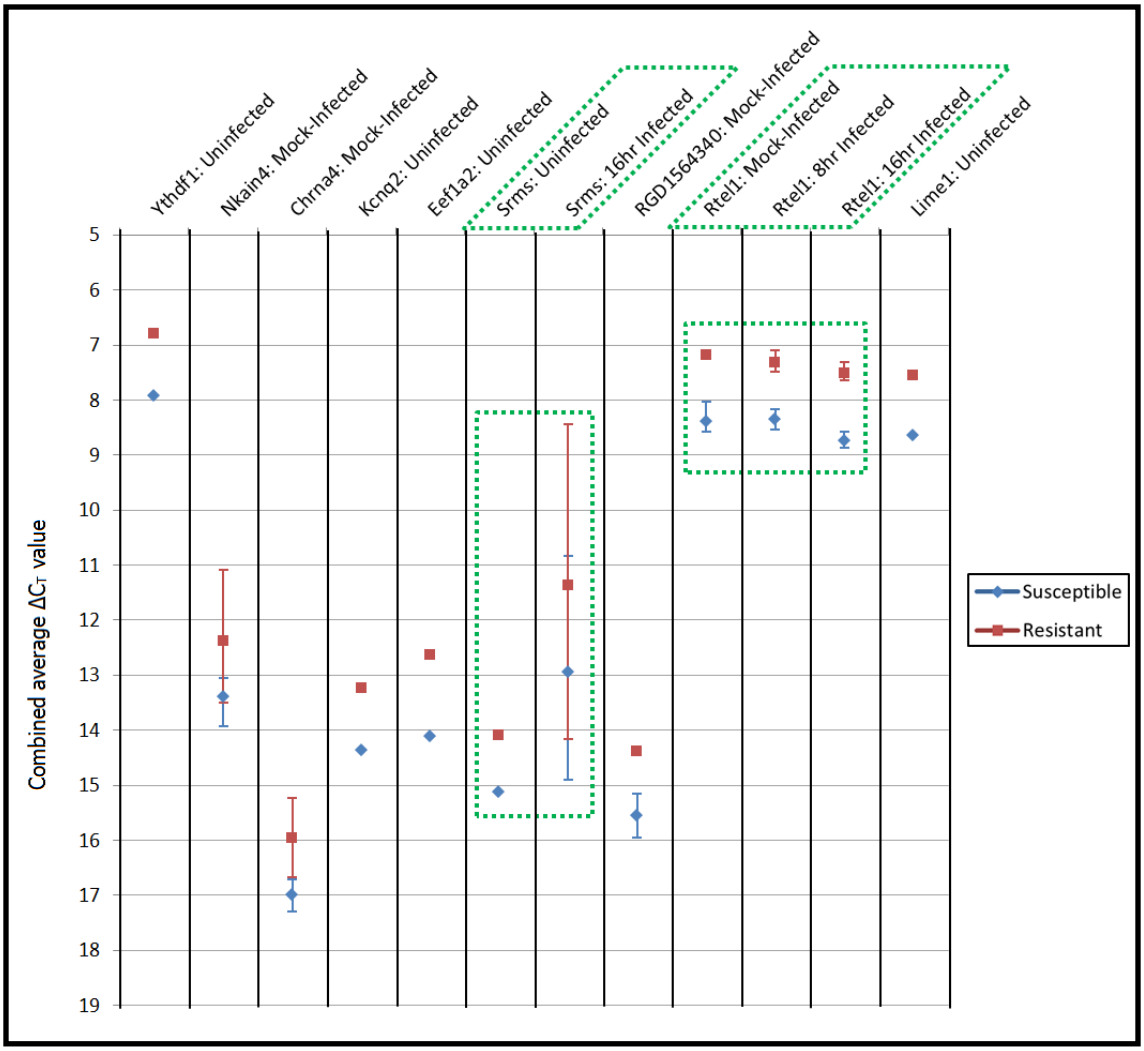

Fig. 10 Graphical representation of combined average ΔC_T values for genes with greater than twofold expression differences of the resistant WF.LEW strain as compared to the susceptible WF/NHsd substrain. "Error bars" represent the range of average ΔC_T values observed in that category for that strain; green boxes associate multiple categories under a single gene.

"Mock-Infected" category only were similarly dubious as one would also expect to observe differences in expression of the gene conferring resistance in the presence of the virus and throughout the course of infection. Furthermore, multiple replicate failures for RGD1564340 and Chrna4 lowered the robustness of those results for that category, and

a closer examination of the wide ranges of the average ΔC_T across the three samples for this condition in Nkain4, Chrna4, and RGD1564340 revealed a notable lack of consistency in results (see Fig. 10.) Results from the "Uninfected" condition for gene Srms suffered the same deficiencies as previously mentioned for that category, but the gene's nearly three-fold increase in WF.LEW expression compared to WF/NHsd expression in the "16-hour Infected" category merited further investigation. However, additional study revealed the seeming contradiction of a nearly twofold decrease in gene expression in mock-infected animals while each of the other conditions showed a rather marked increase, and furthermore, the extreme nature of the inconsistency among the three samples of the same category, particularly in the "16-hour Infected" category which showed the most dramatic fold difference in expression, became apparent. As can be observed in Fig. 10, while the combined average ΔC_Ts of the resistant and susceptible strains for this state may have differed by nearly 1.5 cycles, when it was noted that the range of the average ΔC_Ts among the three samples for the susceptible strain covered nearly 4 cycles and among the three samples for the resistant strain stretched over 5.5 cycles, the excessive overlap of the resistant and susceptible ranges effectively nullified the impact of the purported three-fold difference for this condition.

Thus, the only gene left to consider was the promising Rtel1. With a greater-than-twofold increase in expression in resistant animals in all infected categories and a nearly-twofold increase in resistant expression even in the uninfected category, consistency across all categories was present in the results for this gene. Additionally, the success of all replicates, and thus the presence of all samples in each category for

analysis, preserved the robustness of these results. All C_T values measured were extremely uniform; the C_T values of the three replicates for each sample varied by half a cycle at maximum, and most less than that, and variance in the resulting average ΔC_T among the three samples of each strain for each condition (i.e., for all susceptible mock-infected rats, all resistant mock-infected rats, all susceptible 8hr- or 16hr-infected rats, all resistant 8hr- or 16hr-infected rats, etc.) was minimal, again deviating by half a cycle at most, and with no overlap between the ranges of the resistant and of the susceptible strains. Furthermore, the combined average ΔC_T values were approximately the same (less than half a cycle difference) across all susceptible rats in the mock-infected and infected categories and across all resistant rats in the mock-infected and infected categories. Of additional note was the fact that these highly shared combined average ΔC_T values for the resistant or the susceptible animals, respectively, were approximately one full cycle less (implying a twofold increase in expression according to the $2^{-\Delta\Delta C_T}$ method) from the uninfected animals of their strain, hinting that Rtel1 potentially may be induced by viral infection. Overall, the correlation of the differences between susceptible and resistant animals in combined average ΔC_T values across all three significant categories was striking (see Fig. 10.) Thus, the weak or inconclusive results for the other 19 genes in the ROI only served to emphasize the stark contrast of the clear, consistent, and robust results for gene Rtel1, marking it as a target for additional study.

Results and Discussion: Sequencing

Sequencing results were addressed and analyzed next. In the process, one of the first things observed in the updated v5.0 rat assembly [121] was that three genes originally in the ROI (according to the v3.4 assembly) were missing: Birc7, Col20a1, and Helz2. According to the corresponding mouse and human RefSeq Genes, which were present in the new assembly, the overall gene order was still preserved; however, the homology proved too variable and inexact to predict the beginning and ending of these genes in the rat or the precise location of exons and introns. As such, SNP and DIP variations were mapped only to those 17 genes present in the ROI in the rat v5.0 genome; thus, all SNPs and DIPs which formerly would have been identified as being within Birc7, Col20a1, or Helz2 were instead labeled as being intergenic between the remaining confirmed v5.0 rat genes.

A summary and breakdown of the total variation discovered in the ROI between the resistant WF.LEW and susceptible WF/NHsd strains in the form of SNPs and DIPs can be seen in Fig. 11. Nearly 1000 differences were found in all, the vast majority of which were SNPs; slightly less than half of the variations were found within genes, and most of these were located in introns. As for the non-intronic variations, in total for the entire ~0.5Mb region, 13 5'UTR and 6 3'UTR variations were found along with 19 SNPs in exons, 16 of which were synonymous SNPs (sSNPs) and 3 of which were non-synonymous SNPs (nsSNPs) - two in exon 2 of gene Chrna4 and one in exon 1 of gene Kcnq2. As nsSNPs do not necessarily produce functional or structural consequences, a further examination of these three nsSNPs was conducted utilizing the online program

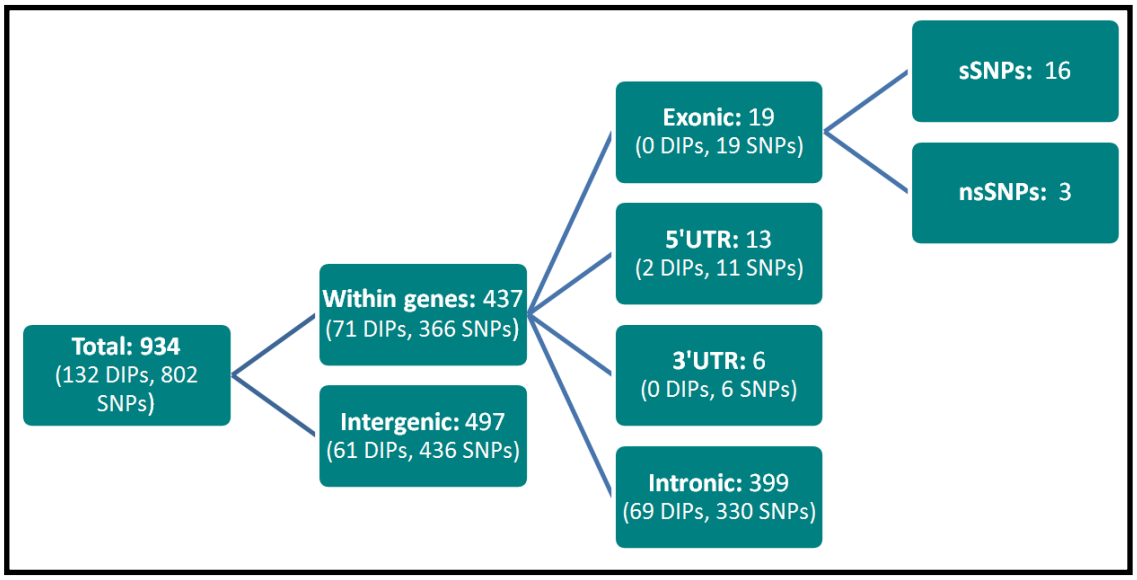

Fig. 11 Breakdown of total variation between WF.LEW and WF/NHsd strains in the ROI discovered by sequencing analysis.

SNAP (Screening for Non-Acceptable Polymorphisms) [125] to predict their effect on protein function. SNAP predicted the single nsSNP in Kcnq2 to be a neutral mutation with a fairly solid reliability index of 7, and while the program predicted the two nsSNPs found in Chrna4 to be non-neutral mutations, the low reliability index of 2 for each of these predictions lessened their impact and encouraged consideration of additional sequence analysis.

A different aspect of the sequencing analysis results is shown in Table 4, breaking down the differences by each gene and intergenic region and identifying the number of each type of variation (SNPs and DIPs) in each category. Additionally, graphical representations by gene of the location (exon, 5'UTR, 3'UTR, intron) and number and type (DIP, SNP, frameshift, non-frameshift, synonymous, non-synonymous)

Table 4 DIPs and SNPs by gene and intergenic region. Each (*) indicates a nsSNP.

Gene	Total Variations	Type	
Ythdf1	19	DIPs	3
		SNPs	16
Intergenic	18	DIPs	2
		SNPs	16
Nkain4	43	DIPs	3
		SNPs	40
Intergenic	16	DIPs	1
		SNPs	15
Arfgap1	24	DIPs	3
		SNPs	21
Intergenic	99	DIPs	15
		SNPs	84
Chrna4	34	DIPs	4
		SNPs	30**
Intergenic	112	DIPs	9
		SNPs	103
Kcnq2	122	DIPs	27
		SNPs	95*
Intergenic	32	DIPs	3
		SNPs	29
Eef1a2	18	DIPs	2
		SNPs	16
Intergenic	72	DIPs	8
		SNPs	64
Ppdpf	5	DIPs	-
		SNPs	5
Intergenic	44	DIPs	7
		SNPs	37
Ptk6	30	DIPs	2
		SNPs	28
Intergenic	10	DIPs	-
		SNPs	10
Srms	10	DIPs	1
		SNPs	9
Intergenic	9	DIPs	-
		SNPs	9

Table 4 Continued.

Gene	Total Variations	Type	
RGD1564340	2	DIPs	-
		SNPs	2
Intergenic	26	DIPs	4
		SNPs	22
Gmeb2	15	DIPs	3
		SNPs	12
Intergenic	28	DIPs	5
		SNPs	23
Stmn3	26	DIPs	5
		SNPs	21
Intergenic	23	DIPs	4
		SNPs	19
Rtel1	40	DIPs	8
		SNPs	32
Intergenic	1	DIPs	-
		SNPs	1
Arfrp1	5	DIPs	1
		SNPs	4
Intergenic	-	DIPs	-
		SNPs	-
Zgpat	21	DIPs	6
		SNPs	15
Intergenic	1	DIPs	-
		SNPs	1
Lime1	1	DIPs	-
		SNPs	1
Intergenic	6	DIPs	3
		SNPs	3
Zbtb46	22	DIPs	3
		SNPs	19

of each variation identified can be found in Appendix C, and Appendix D illustrates the position of each SNP and DIP in the rat v5.0 genome, broken down by gene.

Additional analysis performed on the sequencing data included an examination of differences in read coverage to look for indications of significant CNVs, of which no

prominent or conclusive evidence was found, and an exploration of structural variation between the two strains, which can be seen in Fig. 12. It was noted in this that both strains contained the same approximately 40Kb inversion within the region of 179300000-179400000 on RNO3, slightly outside of the ROI (with the WF/NHsd substrain showing an additional ~36Kb complex variation in the same region) and that each also presented a notable structural variation on the other side of the ROI, within 181000000-181500000 on RNO3 (an ~30Kb inversion in WF.LEW and an ~88Kb complex variation in WF/NHsd) as compared to the reference Brown Norway strain (BN/SsNHsdMCW) used to construct the v5.0 genome. The shared inversion and additional WF/NHsd complex variation above the ROI proved to both be in the intergenic region between genes Edn3 and Ntsr1; meanwhile, the WF.LEW inversion below the ROI contained gene Gata5, and the nearby WF/NHsd complex variation was located in the intergenic region between genes Polr3k and Mrgbp. Further investigation revealed a ~4.5Mb complex rearrangement involving this region at the distal end of RNO3 surrounding the ROI in the v5.0 genome as compared to the v3.4 genome. An illustration of the nature of this rearrangement can be seen in Fig. 13, but while worth noting, the ROI remained intact and did not appear to be clearly affected by this change. However, the structural variation analysis additionally indicated the presence of two noteworthy deletions within the ROI in the WF.LEW strain only: a 776bp intronic deletion within gene Kcnq2 (RNO3 180345935-180346710), and a 406bp intergenic deletion between genes Stmn3 and Rtel1 (RNO3 180529239-180529644). In conjunction with the previously obtained qPCR results, this considerable deletion in the

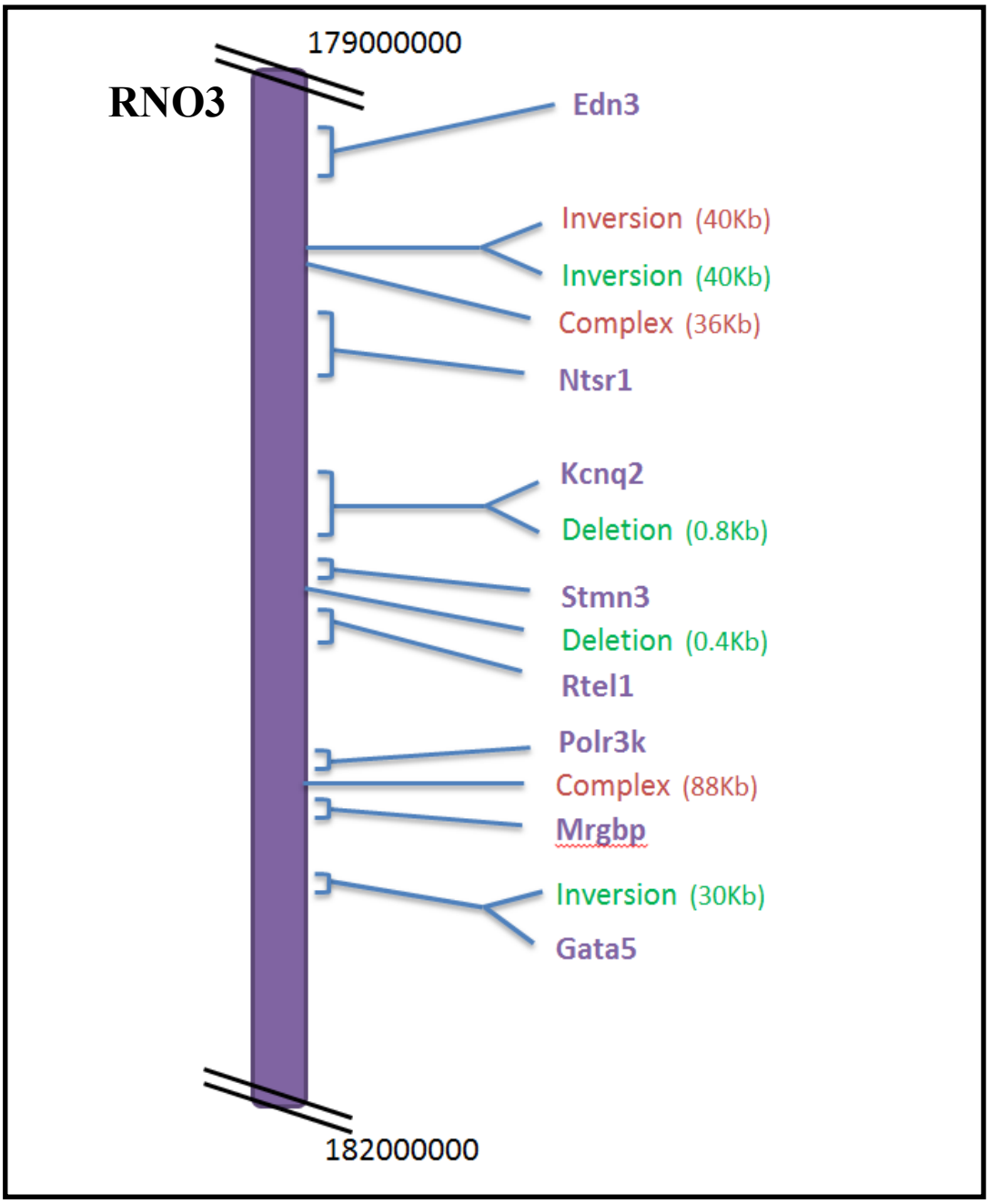

Fig. 12 Representation of relevant genes and structural variations in close proximity to the ROI on RNO3 detected by sequencing analysis of WF/NHsd and WF.LEW. Relative sizes and distances are approximate. Genes are indicated in purple type, WF/NHsd variations in red type, and WF.LEW variations in green type.

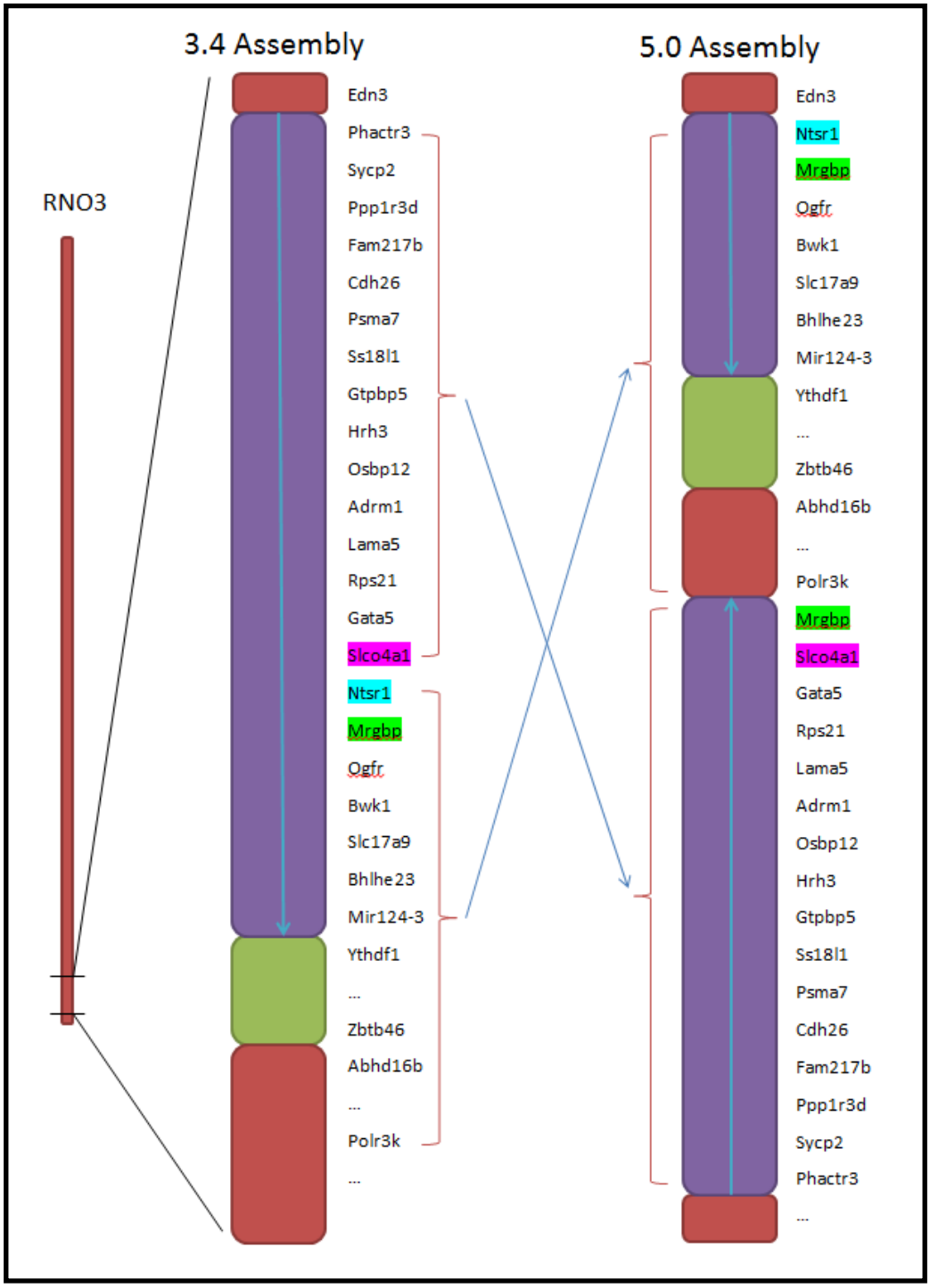

Fig. 13 Chromosomal rearrangement observed in the rat v5.0 assembly as compared to the v3.4 assembly at the distal end of RNO3. The ROI is indicated in green. Figure is not to scale.

vicinity of Rtel1 was particularly intriguing and seemed to merit further investigation.

Rtel1: Investigation and Promoter Search

Further investigation into the region that contained the 406bp deletion, ~2500bp upstream of the beginning of gene Rtel1, was performed in the form of a promoter search. The parameters of this search, which originally encompassed an area extending to approximately 4000bp upstream of the WF.LEW deletion, was eventually expanded to include the entirety of the preceding gene, Stmn3, thus covering an approximately 14,000bp area from RNO3 180518000-180532000. Detection of CpG islands was achieved by use of the online program CpGProD [126], and the online program ProScan was utilized to search for promoters [127]; additionally, masking of repeat regions in the sequence prior to both analyses was performed using the RepeatMasker program [128], as defined in the instructions for the use of CpGProD. Results of this promoter search are summarized in Table 5 and illustrated in Fig. 14. As might be expected, one CpG island was detected by CpGProD and two promoters predicted by ProScan at the beginning of plus-strand gene Rtel1, with the CpG island and one of the two promoters predicted to be on the minus strand. Similarly, one CpG island and one promoter were reported, both on the minus strand, within the first ~1000bp of minus-strand gene Stmn3 and around 10,000bp upstream of the 406bp intergenic deletion. A second minus-strand promoter was indicated in the middle of Stmn3, nearly 7000bp upstream of the deletion. Of further interest were an additional minus-strand CpG island and three additional putative promoters, two on the plus strand and one on the minus strand, reported near the

Table 5 Summary of CpG island and promoter predictions from CpGProD and ProScan, respectively.

Prediction	RNO3 Location	Strand
CpG Island	180518653-180519298	(-)
Promoter	180518854-180519104	(-)
Promoter	180522375-180522625	(-)
Promoter	180525046-180525296	(-)
Promoter	180525190-180525440	(+)
CpG Island	180525519-180526445	(-)
Promoter	180525957-180526207	(+)
CpG Island	180531328-180532972	(-)
Promoter	180531482-180531733	(-)
Promoter	180531554-180531804	(+)

end of Stmn3 and within ~4500bp of the intergenic deletion.

The prediction of promoter regions and a CpG island toward the middle and end of Stmn3 indicates the potential presence of distal regulatory elements, such as enhancers, silencers, insulators, or locus control regions, in this gene. The existence of a Stmn3 enhancer brought into closer proximity to the Rtel1 promoter by the 406bp intergenic deletion is one possible explanation of the increase in Rtel1 expression observed in resistant WF.LEW rats by the qPCR experiments. Enhancers have been proven to exert influence from a distance of several hundred kilobase pairs upstream or downstream of a core promoter and furthermore are orientation-independent elements, rendering the relative location of Rtel1 on the opposite strand from Stmn3 irrelevant to an enhancer's capacity for action [129]. It is also possible that proximity is not the only factor but that the 406bp deletion could also potentially contain an undetected boundary or insulator element which, once eliminated, no longer successfully blocks Stmn3

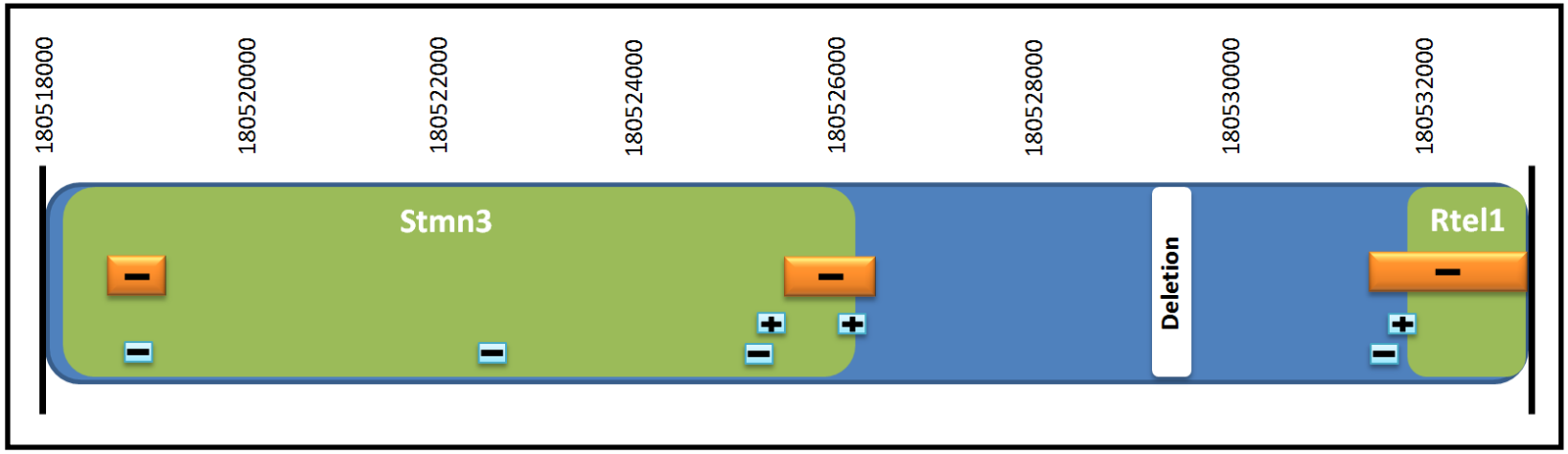

Fig. 14 Depiction of RNO3 chromosomal area involved in promoter search and of investigation results. The underlying chromosome is indicated in dark blue, green covers the area of each gene, the 406bp intergenic deletion is depicted in white, detected CpG islands are orange, and predicted promoters are light blue. Strand orientation of each element is indicated in black.

enhancer action upon the unrelated Rtel1 promoter [130]. Furthermore, by the process of transvection, an active enhancer on one chromosome has the ability, by chromosome pairing, to also affect transcription of the corresponding promoter on the homologous chromosome [131]. If the 406bp intergenic deletion is, in fact, responsible for allowing a Stmn3 enhancer to act upon the Rtel1 promoter and increase Rtel1 expression, then the phenomenon of transvection would further increase this effect. Thus, while it is possible that the observed resistance to RVF shows as a dominant trait because the increase in Rtel1 expression from only one allelic promoter is enough to confer resistance, the potential action of transvection should also be considered. A qPCR comparison of Rtel1 expression in heterozygous F1 rats to homozygous P1 WF.LEW rats and homozygous P1 WF/NHsd rats could demonstrate whether an intermediate level of expression exists, suggesting that only one allelic promoter is being affected, or whether the heterozygous state mimics the homozygous resistant state, implicating the action of transvection. Clearly, additional studies are necessary to confirm these theories and further define the exact mechanism, but the evidence and potential explanations given here support a preliminary conclusion that Rtel1 is likely the gene responsible for conferring resistance to RVF in WF.LEW rats. Whether transvection is occurring or not, the theory of a potential Stmn3 enhancer brought into closer proximity to the Rtel1 promoter and perhaps no longer blocked by an insulator element is a tenable proposal with enough support to merit further investigation in the future.

CHAPTER VI

CONCLUSIONS: CHARACTERIZATION OF FINAL PROPOSED GENE RTEL1 AND ITS POTENTIAL INTERACTIONS AND MECHANISMS

Rtel1

Of the 20 genes in the narrowed ROI of RNO3, Rtel1 is the strongest candidate for providing RVF resistance in WF.LEW rats, based both on qPCR expression data and on sequencing results. The nearly-twofold increase in expression of Rtel1 at a basal level in uninfected WF.LEW rats compared to uninfected WF/NHsd rats, along with the exceptionally consistent greater-than-twofold increase in expression observed in all mock-infected and infected WF.LEW rats compared to mock-infected and infected WF/NHsd rats, is striking and furthermore unparalleled by the qPCR results from any of the other 19 genes. Moreover, the presence of 40 SNPs and DIPs within Rtel1 between the two strains, combined with a noteworthy 406bp deletion in the intergenic region 5' to the gene's starting point in WF.LEW, provides a correlation to and plausible basis for the observed difference in expression. The weight of evidence pointing to Rtel1 thus necessitates an examination of the nature and function of this gene to evaluate its tenability.

The well-conserved Rtel1 gene encodes a helicase involved in regulating telomere elongation. Telomeres consist of DNA repeats at the end of linear chromosomes that function to stabilize and protect the ends of these chromosomes and to support overall genome stability [132]. Among vertebrates, this sequence of

(TTAGGG)n is highly conserved [133]. Interestingly, many DNA viruses also have terminal repeats, and viral-like elements have been suggested as the origins from which cellular telomeres and telomerase evolved [132,134]. This posited evolutionary relationship suggests the possibility of telomeres being potential targets for viruses, and indeed, evidence exists of both DNA and RNA viruses affecting host cell telomeres, including by interacting with host cell telomerase [134,135]. Telomerase itself has proven to be crucial for cell survival, not only by enzymatic activity on telomeric DNA synthesis but also via physical interactions to promote and maintain genome stability in dividing cells [136]. Rtel1 is likewise essential for maintaining telomere length but has similarly also proven itself vital for overall genome stability, with mice deficient in Rtel1 exhibiting not only global telomere loss but additionally chromosome fusions and breaks [137].

A study using mRtel1-deficient mouse ESCs revealed that mRtel1 is not only required for telomere replication of both the leading and lagging strands but is additionally a key protein for DNA replication, homologous recombination, and DNA repair [138]. Human RTEL1, with its non-coding readthrough transcript and also, through alternative splicing, multiple transcript variants encoding different isoforms, has likewise been shown to affect genome stability through its roles in regulating homologous recombination and in repairing DNA double-strand breaks (DSBs) by managing the disassembly of displacement loops (D-loops) [139]. These supplementary capacities of Rtel1 for genome stability and repair are not surprising, as the telomeres with which the helicase is involved as its primarily recognized function resemble fragile

sites, which challenge replication [140]. Telomeres form protective lariat-like structures called telomeric T-loops, which must be resolved before telomere replication can take place [141]. They are also guanine-rich regions, making them capable of forming stable secondary structures, such as G4-DNA [142], that may stall replication forks and possibly cause DNA breaks and loss of telomeric DNA [138]. Recent evidence points to human RTEL1's role in dissociating these T-loops in a similar capacity to its mediatory action on D-loops elsewhere in the genome, and in resolving telomeric G4-DNA structures, reinforcing its importance both specifically at the telomeres and throughout the entire genome [137,143].

Rtel1 has proven not only to mirror telomerase in having function extending beyond merely telomere replication and maintenance but to be necessary itself for the competent action of telomerase on telomeres. In mouse ESCs, mRtel1 was found to localize transiently at the telomeres and furthermore to be required for telomere replication and extension, even when telomerase is present [138]; thus, it appears that telomerase is unable to carry out its main function without the presence of Rtel1 to help facilitate telomere elongation. It is therefore reasonable to theorize that the results of a lack or impairment of Rtel1 should mimic or encompass the detrimental effects of a lack of telomerase, such as those observed in a mouse study by Rudolph et al., 2000. It was found in these experiments that, when subjected to partial hepatectomy (PH) by surgical removal of 2/3 of the liver, mice null for the essential telomerase RNA (mTR) gene ($mTR^{-/-}$), and thus telomerase-deficient, regenerated less liver mass than $mTR^{+/+}$ mice with functional telomerase. Additionally, 3 out of 10 $mTR^{-/-}$ mice died 48-72 hours after

PH, and these exhibited shorter telomeres than the surviving mTR$^{-/-}$ mice. Placed within the context of mitosis, these observations coincide with a regenerative wave of peak S-phase activity at 24-48 hours and maximal mitosis by 72 hours post-PH. Thus, it was concluded that mTR$^{-/-}$ mice are impaired in their cell progression through the mitotic cycle due to the genomic instability resulting from telomere loss, including observed chromosome fusions, the formation of anaphase bridges, and DNA double-strand breaks. This instability interferes with the regeneration process and delays the restoration of liver mass, and it furthermore potentially even triggers DNA damage responses to arrest growth and initiate increased apoptosis [144]. It is of note that the death time window of 48-72 hours post-PH, presumably due to fatally reduced liver competency, observed in the compromised mTR$^{-/-}$ mice in this study is seemingly quite similar in time and cause of death to the time of death at 48-72 hours from terminal liver disease seen in susceptible WF rats infected with RVFV [70, own data]; if Rtel1 is indeed responsible for this RVF resistance, then a lack of sufficient action due to lower gene expression very well might show similar results to those seen from an impairment or lack of telomerase, particularly in fellow rodents. Other studies have similarly linked short telomeres to liver disease and dysfunction, such as liver cirrhosis, even in the absence of any apparent mutation in telomerase [145]. Additionally, studies in humans with cirrhotic livers have found telomere shortening and senescence specifically in hepatocytes, with telomeres consistently short regardless of the age of the patient (age-independent) or of the source of the cirrhosis (disease-independent), including when induced by viral hepatitis, and with hepatocellular senescence restricting the ability of

the injured organ to regenerate [146]. Clearly, even in the absence of a telomerase mutation, shortened telomeres and senescence in hepatocytes resulting from RVF-induced hepatitis could conceivably be responsible for the liver failure and ensuing mortality observed in susceptible WF/NHsd rats, possibly because of a difference in the action of Rtel1 due to lower expression.

In further support of a lack of Rtel1 causing mitotic impairment and potentially cell death, anaphase bridges, which are considered a hallmark of abnormal mitotic events, have similarly been recorded in RTEL1-deficient cells of humans suffering from Hoyeraal-Hreidarsson syndrome (HHS), along with other indicators of genomic instability such as spontaneous DNA damage and telomeric aberrations [147]. HHS, a clinically severe variant of the hereditary disorder dyskeratosis congenita (DC), is characterized by accelerated telomere shortening and dysfunction, which has been proven to occur even in the presence of active telomerase. HHS-causing mutations have been discovered in genes encoding various telomerase subunits and telomere proteins, and more recently, in RTEL1 [148]. Investigation of various RTEL1 mutations resulting in HHS symptoms has reinforced previous evidence of the roles of RTEL1 in enabling telomere elongation by telomerase and in properly resolving T-loops, and has further elucidated its functions in stabilizing telomeres, suppressing the DNA damage response, and repressing inappropriate recombination throughout the genome, emphasizing its action in both telomeric and non-telomeric aspects of cell function; furthermore, it has implicated the impairment or lack of RTEL1 as a cause of severe immunodeficiency (a prominent and serious symptom of HHS) [148,149]. The RTEL1 mutations investigated

in those experiments included compound heterozygous mutations as well as homozygous autosomal recessive mutations, and it must be addressed that while the concluding focus of the current study reported here proposes the work of an enhancer as the probable mechanism of increased Rtel1 expression conferring resistance to RVF by increasing or improving immune system response, it cannot be ruled out, without further study and evidence, that one or even several of the 40 SNPs and DIPs within Rtel1 found to differ between the resistant and susceptible strains could be responsible for or add to the effect, particularly in light of the fact that non-coding SNPs and sSNPs as well as nsSNPs in RTEL1 have a reported association with susceptibility to glioma [150]. Clearly this gene plays a significant role in immune system function, and even slight changes can have a noticeable physiological impact, potentially crippling immune response and increasing susceptibility to disease and dysfunction.

TNFRSF6B

Another potential theory to explain the rescuing action of Rtel1 involves the anti-apoptotic TNFRSF6B decoy receptor gene of the tumor necrosis factor receptor superfamily. This theory connects the gene's genomic location immediately following RTEL1 on chromosome 20 in humans and on the opposite strand overlapping RTEL1 on chromosome 13 in cattle to the significance of tumor necrosis factor alpha (TNF-α) for hepatocytes in particular and for protection against viral hemorrhagic fever (VHF), particularly in the lack of a sufficient IFN response.

TNF-α is a cytokine mainly secreted by macrophages in response to an injury or pathogen; it has the capacity to induce apoptotic cell death and to inhibit viral replication [151]. Macrophages are the primary component of the reticuloendothelial system, and these largely mediate the innate resistance or susceptibility of animals to viral infections due to their functions of monitoring the body, of clearing the bloodstream of viral particles, and of controlling the entry of viruses into target organs, including the liver. Macrophages play an important role in the infection and growth of viruses in the liver, as the virus must pass through a macrophage "barrier" in order to reach hepatic cells [152]. Disease resistance may originate from the relative susceptibility of the macrophages themselves to viral hepatitis, as seen in a study by Bang and Warwick, 1960, in which a genetic difference in susceptibility of two mouse strains to mouse hepatitis was determined to be linked to the survival or destruction of mouse liver macrophages [153]; however, RVFV appears not to directly infect liver macrophages but instead to be taken up by them and then passed on to hepatic cells [152]. It has been acknowledged that macrophages play a significant role in the pathogenesis of RVF viral infection, as enhancing macrophage function by stimulation with glucan prior to infection reduces the pathogenicity of RVFV in mice, increasing their survival rate from 50% to 84% [154]; thus, a different immune function of macrophages, such as their secretion of TNF-α, may be the factor that plays an important part in RVF resistance. Interestingly, in a similar later experiment, pre-glucan-treatment of mice which were subsequently infected with RVFV only delayed death; however, the cause of these deaths was encephalitis rather than hepatitis [72]. As such, it appears that in this case macrophage stimulation

preserved and protected the liver of these rodents but failed to effect clearance of the virus from the bloodstream and thus allowed infection of the brain, mimicking the results observed in the RVFV infection of resistant LEW rats which are protected from hepatic disease but may occasionally succumb to encephalitis [70].

As referenced earlier, a delayed IFN response to RVFV is correlated with mortality in rhesus monkeys [68], suggesting that a prompt immune response is critical in limiting the severity of RVF disease. It is speculated that the RVFV NSs protein must be a potent repressor of IFN type I production early on, perhaps using its inhibition of TFIIH to limit IFN transcription. While this inhibition of general transcription means that viral transcription by the captive host cell is restricted and slowed as well, it appears that this disadvantage in viral growth is worth the benefit of preventing an IFN response [44]. The Ebola virus, another cause of VHF, similarly produces a protein with antagonistic function toward IFN type I (VP35), and for it as well, early immune response has been implicated as the determining factor in the restriction of viral replication and in successful recovery from the disease; however, from observation of asymptomatic Ebola virus infection in human patients, an early and strong cytokine response that included TNF-α effectively controlled viral dissemination and protected against fatality in the absence of a sufficient IFN response [155,156]. Thus, it appears possible for macrophage-produced TNF-α to help provide a successful immune response against VHFs when IFN action is inadequate. This throws into an interesting light previous evidence that female Lewis rats (LEW/N) demonstrate a defect in the production of glucocorticoids, hormones responsible for the immunosuppression of NF-

κB, a transcription factor induced by TNF-α. This lowered glucocorticoid production level would inhibit immunosuppression, resulting in the increase in autoimmune inflammatory diseases such as arthritis observed in the study but also presumably resulting in an increase in antiviral function via this TNF-α-induced pathway in Lewis rats [157].

TNF-α is not only related to VHF survival but to liver function as well. In striking similarity to the critical nature of telomerase for liver regeneration mentioned previously, rats lacking TNF-α action and mice lacking the TNF-R1 receptor likewise demonstrated an inability to recover from partial hepatectomy, showing decreased DNA synthesis, delayed liver restoration, and higher fatality than the respective wild-type [158,159]. Curiously, both the hepatitis B and C viruses induce TNF-α expression in the human liver, and elevated serum levels of TNF-α have been observed in patients exhibiting fulminant hepatitis, with those levels significantly higher in fatal cases than in survivors [160,161]. This possibly implicates TNF-α in initiating or perpetuating liver damage in hepatitis, perhaps related to the cytokine's function of inducing apoptosis, as through this mechanism, TNF-α has proven to be capable of aggravating liver injury. Co-administration of TNF-α with D-galactosamine (GaIN) to inhibit the transcription of hepatocytes and therefore induce liver injury activates apoptosis of mouse hepatocytes, both *in vivo* and *in vitro* [162]. Evidence indicates that the TNF-R1 receptor is involved in this pathway, as TNF-R1 knockout mice are resistant to this treatment; interestingly, TNF-R2 receptor knockout mice are more susceptible than wild-type mice, which can perhaps be explained by the fact that without TNF-R2, more TNF-α is available to bind

to TNF-R1 and induce apoptosis, thus increasing the cytotoxic effect [163,164]. Considering the effects of competitive binding, a decoy receptor that inhibits apoptosis, such as TNFRSF6B, could function in a similar capacity and produce a comparable effect to the presence of competing receptor TNF-R2 in mitigating apoptosis and preventing further liver injury.

Part of the TNF receptor superfamily, the product of gene TNFRSF6B acts as a decoy receptor that competes with death receptors for binding of apoptosis-mediating ligands FasL, LIGHT, and TL1A. This gene thereby plays a role in regulating apoptosis by providing protection against it, which explains why overexpression of this gene has been observed in tumors of various tissues [165]. A readthrough transcript from RTEL1 into TNFRSF6B exists in humans, although this RTEL1-TNFRSF6B transcript generated is non-coding. Currently, no RTEL1-TNFRSF6B readthrough transcript is annotated in the rat v5.0 genome, nor has a mouse or rat gene homologue to TNFRSF6B been identified anywhere in their respective genomes; however, a study of basal macrophages from Wistar-Kyoto rats (WKY/NCrl) and Lewis rats (LEW/Crl), which are susceptible and resistant, respectively, to crescentic glomerulonephritis (CRGN), discovered four differentially expressed, alternatively spliced isoforms of Rtel1 between the two strains [166]. It therefore does not seem unreasonable to assume that currently unannotated transcripts may exist which have yet be identified. (It is additionally interesting to note that, for all four isoforms, Rtel1 expression in the resistant LEW rats was higher than in the susceptible WKY rats.) Fascinatingly, TNFRSF6B gene therapy was demonstrated in mice to be effective in preventing the development of autoimmune

crescentic glomerulonephritis (ACGN), a variant of CRGN, at least partially due to inhibiting apoptosis [167]; thus, there is evidence of the amplified presence of both Rtel1 and TNFRSF6B providing protection from or resistance to disease. Moreover, *in vivo* treatment of a murine model with a TNFRSF6B analogue was discovered to alleviate lung inflammation caused by FasL, further illustrating its potential therapeutic utility; also, TNFRSF6B inhibits FasL-mediated cell death in human hepatocytes *in vitro*, and pre-treatment with TNFRSF6B prevents FasL-produced fatality in mice, ostensibly by attenuating FasL-induced hepatocyte apoptosis [168,169]. Naturally increased TNFRSF6B expression has been observed in human chronic liver disease, which may facilitate liver cell survival through its anti-apoptotic activity [170]. Thus, TNFRSF6B can be beneficial under disease conditions, including particularly to the liver.

While apoptosis of virus-infected hepatocytes can contribute to viral clearance, it can also result in excessive or unnecessary destruction of liver cells once the apoptotic pathway has been activated, leading to liver dysfunction and possible necrosis. For example, during the acute phase of hepatitis B virus (HBV) infection, a significant proportion of hepatocytes are infected and likely replicating the virus; however, widespread apoptosis of these liver cells in an attempt to control viral spread would greatly damage this vital organ of the host. Thus, apoptosis is not universally advantageous for the infected host, making an anti-apoptotic factor such as TNFRSF6B valuable for host survival [151,171]. Both TNF and FasL are implicated in the injury of liver cells, with TNF additionally suspected of potentially directly causing organ failure via a “suicide program” under disease conditions [163,170]. Furthermore, TNF-α can

affect FasL apoptotic activity, as its regulation of FasL-mediated apoptosis has been observed both *in vivo* & *in vitro* in mice, and an *in vitro* study of human eosinophils discovered that TNF-α together with IFN-γ increases expression of the Fas cell surface death receptor (CD95) and thereby increases FasL-induced apoptosis [172,173]. Thus, while macrophage production of TNF-α appears to be capable of helping to compensate for the lack of IFN type I response by itself participating in inducing a sufficient immune response to provide resistance to VHFs similar to RVF, it is possible that an unintended additional effect of this TNF-α production could be increased inducement of apoptosis, particularly in infected hepatocytes, via its influence on FasL, leading to fatal liver necrosis. It is therefore plausible that decoy receptor TNFRSF6B, by competing with death receptors, prevents ensuing liver necrosis due to unrestrained host-immune-system-mediated apoptosis related to TNF, allowing the host to survive hepatic disease while TNF-α induces its cascade, assisting in initiating a successful immune response against RVFV in lieu of proper IFN action. Additional subsequent factors of resistance may include the limitations of transcription via TFIIH due to the inhibitory action of RVFV NSs becoming disadvantageous to the virus by slowing its replication enough for it to be overwhelmed by the TNF-α-induced immune response, and possibly the assistance of the elevated levels of TNF-α in eventual liver regeneration. While the involvement of TNFRSF6B in this pathway would require confirmation, the potential implications of its established location relative to RTEL1 in the human and cattle genomes should not be ignored. The protection that an anti-apoptotic decoy receptor such as TNFRSF6B could conceivably provide to target organs of RVFV, such as the

liver, while macrophage-secreted TNF-α participates in inducing a sufficient early immune response in compensation for deficient IFN action, is an interesting theory of action that demands further attention.

Summary and Conclusions

In light of this current study that identifies Rtel1 as the most likely candidate gene for providing resistance to RVFV, its established role as a regulator of telomere elongation correlates to the postulated evolutionary and proven interactive relationships between viruses and telomeres; moreover, recent evidence clearly shows that it affects several additional processes and is involved in various other pathways. Previous evidence indicating the critical nature of Rtel1 for genome stability, its necessity for the proper functionality of telomerase, its implied effect on principal mitotic events, and its considerable influence on the immune system, all corroborates the acquired data of this study indicating Rtel1 to be the gene of significance conferring resistance to RVFV in WF.LEW rats. Additionally, its potential association with TNFRSF6B, especially in light of the proven effects of TNF-α in connection with the liver and with VHFs and considering the protective aspects of the anti-apoptotic decoy receptor itself, further endorses the candidate gene status of Rtel1. Further exploration and confirmation, through studies such as Rtel1 gene knockdown in resistant WF.LEW rats and the use of targeted excision, via methods such as Cre-Lox recombination, of the purportedly responsible 406bp intergenic deletion in susceptible WF/NHsd rats to mimic the structure of the WF.LEW genomic region, will be necessary to verify these conclusions

and to determine the exact pathway and mechanism by which this resistance is attained, but based on the evidence gathered by this current study, further supported by its known functions and established consequential nature, Rtel1 remains a promising final candidate gene for additional investigation in order to eventually provide a basis for the development of new protective and preventive measures against RVFV in threatened target species.

REFERENCES

[1] R.E. Shope, C.J. Peters, J.S. Walker, Serological relation between Rift Valley fever virus and viruses of phlebotomus fever serogroup, Lancet 315 (1980) 886-887.

[2] World Health Organization, Rift Valley fever: fact sheet no. 207, updated May 2010, accessed May 2015. Available online <http://www.who.int/mediacentre/factsheets/fs207/en/>.

[3] A.I. Dement, Rift Valley Fever, in: Quick Facts about Foreign and Endemic Animal Diseases, FAZD Center, 2008, pp. 75-76.

[4] R. Daubney, J.R. Hudson, P.C. Garnham, Enzootic hepatitis or Rift Valley fever: an undescribed virus disease of sheep, cattle and man from East Africa, J. Pathol. Bacteriol. 34 (1931) 545–579.

[5] R. Daubney, J.R. Hudson, Rift Valley fever, Lancet 219 (1932) 611–612.

[6] J.M. Meegan, The Rift Valley fever epizootic in Egypt 1977-1978: 1. Description of the epizootic and virological studies, Trans. R. Soc. Trop. Med. Hyg. 73 (1979) 618-623.

[7] K.S.E. Abdel-Wahab, L.M. El Baz, E.M. El Tayeb, H. Omar, M.A.M. Ossman, W. Yasin, Rift Valley Fever virus infections in Egypt: pathological and virological findings in man, Trans. R. Soc. Trop. Med. Hyg. 74 (1978) 417-419.

[8] J.D.S. Joubert, A.L. Fergusson, J. Gear, Rift Valley fever in South Africa: 2. The occurence of human cases in the Orange Free State, the North-Western Cape

province, the Western and Southern Transvaal: A. Epidemiological and clinical findings, S. Afr. Med. J. 25 (1951) 890-891.

[9] B.M. McIntosh, D. Russell, I. Dos Santos, J.H.S. Gear, Rift Valley fever in humans in South Africa, S. Afr. Med. J. 58 (1980) 803-806.

[10] F.G. Davies, Observations on the epidemiology of Rift Valley fever in Kenya, J. Hyg. 75 (1975) 219-230.

[11] H.G. Zeller, D. Fontenille, M. Traore-Lamizana, Y. Thiongane, J.P. Digoutte, Enzootic activity of Rift Valley fever virus in Senegal, Am. J. Trop. Med. Hyg. 56 (1997) 265–272.

[12] J.P. Digoutte, C.J. Peters, General aspects of the 1987 Rift Valley fever epidemic in Mauritania, Res. Virol. 140 (1989) 27-30.

[13] T.G. Ksiazek, A. Jouan, J.M. Meegan, B. Le Guenno, M.L. Wilson, C.J. Peters, J.P. Digoutte, M. Guillaud, N.O. Merzoug, E.M. Touray, Rift Valley fever among domestic animals in the recent West African outbreak, Res. Virol. 140 (1989) 67-77.

[14] J.F. Saluzzo, J.P. Digoutte, C. Chartier, D. Martinez, R. Bada, Focus of Rift Valley fever virus transmission in southern Mauritania, Lancet 329 (1987) 504.

[15] A. Jouan, I. Coulibaly, F. Adam, B. Phillippe, O. Riou, B. Leguenno, R. Christie, N.O. Merzoug, T. Ksiazek, J.P. Digoutte, Analytical study of a Rift Valley fever epidemic, Res. Virol. 140 (1989) 175-186.

[16] J. Morvan, P.E. Rollin, S. Laventure, I. Rakotoarivony, J. Roux, Rift Valley fever epizootic in the central highlands of Madagascar, Res. Virol. 143 (1992) 407-415.

[17] Centers for Disease Control and Prevention, Outbreak of Rift Valley fever – Yemen, August-October 2000, Morb. Mort. Wkly. Rep. 49 (2000) 1065-1066. Available online <http://www.cdc.gov/mmwr/preview/mmwrhtml/mm4947a3.htm>.

[18] H.H. Balkhy, Z.A. Memish, Rift Valley fever: an uninvited zoonosis in the Arabian peninsula, Int. J. Antimicrob. Agents 21 (2003) 153-157.

[19] T.A. Madani, Y.Y. Al-Mazrou, M.H. Al-Jeffri, A.A. Mishkhas, A.M. Al-Rabeah, A.M. Turkistani, M.O. Al-Sayed, A.A. Abodahish, A.S. Khan, T.G. Ksiazek, O. Shobokshi, Rift Valley fever epidemic in Saudi Arabia: epidemiological, clinical, and laboratory characteristics, Clin. Infect. Dis. 37 (2003) 1084-1092.

[20] M. Pépin, M. Bouloy, B.H. Bird, A. Kemp, J. Paweska, Rift Valley fever virus (Bunyaviridae: Phlebovirus): an update on pathogenesis, molecular epidemiology, vectors, diagnostics and prevention, Vet. Res. 41 (2010) 61.

[21] Centers for Disease Control and Prevention, Rift Valley fever outbreak – Kenya, November 2006-January 2007, Morb. Mort. Wkly. Rep. 56 (2007) 73-76. Available online <http://www.cdc.gov/mmwr/preview/mmwrhtml/mm5604a3.htm>.

[22] World Health Organization, Global Alert and Response: Rift Valley Fever in South Africa, published Mar. 2010, accessed May 2015. Available online <http://www.who.int/csr/don/2010_03_30a/en/index.html>.

[23] S. Moutailler, G. Krida, F. Schaffner, M. Vazeille, A.B. Failloux, Potential vectors of Rift Valley fever virus in the Mediterranean region, Vector Borne Zoonotic Dis. 8 (2008) 749-754.

[24] T.P. Gargan II, G.G. Clark, D.J. Dohm, M.J. Turell, C.L. Bailey, Vector potential of selected North American mosquito species for Rift Valley fever virus, Am. J. Trop. Med. Hyg. 38 (1988) 440-446.

[25] M.J. Turell, D.J. Dohm, C.N. Mores, L. Terracina, D.L. Wallette, Jr., L.J. Hribar, J.E. Pecor, J.A. Blow, Potential for North American mosquitoes to transmit Rift Valley fever virus, J. Am. Mosq. Control Assoc. 24 (2008) 502-507.

[26] R.F. Breiman, M.K. Njenga, S. Cleaveland, S.K. Sharif, M. Mbabu, L. King, Lessons from the 2006–2007 Rift Valley fever outbreak in East Africa: Implications for prevention of emerging infectious diseases, Future Virol. 3 (2008) 411-417.

[27] V. Martin, V. Chevalier, P. Ceccato, A. Anyamba, L. De Simone, J. Lubroth, S. de La Rocque, J. Domenech, The impact of climate change on the epidemiology and control of Rift Valley fever, Rev. Sci. Tech. Off. Int. Epizoot. 27 (2008) 413-426.

[28] S.C. Weaver, W.K. Reisen, Present and future arboviral threats, Antiviral Res. 85 (2010) 328-345.

[29] D. Pfeiffer, M. Pépin, M. Wooldridge, A. Schudel, M. Pensaert, D. Collins, T. Baldet, G. Davies, A. Kemp, V. Martin, J. Paweska, R. Swanepoel, Y. Thiongane, Opinion of the Scientific Panel on Animal Health and Welfare (AHAW) on a request from the Commission related to "The risk of a Rift Valley Fever incursion and its persistence within the community", EFSA J. 238 (2005) 1-130. Available online <http://www.efsa.europa.eu/en/efsajournal/doc/238.pdf>.

[30] B. Dufour, F. Moutou, A.M. Hattenberger, F. Rodhain, Global change: impact, management, risk approach and health measures – the case of Europe, Rev. Sci. Tech. Off. Int. Epizoot. 27 (2008) 529-550.

[31] V. Chevalier, M. Pépin, L. Plee, R. Lancelot, Rift Valley fever – a threat for Europe? Eurosurveillance 15 (11 Mar. 2010) 4. Available online <http://www.eurosurveillance.org/ViewArticle.aspx?Articleid=19506>.

[32] P. Gale, A. Brouwer, V. Ramnial, L. Kelly, R. Kosmider, A.R. Fooks, E.L. Snary, Assessing the impact of climate change on vector-borne viruses in the EU through the elicitation of expert opinion, Epidemiol. Infect. 138 (2010) 214-225.

[33] R.J. Zabransky, Is Rift Valley fever a threat in the United States?, Clin. Microbiol. Newsl. 27 (2005) 41.

[34] T.R. Kasari, D.A. Carr, T.V. Lynn, J.T. Weaver, Evaluation of pathways for release of Rift Valley fever virus into domestic ruminant livestock, ruminant wildlife, and human populations in the continental United States, J. Am. Vet. Med. Assoc. 232 (2008) 514-529.

[35] D.R. Smith, K.E. Steele, J. Shamblin, A. Honko, J. Johnson, C. Reed, M. Kennedy, J.L. Chapman, L.E. Hensley, The pathogenesis of Rift Valley fever virus in the mouse model, Virol. 407 (2010) 256-267.

[36] R. Muller, O. Poch, M. Delarue, D.H.L. Bishop, M. Bouloy, Rift Valley fever virus L segment: correction of the sequence and possible functional role of newly identified regions conserved in RNA-dependent polymerases, J. Gen. Virol. 75 (1994) 1345-1352.

[37] M.S. Collett, A.F. Purchio, K. Keegan, S. Frazier, W. Hays, D.K. Anderson, M.D. Parker, C. Schmaljohn, J. Schmidt, J.M. Dalrymple, Complete nucleotide sequence of the M RNA segment of Rift Valley fever virus, Virol. 144 (1985) 228-245.

[38] M.S. Collett, Messenger RNA of the M segment RNA of Rift Valley fever virus, Virol. 151 (1986) 151-156.

[39] C. Giorgi, L. Accardi, L. Nicoletti, M.C. Gro, K. Takehara, C. Hilditch, S. Morikawa, D.H.L. Bishop, Sequences and coding strategies of the S RNAs of Toscana and Rift Valley fever viruses compared to those of Punta Toro, Sicilian sandfly fever, and Uukuniemi viruses, Virol. 180 (1991) 738-753.

[40] T. Ikegami, S. Makino, Rift Valley fever vaccines, Vaccine 27 (2009) D69-D72.

[41] S. Won, T. Ikegami, C.J. Peters, S. Makino, NSm protein of Rift Valley fever virus suppresses virus-induced apoptosis, J. Virol. 81 (2007) 13335-13345.

[42] P. Vialat, A. Billecocq, A. Kohl, M. Bouloy, The S segment of Rift Valley Fever Phlebovirus (*Bunyaviridae*) carries determinants for attenuation and virulence in mice, J. Virol. 74 (2000) 1538-1543.

[43] M. Bouloy, C. Janzen, P. Vialat, H. Khun, J. Pavlovic, M. Huerre, O. Haller, Genetic evidence for an interferon-antagonistic function of Rift Valley Fever virus nonstructural protein NSs, J. Virol. 75 (2001) 1371-1377.

[44] A. Billecocq, M. Spiegel, P. Vialat, A. Kohl, F. Weber, M. Bouloy, O. Haller, NSs protein of Rift Valley Fever virus blocks interferon production by inhibiting host gene transcription, J. Virol. 78 (2004) 9798-9806.

[45] M. Bouloy, F. Weber, Molecular biology of Rift Valley Fever virus, Open Virol. 4 (2010) 8-14.

[46] N. Le May, Z. Mansuroglu, P. Leger, T. Josse, G. Blot, A. Billecocq, R. Flick, Y. Jacob, E. Bonnefoy, M. Bouloy, A SAP30 complex inhibits IFN-β expression in Rift Valley Fever virus infected cells, PLoS Pathog. 4 (2008) 134-144.

[47] R. Swanepoel, N.K. Blackburn, Demonstration of nuclear immunofluorescence in Rift Valley fever infected cells, J. Gen. Virol. 34 (1977) 557-561.

[48] J.K. Struthers, R. Swanepoel, Identification of a major non-structural protein in the nuclei of Rift Valley fever virus-infected cells, J. Gen. Virol. 60 (1982) 381-384.

[49] J.K. Struthers, R. Swanepoel, S.P. Shepherd, Protein synthesis in Rift Valley fever virus-infected cells, Virol. 134 (1984) 118-124.

[50] A. Dasgupta, Targeting TFIIH to inhibit host cell transcription by Rift Valley fever virus, Mol. Cell 13 (2004) 456-458.

[51] N. Le May, S. Dubaele, L.P. De Santis, A. Billecocq, M. Bouloy, J. Egly, TFIIH transcription factor, a target for the Rift Valley Hemorrhagic Fever virus, Cell 116 (2004) 541-550.

[52] M. Habjan, A. Pichlmair, R.M. Elliott, A.K. Överby, T. Glatter, M. Gstaiger, G. Superti-Furga, H. Unger, F. Weber, NSs protein of Rift Valley fever virus induces the specific degradation of the double-stranded RNA-dependent protein kinase, J. Virol. 83 (2009) 4365-4375.

[53] T. Ikegami, K. Narayanan, S. Won, W. Kamitani, C.J. Peters, S. Makino, Dual functions of Rift Valley fever virus NSs protein: inhibition of host mRNA transcription and post-transcriptional down-regulation of protein kinase PKR, Ann. N.Y. Acad. Sci. 1171 (2009) E75-E85.

[54] T. Ikegami, K. Narayanan, S. Won, W. Kamitani, C.J. Peters, S. Makino, Rift Valley fever virus NSs protein promotes post-transcriptional downregulation of protein kinase PKR and inhibits eIF2α phosphorylation, PLoS Pathog. 5 (2009) e1000287.

[55] A.J. Sadler, B.R. Williams, Interferon-inducible antiviral effectors, Nat. Rev. Immunol. 8 (2008) 559-568.

[56] Z. Mansuroglu, T. Josse, J. Gilleron, A. Billecocq, P. Leger, M. Bouloy, E. Bonnefoy, Nonstructural NSs protein of Rift Valley Fever virus interacts with

pericentromeric DNA sequences of the host cell, inducing chromosome cohesion and segregation defects, J. Virol. 84 (2010) 928-939.

[57] R. Flick, M. Bouloy, Rift Valley fever virus, Curr. Mol. Med. 5 (2005) 827-834.

[58] G.H. Gerdes, Rift Valley fever, Rev. Sci. Tech. Off. Int. Epizoot. 23 (2004) 613-623.

[59] B.J. Erasmus, J.A. Coetzer, The symptomatology and pathology of Rift Valley fever in domestic animals, Contrib. Epidemiol. Biostatist. 3 (1981) 77-82.

[60] C.J. Peters, C.T. Liu, G.W. Anderson, J.C. Morrill, P.B. Jahrling, Pathogenesis of viral hemorrhagic fevers: Rift Valley Fever and Lassa Fever contrasted, Rev. Infect. Dis. 11 (1989) S743-S749.

[61] J.F. Smith, D.Y. Pifat, Morphogenesis of sandfly fever viruses (Bunyaviridae family), Virol. 121 (1982) 61-81.

[62] G.W. Anderson, Jr., J.F. Smith, Immunoelectron microscopy of Rift Valley fever viral morphogenesis in primary rat hepatocytes, Virol. 161 (1987) 91-100.

[63] K.A. Hubbard, A. Baskerville, J.R. Stephenson, Ability of a mutagenized virus variant to protect young lambs from Rift Valley fever, Am. J. Vet. Res. 52 (1991) 50-55.

[64] J.C. Morrill, G.B. Jennings, H. Caplen, M.J. Turell, A.J. Johnson, C.J. Peters, Pathogenicity and immunogenicity of a mutagen-attenuated Rift Valley fever virus immunogen in pregnant ewes, Am. J. Vet. Res. 48 (1987) 1042-1047.

[65] J.C. Morrill, C.A. Mebus, C.J. Peters, Safety and efficacy of a mutagen-attenuated Rift Valley fever virus vaccine in cattle, Am. J. Vet. Res. 58 (1997) 1104-1109.

[66] J.T. Paweska, E. Mortimer, P.A. Leman, R. Swanepoel, An inhibition enzyme-linked immunosorbent assay for the detection of antibody to Rift Valley fever virus in humans, domestic and wild ruminants, J. Virol. Methods 127 (2005) 10-18.

[67] A. McElroy, C. Albarino, S. Nichol, Development of a RVFV ELISA that can distinguish infected from vaccinated animals, Virol. J. 6 (2009) 125.

[68] J.C. Morrill, G.B. Jennings, A.J. Johnson, T.M. Cosgriff, P.H. Gibbs, C.J. Peters, Pathogenesis of Rift Valley fever in rhesus monkeys: role of interferon response, Arch. Virol. 110 (1990) 195-212.

[69] C.J. Peters, D. Jones, R. Trotter, J. Donaldson, J. White, E. Stephen, T.W. Slone, Jr., Experimental Rift Valley fever in rhesus macaques, Arch. Virol. 99 (1988) 31-44.

[70] G.W. Anderson, Jr., T.W. Slone, C.J. Peters, Pathogenesis of Rift Valley fever virus (RVFV) in inbred rats, Microb. Pathog. 2 (1987) 283-293.

[71] D.G. Bennett, R.D. Glock, P.J. Gerone, Protection of mice and lambs against pantropic Rift Valley fever virus using immune serum, Am. J. Vet. Res. 26 (1965) 57-62.

[72] C.J. Peters, J.A. Reynolds, T.W. Slone, D.E. Jones, E.L. Stephen, Prophylaxis of Rift Valley fever with antiviral drugs, immune serum, an interferon inducer, and a macrophage activator, Antivir. Res. 6 (1986) 285-297.

[73] G.A. Eddy, C.J. Peters, G. Meadors, F.E. Cole, Jr., Rift Valley fever vaccine for humans, Contrib. Epidemiol. Biostatist. 3 (1981) 124-141.

[74] J.C. Morrill, G.B. Jennings, T.M. Cosgriff, P.H. Gibbs, C.J. Peters, Prevention of Rift Valley fever in rhesus monkeys with interferon-α, Rev. Infect. Dis. 2 (1989) S815-S825.

[75] C.J. Peters, G.W. Anderson, Jr., Pathogenesis of Rift Valley fever, Contrib. Epidemiol. Biostatist. 3 (1981) 21-41.

[76] C.J. Peters, T.W. Slone, Inbred rat strains mimic the disparate human response to Rift Valley fever virus infection, J. Med. Virol. 10 (1982) 45-54.

[77] M. Kende, H.W. Lupton, W.L. Rill, H.B. Levy, P.G. Canonico, Enhanced therapeutic efficacy of poly(ICLC) and ribavirin combinations against Rift Valley fever virus infection in mice, Antimicrob. Agents Chemother. 31 (1987) 986-990.

[78] M. Bouloy, C. Janzen, P. Vialat, M. Huerre, J. Pavlovic, O. Haller, High virulence of attenuated Rift Valley fever virus strains in mice lacking a functional type I interferon system, J. Interferon Cytokine Res. 19 (1999) S75.

[79] G.W. Anderson, Jr., C.J. Peters, Viral determinants of virulence for Rift Valley fever (RVF) in rats, Microb. Pathog. 5 (1988) 241-250.

[80] J.A. Rosebrock, C.J. Peters, Cellular resistance to Rift Valley fever virus (RVFV) infection in cultured macrophages and fibroblasts from genetically resistant and susceptible rats, In Vitro 18 (1982) 308.

[81] J.A. Rosebrock, H. Schellekens, C.J. Peters, The effects of ageing *in vitro* and interferon on the resistance of rat macrophages to Rift Valley fever virus, Anat. Rec. 205 (1983) A165-A166.

[82] G.W. Anderson, Jr., Viral and host determinants of resistance to Rift Valley fever in a rat model, Ph.D. dissertation, Johns Hopkins University (1988).

[83] M. Frese, G. Kochs, H. Feldmann, C. Hertkorn, O. Haller, Inhibition of Bunyaviruses, Phleboviruses, and Hantaviruses by human MxA protein, J. Virol. 70 (1996) 915-923.

[84] S. Stertz, J. Dittmann, J.C.G. Blanco, L.M. Pletneva, O. Haller, G. Kochs, The antiviral potential of interferon-induced cotton rat Mx proteins against Orthomyxovirus (influenza), Rhabdovirus, and Bunyavirus, J. Interferon Cytokine Res. 27 (2007) 847-855.

[85] M. Sandrock, M. Frese, O. Haller, G. Kochs, Interferon-induced rat Mx proteins confer resistance to Rift Valley Fever virus and other arthropod-borne viruses, J. Interferon Cytokine Res. 21 (2001) 663-668.

[86] K.J. Linthicum, F.G. Davies, A. Kairo, Rift Valley fever virus (family Bunyaviridae, genus *Phlebovirus*). Isolations from Diptera collected during an inter-epizootic period in Kenya, J. Hyg. 95 (1985) 197-209.

[87] T.P. Gargan II, P.G. Jupp, R.J. Novak, Panveld oviposition sites of floodwater *Aedes* mosquitoes and attempts to detect transovarial transmission of Rift Valley fever virus in South Africa, Med. Vet. Entomol. 2 (1988) 231-236.

[88] K.J. Linthicum, F.G. Davies, C.L. Bailey, A. Kairo, Mosquito species succession in a dambo in an East African forest, Mosq. News 43 (1983) 464-470.

[89] T.M. Logan, K.J. Linthicum, F.G. Davies, Y.S. Binepal, C.R. Roberts, Isolation of Rift Valley fever virus from mosquitoes (Diptera: Culicidae) collected during an outbreak in domestic animals in Kenya, J. Med. Entomol. 28 (1991) 293-295.

[90] D.J.J. Van Velden, J.D. Meyer, J. Olivier, J.H.S. Gear, B. McIntosh, Rift Valley fever affecting humans in South Africa: a clinicopathological study, S. Afr. Med. J. 51 (1977) 867-871.

[91] L.W. Laughlin, J.M. Meegan, L.J. Strausbaugh, D.M. Morens, R.H. Watten, Epidemic Rift Valley fever in Egypt: observations of the spectrum of human illness, Trans. R. Soc. Trop. Med. Hyg. 73 (1979) 630-633.

[92] J.M. Meegan, H. Hoogstraal, M.I. Moussa, An epizootic of Rift Valley fever in Egypt in 1977, Vet. Rec. 105 (1979) 124-125.

[93] J.A.W. Coetzer, J. Musser, S. Burnham, Rift Valley Fever Symptoms, created 2006, accessed May 2015. Available online <http://www.cvm.tamu.edu/FADR/Files/RiftValleyFeverSymptoms.pdf>.

[94] USDA APHIS and CDC, Federal Select Agent Program: Select Agents and Toxins List, updated 2014, accessed May 2015. Available online <http://www.selectagents.gov/SelectAgentsandToxinsList.html>.

[95] Institute for Infectious Animal Diseases, Quick facts about IIAD, accessed May 2015. Available online <http://iiad.tamu.edu/quick-facts-about-fazds-2/>.

[96] H. Caplen, C.J. Peters, D.H.L. Bishop, Mutagen-directed attenuation of Rift Valley fever virus as a method for vaccine development, J. Gen. Virol. 66 (1985) 2271-2277.

[97] R. Muller, J.F. Saluzzo, N. Lopez, T. Dreier, M. Turell, J. Smith, M. Bouloy, Characterization of clone 13, a naturally attenuated avirulent isolate of Rift Valley fever virus, which is altered in the small segment, Am. J. Trop. Med. Hyg. 53 (1995) 405-411.

[98] R. Randall, L.N. Binn, V.R. Harrison, Immunization against Rift Valley fever virus: studies on the immunogenicity of lyophilized, formalin-inactivated vaccine, J. Immunol. 93 (1964) 293-299.

[99] B.J. Barnard, M.J. Botha, An inactivated Rift Valley fever vaccine, J. S. Afr. Vet. Assoc. 48 (1977) 45-48.

[100] J.F. Saluzzo, J.F. Smith, Use of reassortant viruses to map attenuating and temperature-sensitive mutations of the Rift Valley fever virus MP-12 vaccine, Vaccine 8 (1990) 369-375.

[101] A. Baskerville, K.A. Hubbard, J.R. Stephenson, Comparison of the pathogenicity for pregnant sheep of Rift Valley fever virus and a live attenuated vaccine, Res. Vet. Sci. 52 (1992) 302-311.

[102] J.C. Morrill, C.A. Mebus, C.J. Peters, Safety of a mutagen-attenuated Rift Valley fever virus vaccine in fetal and neonatal bovids, Am. J. Vet. Res. 58 (1997) 1110-1114.

[103] J.C. Morrill, C.J. Peters, Pathogenicity and neurovirulence of a mutagen-attenuated Rift Valley fever vaccine in rhesus monkeys, Vaccine 21 (2003) 2994-3002.

[104] P. Hunter, B.J. Erasmus, J.H. Vorster, Teratogenicity of a mutagenised Rift Valley fever virus (MVP 12) in sheep, Onderstepoort J. Vet. Res. 69 (2001) 95-98.

[105] B.H. Bird, T.G. Ksiazek, S.T. Nichol, N.J. Maclachlan, Rift Valley fever virus, J. Am. Vet. Med. Assoc. 234 (2009) 883-893.

[106] G.W. Anderson, T.W. Slone, Jr., C.J. Peters, The gerbil, Meriones unguiculatus, a model for Rift Valley fever viral encephalitis, Arch. Virol. 102 (1988) 187-196.

[107] C. Reed, K.E. Steele, A. Honko, J. Shamblin, L.E. Hensley, D.R. Smith, Ultrastructural study of Rift Valley fever virus in the mouse model, Virol. 431 (2012) 58-70.

[108] G.W. Anderson, Jr., J.A. Rosebrock, A.J. Johnson, G.B. Jennings, C.J. Peters, Infection of inbred rat strains with Rift Valley fever virus: development of a congenic resistant strain and observations on age-dependence of resistance, Am. J. Trop. Med. Hyg. 44 (1991) 475-480.

[109] M. Ritter, M. Bouloy, P. Vialat, C. Janzen, O. Haller, M. Frese, Resistance to Rift Valley fever virus in *Rattus norvegicus*: genetic variability within certain 'inbred' strains, J. Gen. Virol. 81 (2000) 2683-2688.

[110] P. Olofsson, A. Johansson, D. Wedekind, I. Klöting, K. Klinga-Levan, S. Lu, R. Holmdahl, Inconsistent susceptibility to autoimmunity in inbred LEW rats is due to genetic crossbreeding involving segregation of the arthritis-regulating gene *Ncf1*, Genomics 83 (2004) 765-771.

[111] R.J. Callicott, S.T. Ballard, J.E. Womack, Genomic comparison of Lewis and Wistar-Furth rat substrains by use of microsatellite markers, J. Am. Assoc. Lab Anim. Sci. 46 (2007) 25-29.

[112] R.J. Callicott, Characterization and mapping of the gene conferring resistance to Rift Valley Fever Virus hepatic disease in WF.LEW rats, Ph.D. dissertation, Texas A&M University (2008); AAT 3347892. Available online <http://repository.tamu.edu/bitstream/handle/1969.1/ETD-TAMU-2008-12-196/CALLICOTT-DISSERTATION.pdf?sequence=2>.

[113] D. Moore, Phenol extraction and ethanol precipitation of DNA, in: F.M. Ausubel, R. Brent, R.E. Kingston, D.D. Moore, J.G. Seidman, J.A. Smith, K. Struhl (Eds.), Current Protocols in Molecular Biology, John Wiley and Sons, New Jersey, 1996, pp. 2.1.1-2.1.3.

[114] G.E. Truett, P. Heeger, R.L. Mynatt, A.A. Truett, J.A. Walker, M.L. Warman, Preparation of PCR-quality mouse genomic DNA with hot sodium hydroxide and Tris (HotSHOT), BioTechniques 29 (2000) 52-54.

[115] S.J. Laulederkind, G.T. Hayman, S.J. Wang, J.R. Smith, T.F. Lowry, R. Nigam, V. Petri, J. de Pons, M.R. Dwinell, M. Shimoyama, D.H. Munzenmaier, E.A. Worthey, H.J. Jacob, The Rat Genome Database 2013 – data, tools, and users, Brief Bioinform 14 (2013) 520-526, <http://rgd.mcw.edu>.

[116] T. Koressaar, M. Remm, Enhancements and modifications of primer design program Primer3, Bioinformatics 23 (2007) 1289-1291, <http://bioinfo.ut.ee/primer3-0.4.0>.

[117] I. Boutin-Ganache, M. Raposo, M. Raymond, C.F. Deschepper, M13-tailed primers improve the readability and usability of microsatellite analyses performed with two different allele-sizing methods, BioTechniques 31 (2001) 24-28.

[118] M.F. Kramer, D.M. Coen, Enzymatic amplification of DNA by PCR: standard procedures and optimization, in: F.M. Ausubel, R. Brent, R.E. Kingston, D.D. Moore, J.G. Seidman, J.A. Smith, K. Struhl (Eds.), Current Protocols in Molecular Biology, John Wiley and Sons, New Jersey, 1995, pp. 15.1.1-15.1.9.

[119] M.I. Jensen-Seaman, T.S. Furey, B.A. Payseur, Y. Lu, K.M. Roskin, C. Chen, M.A. Thomas, D. Haussler, H.J. Jacob, Comparative recombination rates in the rat, mouse, and human genomes, Genome Res. 14 (2004) 528-538.

[120] National Center for Biotechnology Information - Genome, <http://www.ncbi.nlm.nih.gov/ genome>.

[121] W.J. Kent, C.W. Sugnet, T.S. Furey, K.M. Roskin, T.H. Pringle, A.M. Zahler, D. Haussler, The human genome browser at UCSC, Genome Res 12 (2002) 996-1006, <http://genome.ucsc.edu/index.html>.

[122] K.J. Livak, T.D. Schmittgen, Analysis of relative gene expression data using real-time quantitative PCR and the $2^{-\Delta\Delta C}{}_T$ method, Methods 25 (2001) 402-408.

[123] Life Technologies Corporation, Amplification efficiency of TaqMan® Gene Expression Assays, 2012, <http://www3.appliedbiosystems.com/cms/groups/mcb_marketing/documents/generaldocuments/cms_040377.pdf>.

[124] Thermo Fisher Scientific, Assessment of Nucleic Acid Purity, 2011, <http://www.nanodrop.com/Library/T042-NanoDrop-Spectrophotometers-Nucleic-Acid-Purity-Ratios.pdf>.

[125] Y. Bromberg, B. Rost, SNAP: predict effect of non-synonymous polymorphisms on function, Nucl Acids Res 35 (2007) 3823-3835, <https://www.rostlab.org/services/snap/>.

[126] L. Ponger, D. Mouchiroud, CpGProD: identifying CpG islands associated with transcription start sites in large genomic mammalian sequences, Bioinformatics 18 (2001) 631-633, <http://pbil.univ-lyon1.fr/software/cpgprod.html>.

[127] D.S. Prestridge, Predicting Pol II promoter sequences using transcription factor binding sites, J Mol Biol 249 (1995) 923-932, <http://www-bimas.cit.nih.gov/molbio/proscan/>.

[128] A.F.A. Smit, R. Hubley, P. Green, RepeatMasker Open-3.0, 1996-2010, <http://www.repeatmasker.org/>.

[129] G.A. Maston, S.K. Evans, M.R. Green, Transcriptional regulatory elements in the human genome, Annu Rev Genomics Hum Genet 7 (2006) 29-59.

[130] N.D. Heintzman, B. Ren, Finding distal regulatory elements in the human genome, Curr Opin Genet Dev 19 (2009) 541-549.

[131] E.M. Blackwood, J.T. Kadonaga, Going the distance: a current view of enhancer action, Science 281 (1998) 60-63.

[132] J. Nosek, P. Kosa, L. Tomaska, On the origin of telomeres: a glimpse at the pre-telomerase world, BioEssays 28 (2006) 182-190.

[133] J. Meyne, R. Ratliff, R. Moyzis, Conservation of the human telomere sequence (TTAGGG)n among vertebrates, Proc. Natl. Acad. Sci. USA 86 (1989) 7049-7053.

[134] Z. Deng, Z. Wang, P. Lieberman, Telomeres and viruses: common themes of genome maintenance, Front. Oncol. 2 (2012) 201.

[135] Z. Zhu, A.T. Wilson, K. Gopalakrishna, K.E. Brown, B.A. Luxon, W.N. Schmidt, Hepatitis C virus core protein enhances telomerase activity in Huh7 cells, J. Med. Virol. 82 (2010) 239-248.

[136] Y. Cao, H. Li, S. Deb, J. Liu, TERT regulates cell survival independent of telomerase enzymatic activity, Oncogene 21 (2002) 3130-3138.

[137] H. Ding, M. Schertzer, X. Wu, M. Gertsenstein, S. Selig, M. Kammori, R. Pourvali, S. Poon, I. Vulto, E. Chavez, P.P.L. Tam, A. Nagy, P.M. Lansdorp, Regulation of murine telomere length by Rtel: an essential gene encoding a helicase-like protein, Cell 117 (2004) 873-886.

[138] E. Uringa, K. Lisaingo, H.A. Pickett, J. Brind'Amour, J. Rohde, A. Zelensky, J. Essers, P.M. Lansdorp, RTEL1 contributes to DNA replication and repair and telomere maintenance, Mol. Biol. Cell 23 (2012) 2782-2792.

[139] L.J. Barber, J.L. Youds, J.D. Ward, M.J. McIlwraith, N.J. O'Neil, M.I.R. Petalcorin, J.S. Martin, S.J. Collis, S.B. Cantor, M. Auclair, H. Tissenbaum, S.C. West, A.M. Rose, S.J. Boulton, RTEL1 maintains genomic stability by suppressing homologous recombination, Cell 135 (2008) 261-271.

[140] A. Sfeir, S.T. Kosiyatrakul, D. Hockemeyer, S.L. MacRae, J. Karlseder, C.L. Schildkraut, T. de Lange, Mammalian telomeres resemble fragile sites and require TRF1 for efficient replication, Cell 138 (2009) 90-103.

[141] T. de Lange, T-loops and the origin of telomeres, Nat. Rev. Mol. Cell Biol. 19 (2004) 323-329.

[142] D. Sen, W. Gilbert, Guanine quartet structures, Methods Enzymol. 211 (1992) 191-199.

[143] J.B. Vannier, V. Pavicic-Kaltenbrunner, M.I.R. Petalcorin, H. Ding, S.J. Boulton, RTEL1 dismantles T loops and counteracts telomeric G4-DNA to maintain telomere integrity, Cell 149 (2012) 795-806.

[144] K.L. Rudolph, S. Chang, M. Millard, N. Schreiber-Agus, R.A. DePinho, Inhibition of experimental liver cirrhosis in mice by telomerase gene delivery, Science 287 (2000) 1253-1258.

[145] A. Chavez, A.M. Tsou, F.B. Johnson, Telomeres do the (un)twist: helicase action at chromosome termini, Biochim. Biophys. Acta 1792 (2009) 329-340.

[146] S.U. Wiemann, A. Satyanarayana, M. Tsahuridu, H.L. Tillmann, L. Zender, J. Klempnauer, P. Flemming, S. Franco, M.A. Blasco, M.P. Manns, K.L. Rudolph, Hepatocyte telomere shortening and senescence are general markers of human liver cirrhosis, FASEB J. 16 (2002) 935-942.

[147] T. Le Guen, L. Jullien, F. Touzot, M. Schertzer, L. Gaillard, M. Perderiset, W. Carpentier, P. Nitschke, C. Picard, G. Couillault, J. Soulier, A. Fischer, I. Callebaut, N. Jabado, A. Londono-Vallejo, J. de Villartay, P. Revy, Human RTEL1 deficiency causes Hoyeraal-Hreidarsson syndrome with short telomeres and genome instability, Hum. Mol. Genet. 22 (2013) 3239-3249.

[148] Z. Deng, G. Glousker, A. Molczan, A.J. Fox, N. Lamm, J. Dheekollu, O. Weizman, M. Schertzer, Z. Wang, O. Vladimirova, J. Schug, M. Aker, A. Londono-Vallejo, K.H. Kaestner, P.M. Lieberman, Y. Tzfati, Inherited mutations in the helicase RTEL1 cause telomere dysfunction and Hoyeraal-Hreidarsson syndrome, Proc. Natl. Acad. Sci. U.S.A. 110 (2013) E3408-E3416.

[149] B.J. Ballew, V. Joseph, S. De, G. Sarek, J.B. Vannier, T. Stracker, K.A. Schrader, T.N. Small, R. O'Reilly, C. Manschreck, M.M.H. Fleischut, L. Zhang, J. Sullivan, K. Stratton, M. Yeager, K. Jacobs, N. Giri, B.P. Alter, J. Boland, L. Burdett, K. Offit, S.J. Boulton, S.A. Savage, J.H.J. Petrini, A recessive founder mutation in regulator of telomere elongation helicase 1, RTEL1, underlies severe immunodeficiency and features of Hoyeraal Hreidarsson syndrome, PLoS Genet. 9 (2013) e1003695.

[150] K.M. Egan, R.C. Thompson, L.B. Nabors, J.J. Olson, D.J. Brat, R.V. LaRocca, S. Brem, P.L. Moots, M.H. Madden, J.E. Browning, Y.A. Chen, Cancer susceptibility variants and the risk of adult glioma in a US case-control study, J. Neurooncol. 104 (2011) 535-542.

[151] C.A. Benedict, Viruses and the TNF-related cytokines, an evolving battle, Cytokine Growth Factor Rev. 14 (2003) 349-357.

[152] C.A. Mims, Aspects of the pathogenesis of virus diseases, Bacteriol. Rev. 28 (1964) 30-71.

[153] F.B. Bang, A. Warwick, Mouse macrophages as host cells for the mouse hepatitis virus and the genetic basis of their susceptibility, Proc. Natl. Acad. Sci. 46 (1960) 1065-1075.

[154] J.A. Reynolds, M.D. Kastello, D.G. Harrington, C.L. Crabbs, C.J. Peters, J.V. Jemski, G.H. Scott, N.R. Di Luzio, Glucan-induced enhancement of host resistance to selected infectious diseases, Infect. Immun. 30 (1980) 51-57.

[155] C.F. Basler, X. Wang, E. Muhlberger, V. Volchkov, J. Paragas, H.D. Klenk, A. Garcia-Sastre, P. Palese, The Ebola virus VP35 protein functions as a type I IFN antagonist, Proc. Natl. Acad. Sci. 97 (2000) 12289-12294.

[156] E.M. Leroy, S. Baize, V.E. Volchkov, S.P. Fisher-Hoch, M.C. Georges-Courbot, J. Lansoud-Soukate, M. Capron, P. Debre, J.B. McCormick, A.J. Georges, Human asymptomatic Ebola infection and strong inflammatory response, Lancet 355 (2000) 2210-2215.

[157] E.M. Sternberg, J.M. Hill, G.P. Chrousos, T. Kamilaris, S.J. Listwak, P.W. Gold, R.L. Wilder, Inflammatory mediator-induced hypothalamic-pituitary-adrenal axis activation is defective in streptococcal cell wall arthritis-susceptible Lewis rats, Proc. Natl. Acad. Sci. 86 (1989) 2374-2378.

[158] P. Akerman, P. Cote, S.Q. Yang, C. McClain, S. Nelson, G.J. Bagby, A.M. Diehl, Antibodies to tumor necrosis factor-alpha inhibit liver regeneration after partial hepatectomy, Am. J. Physiol. 263 (1992) G579-G585.

[159] Y. Yamada, I. Kirillova, J.J. Peschon, N. Fausto, Initiation of liver growth by tumor necrosis factor: deficient liver regeneration in mice lacking type I tumor necrosis factor receptor, Proc. Natl. Acad. Sci. 94 (1997) 1441-1446.

[160] Y. Muto, K.T. Nouri-Aria, A. Meager, G.J. Alexander, A.L. Eddleston, R. Williams, Enhanced tumour necrosis factor and interleukin-1 in fulminant hepatic failure, Lancet 332 (1988) 72-74.

[161] G.L.A. Bird, N. Sheron, A.K.J. Goka, G.J. Alexander, R.S. Williams, Increased plasma tumor necrosis factor in severe alcoholic hepatitis, Ann. Intern. Med. 112 (1990) 917-920.

[162] V. Lehmann, M.A. Freudenberg, C. Galanos, Lethal toxicity of lipopolysaccharide and tumor necrosis factor in normal and D-galactosamine-treated mice, J. Exp. Med. 165 (1987) 657-663.

[163] M. Leist, F. Gantner, S. Jilg, A. Wendel, Activation of the 55 kDa TNF receptor is necessary and sufficient for TNF-induced liver failure, hepatocyte apoptosis, and nitrite release, J. Immunol. 154 (1995) 1307-1316.

[164] C.A. Bradham, J. Plumpe, M.P. Manns, D.A. Brenner, C. Trautwein, Mechanisms of hepatic toxicity. I. TNF-induced liver injury, Am. J. Physiol. 275 (1998) G387-G392.

[165] J. Wu, B. Han, TNFRSF6B (tumor necrosis factor receptor superfamily, member 6b, decoy), Atlas Genet. Cytogenet. Oncol. Haematol. Dec. 2007. <http://AtlasGeneticsOncology.org/Genes/TNFRSF6BID42628ch20q13.html>

[166] K. Maratou, J. Behmoaras, C. Fewings, P. Srivastava, Z. D'Souza, J. Smith, L. Game, T. Cook, T. Aitman, Characterization of the macrophage transcriptome in glomerulonephritis-susceptible and -resistant rat strains, Genes Immun. 12 (2011) 78-89.

[167] S.M. Ka, H.K. Sytwu, D.M. Chang, S.L. Hsieh, P.Y. Tsai, A. Chen, Decoy receptor 3 ameliorates an autoimmune crescentic glomerulonephritis model in mice, J. Am. Soc. Nephrol. 18 (2007) 2473-2485.

[168] M.A. Wortinger, J.W. Foley, P. Larocque, D.R. Witcher, M. Lahn, J.A. Jakubowski, A. Glasebrook, H.Y. Song, Fas ligand-induced murine pulmonary inflammation is reduced by a stable decoy receptor 3 analogue, Immunology 110 (2003) 225-233.

[169] K. Connolly, Y.H. Cho, R. Duan, J. Fikes, T. Gregorio, D.W. LaFleur, Z. Okoye, T.W. Salcedo, G. Santiago, S. Ullrich, P. Wei, K. Windle, E. Wong, X.T. Yao, Y.Q. Zhang, G. Zheng, P.A. Moore, In vivo inhibition of Fas ligand-mediated killing by TR6, a Fas ligand decoy receptor, J. Pharmacol. Exp. Ther. 298 (2001) 25-33.

[170] S. Kim, V. Kotoula, P. Hytiroglou, D. Zardavas, L. Zhang, Significance of increased expression of decoy receptor 3 in chronic liver disease, Dig. Liver Dis. 41 (2009) 591-598.

[171] L.G. Guidotti, F.V. Chisari, Noncytolytic control of viral infections by the innate and adaptive immune response, Annu. Rev. Immunol. 19 (2001) 65-91.

[172] B.D. Elzey, T.S. Griffith, J.M. Herndon, R. Barreiro, J. Tschopp, T.A. Ferguson, Regulation of Fas ligand-induced apoptosis by TNF, J. Immunol. 15 (2001) 3049-3056.

[173] W. Luttmann, E. Dauer, S. Schmidt, O. Marx, M. Hossfeld, H. Matthys, J.C. Virchow, Jr., Effects of interferon-gamma and tumour necrosis factor-alpha on CD95/Fas ligand-mediated apoptosis in human blood eosinophils, Scand. J. Immunol. 51 (2000) 54-59.

APPENDIX A

SSLP MARKERS AND SIZES*

Marker	LEW/SsNHsd	LEW/Crl	WF.LEW	LEW/MolTac	WF/NHsd	WF/Crl
RH140313	211	211	211	211	211	211
BI301396	231	231	231	231	231	231
D3Wox1	216	216	218	224	218	220
BF412371	148	148	148	148	148	148
BF401071	220	220	220	220	220	220

*Allele sizes include the additional 19 base pairs of the M13 primer.

APPENDIX B

SNP MARKERS AND ALLELES

Marker	LEW/SsNHsd	LEW/Crl	WF.LEW	LEW/MolTac	WF/NHsd	WF/Crl
rs8149191	T	T	T	T	T	T
rs8164532	A	A	A	G	G	G
rs8154944	A	A	A	G	G	G
rs8163789	A	A	A	G	G	G
rs8168846	G	G	G	G	G	G
rs8152155	G	G	G	G	G	G
rs8156398	C	C	C	T	T	T
rs8164870	T	T	T	T	T	T
rs8166193	G	G	G	G	G	G
rs8146600	T	T	T	T	T	T
rs8145897	C	C	C	C	C	C
rs8167610	G	G	G	A	A	A
rs13457129	C	C	C	G	G	G

APPENDIX C

ROI SNP AND DIP BREAKDOWN BY GENE

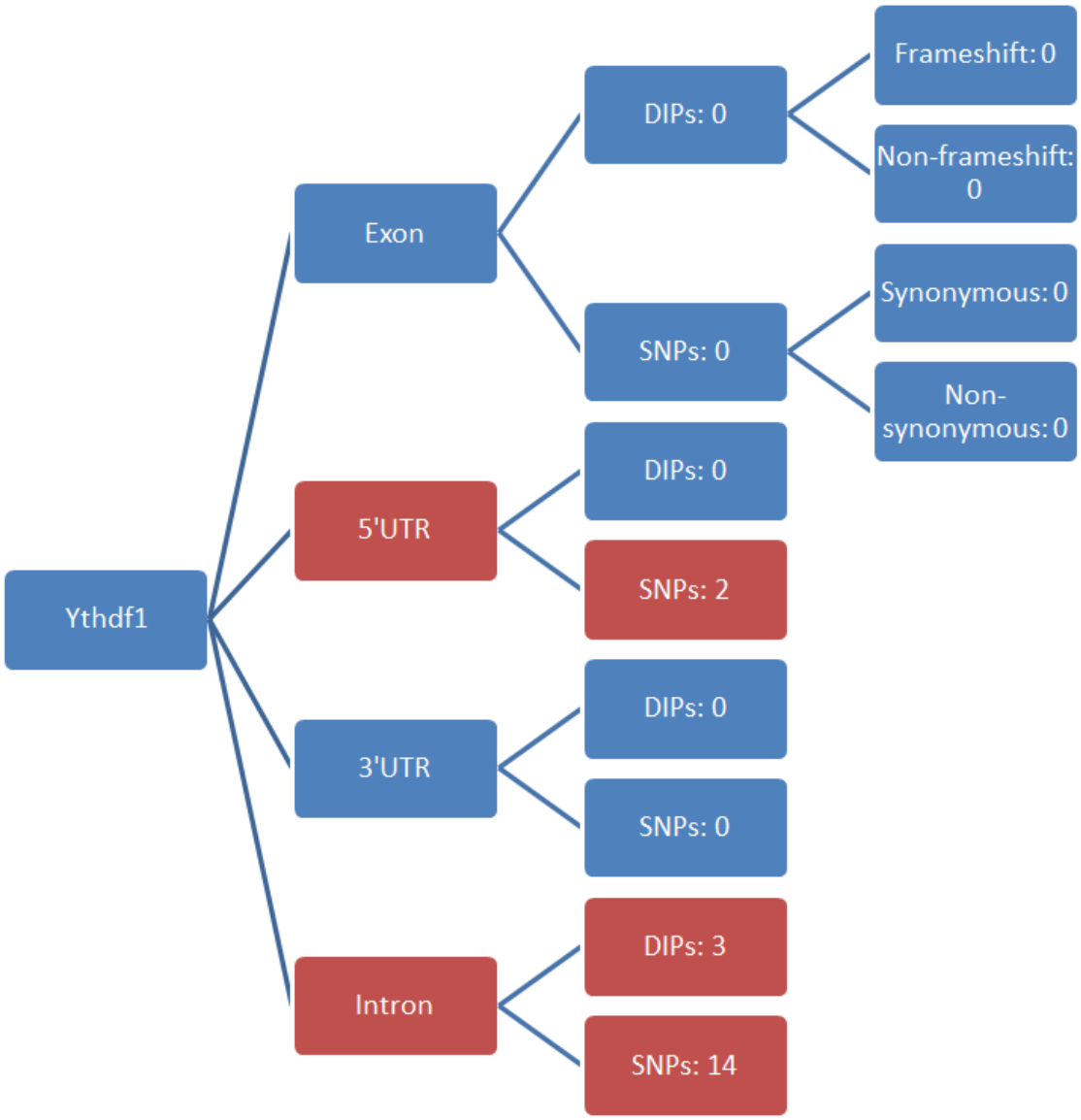

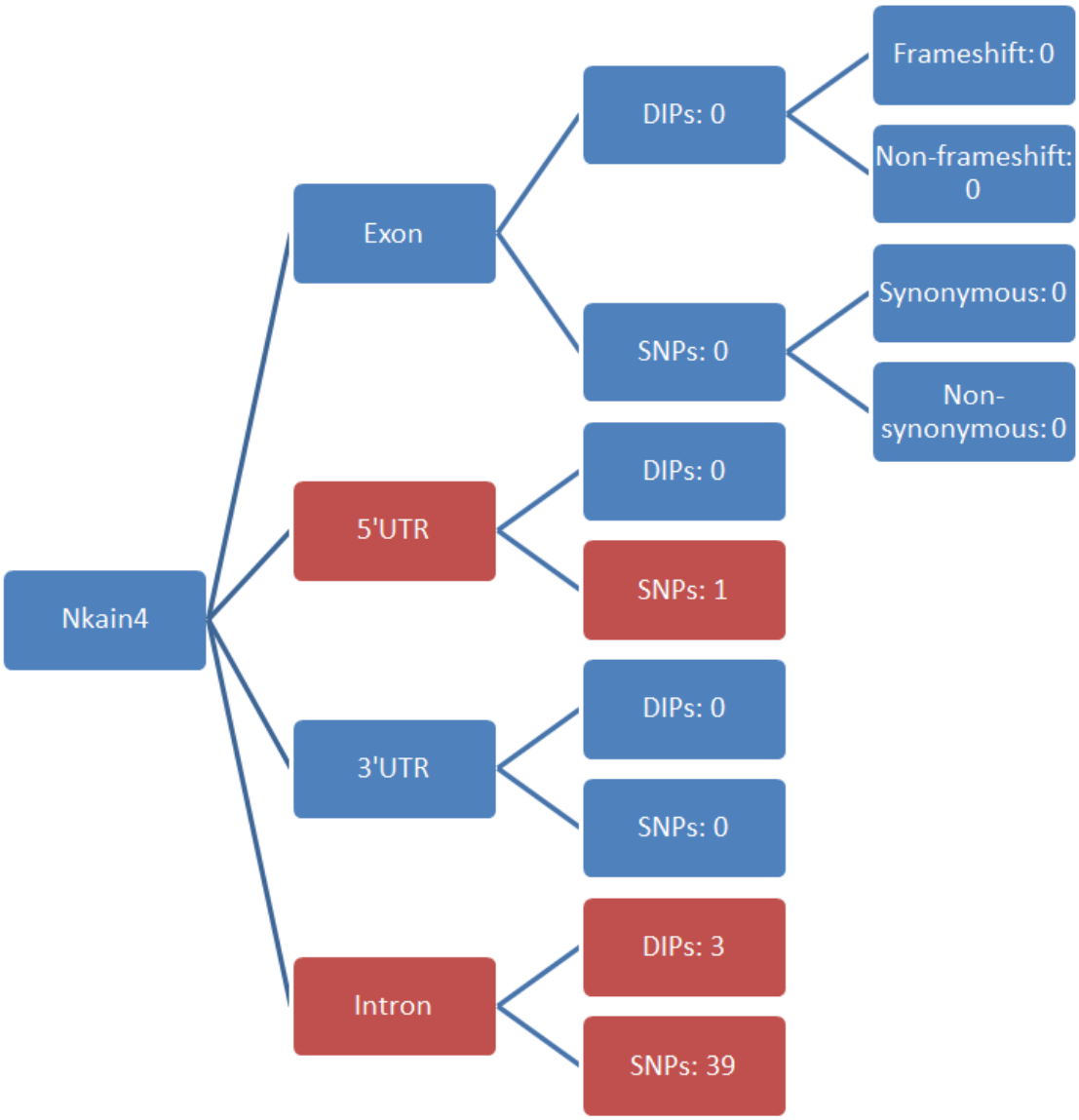
Nkain4
Exon
DIPs: 0
Frameshift: 0
Non-frameshift: 0
SNPs: 0
Synonymous: 0
Non-synonymous: 0
5'UTR
DIPs: 0
SNPs: 1
3'UTR
DIPs: 0
SNPs: 0
Intron
DIPs: 3
SNPs: 39

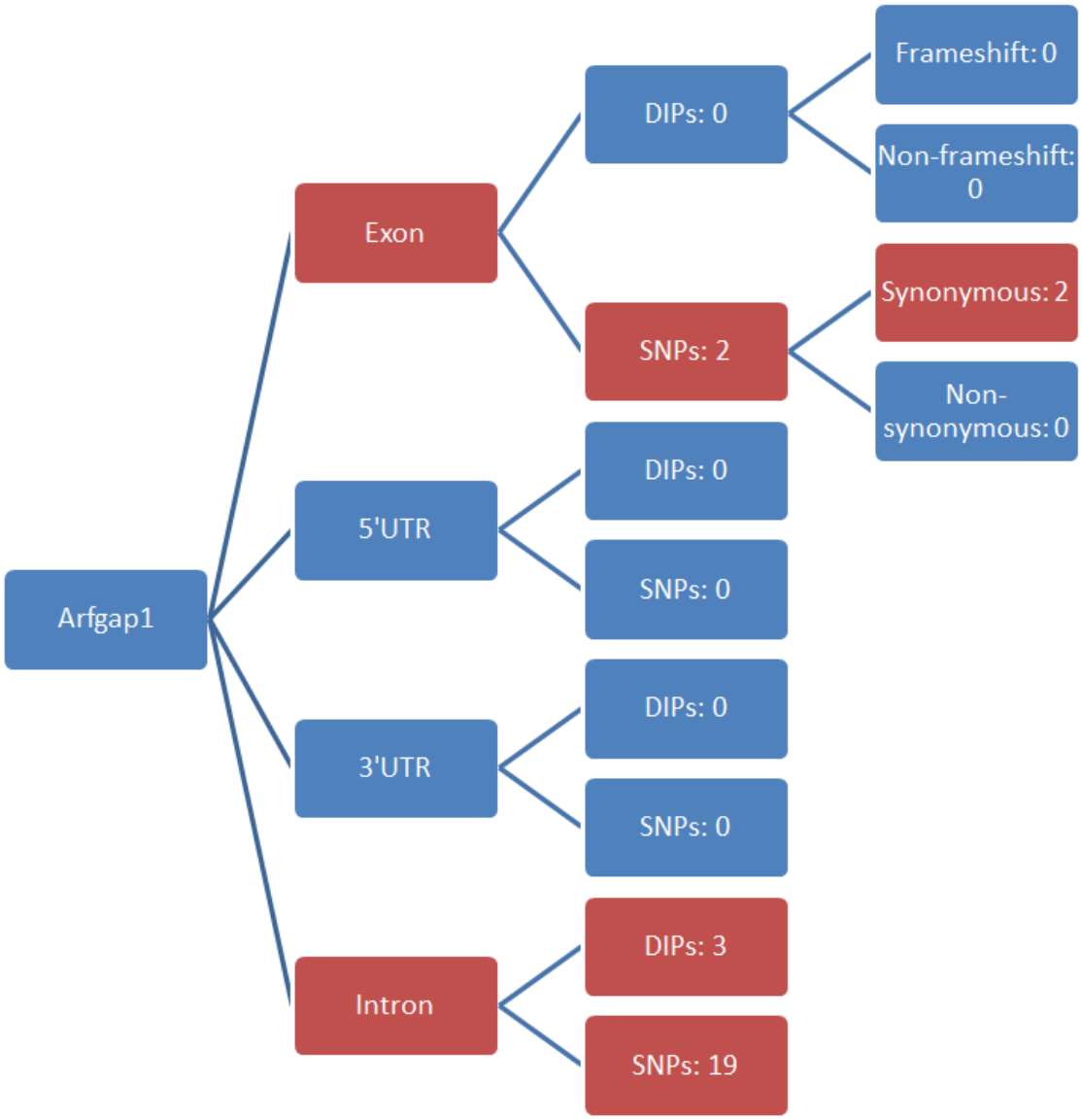
Arfgap1
Exon
DIPs: 0
Frameshift: 0
Non-frameshift: 0
SNPs: 2
Synonymous: 2
Non-synonymous: 0
5'UTR
DIPs: 0
SNPs: 0
3'UTR
DIPs: 0
SNPs: 0
Intron
DIPs: 3
SNPs: 19

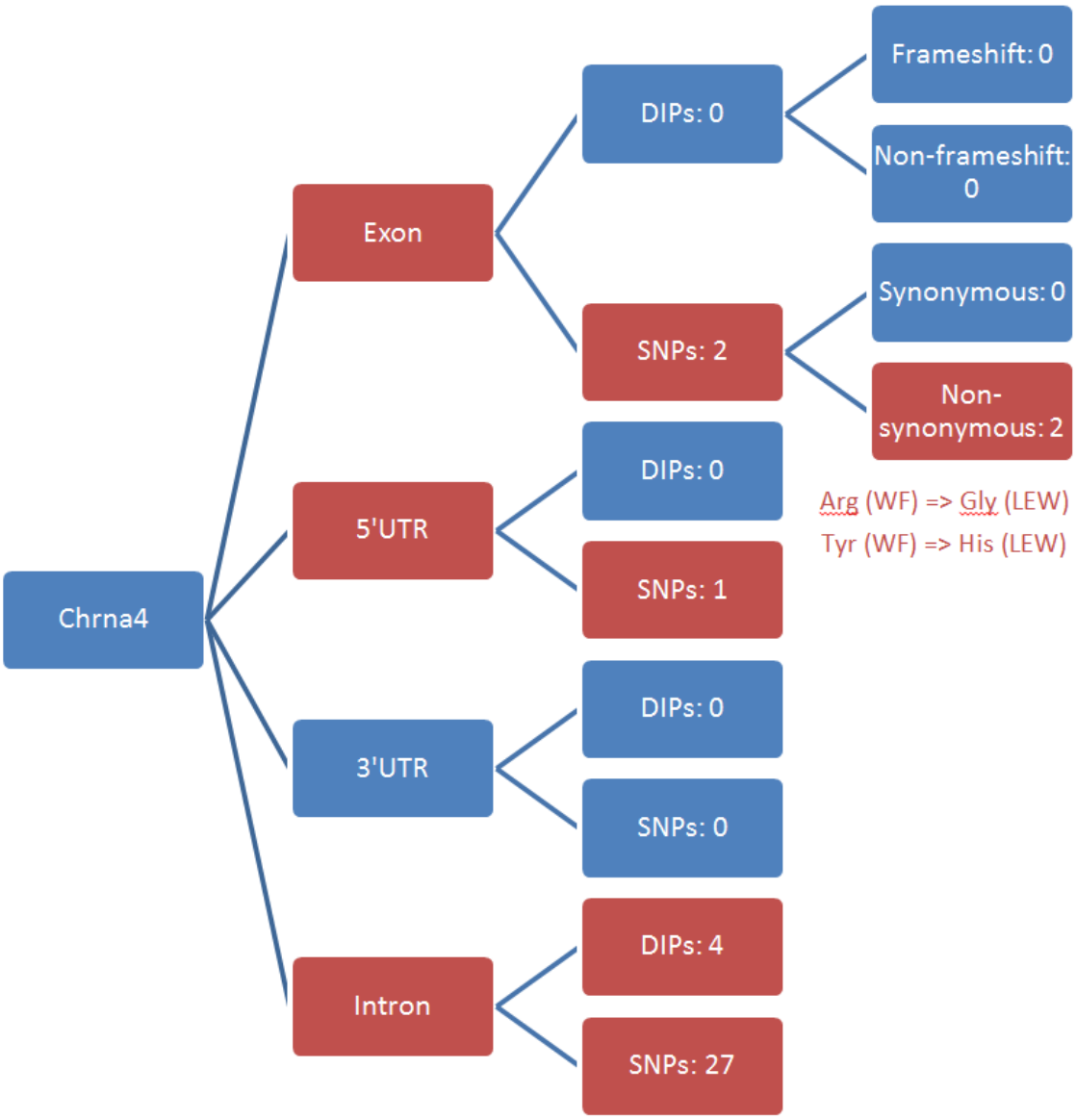
Chrna4
Exon
DIPs: 0
Frameshift: 0
Non-frameshift: 0
SNPs: 2
Synonymous: 0
Non-synonymous: 2
Arg (WF) => Gly (LEW)
Tyr (WF) => His (LEW)
5'UTR
DIPs: 0
SNPs: 1
3'UTR
DIPs: 0
SNPs: 0
Intron
DIPs: 4
SNPs: 27

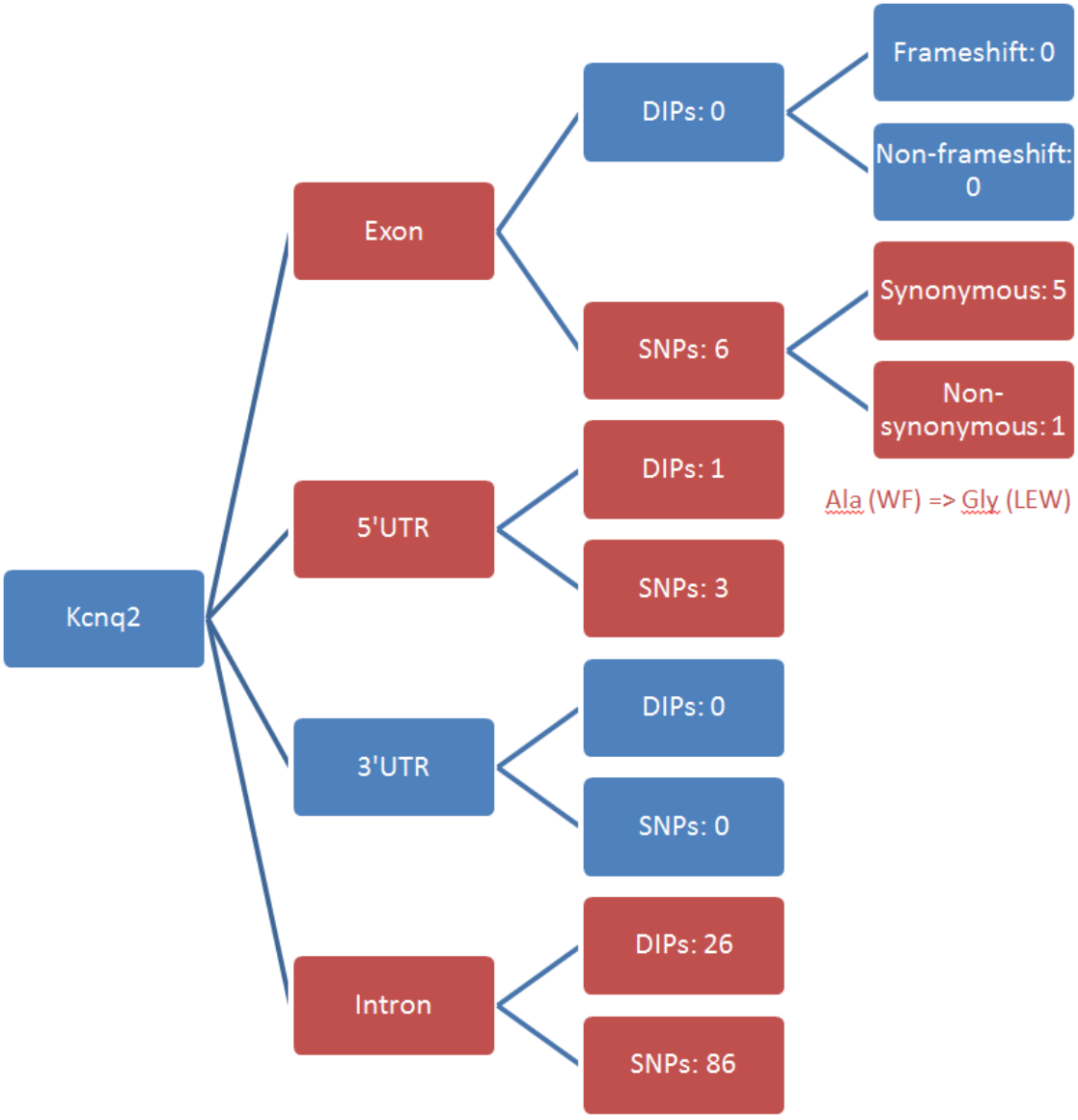
Kcnq2
Exon
5'UTR
3'UTR
Intron
DIPs: 0
SNPs: 6
DIPs: 1
SNPs: 3
DIPs: 0
SNPs: 0
DIPs: 26
SNPs: 86
Frameshift: 0
Non-frameshift: 0
Synonymous: 5
Non-synonymous: 1
Ala (WF) => Gly (LEW)

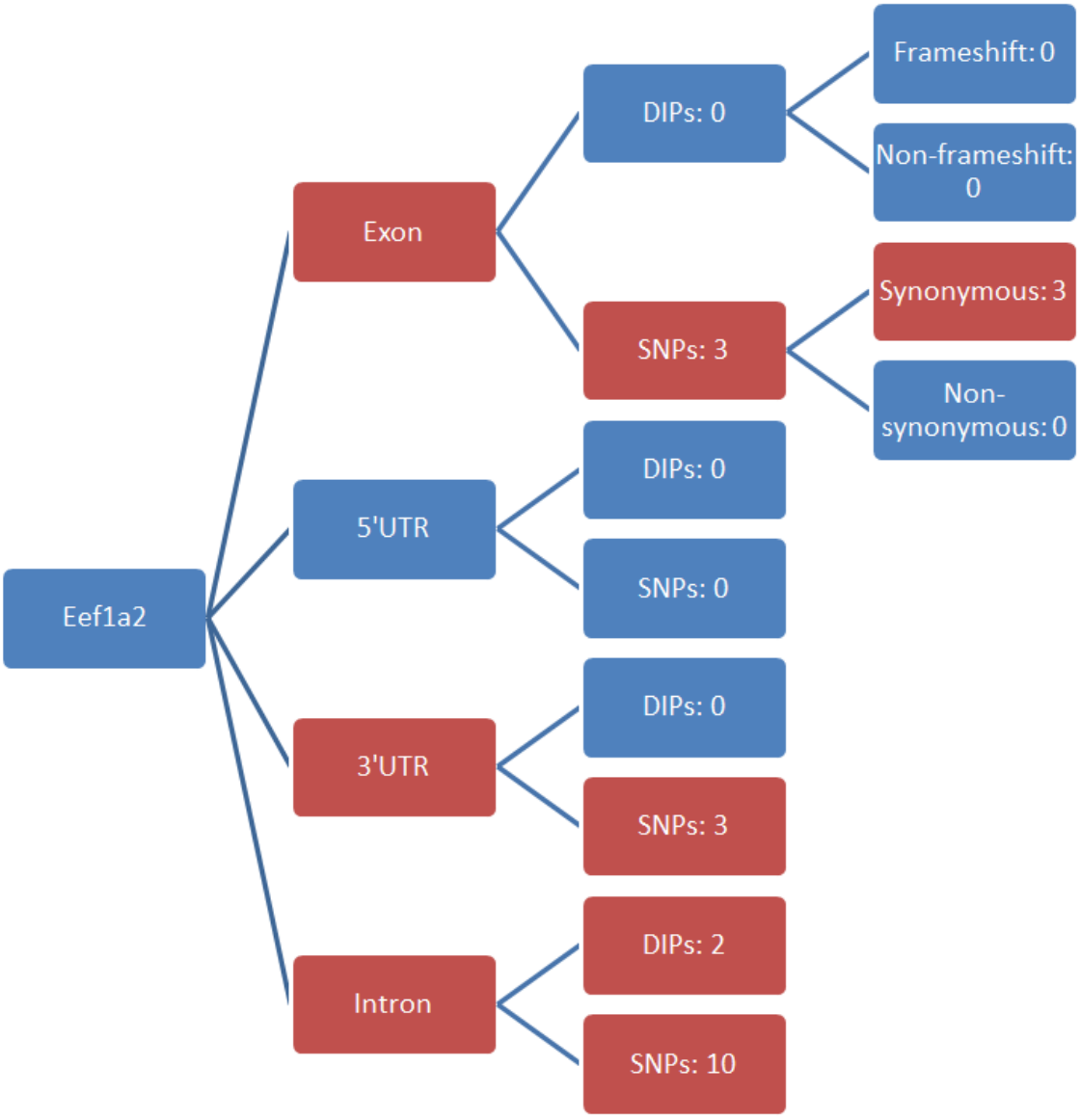
Eef1a2
Exon
DIPs: 0
Frameshift: 0
Non-frameshift: 0
SNPs: 3
Synonymous: 3
Non-synonymous: 0
5'UTR
DIPs: 0
SNPs: 0
3'UTR
DIPs: 0
SNPs: 3
Intron
DIPs: 2
SNPs: 10

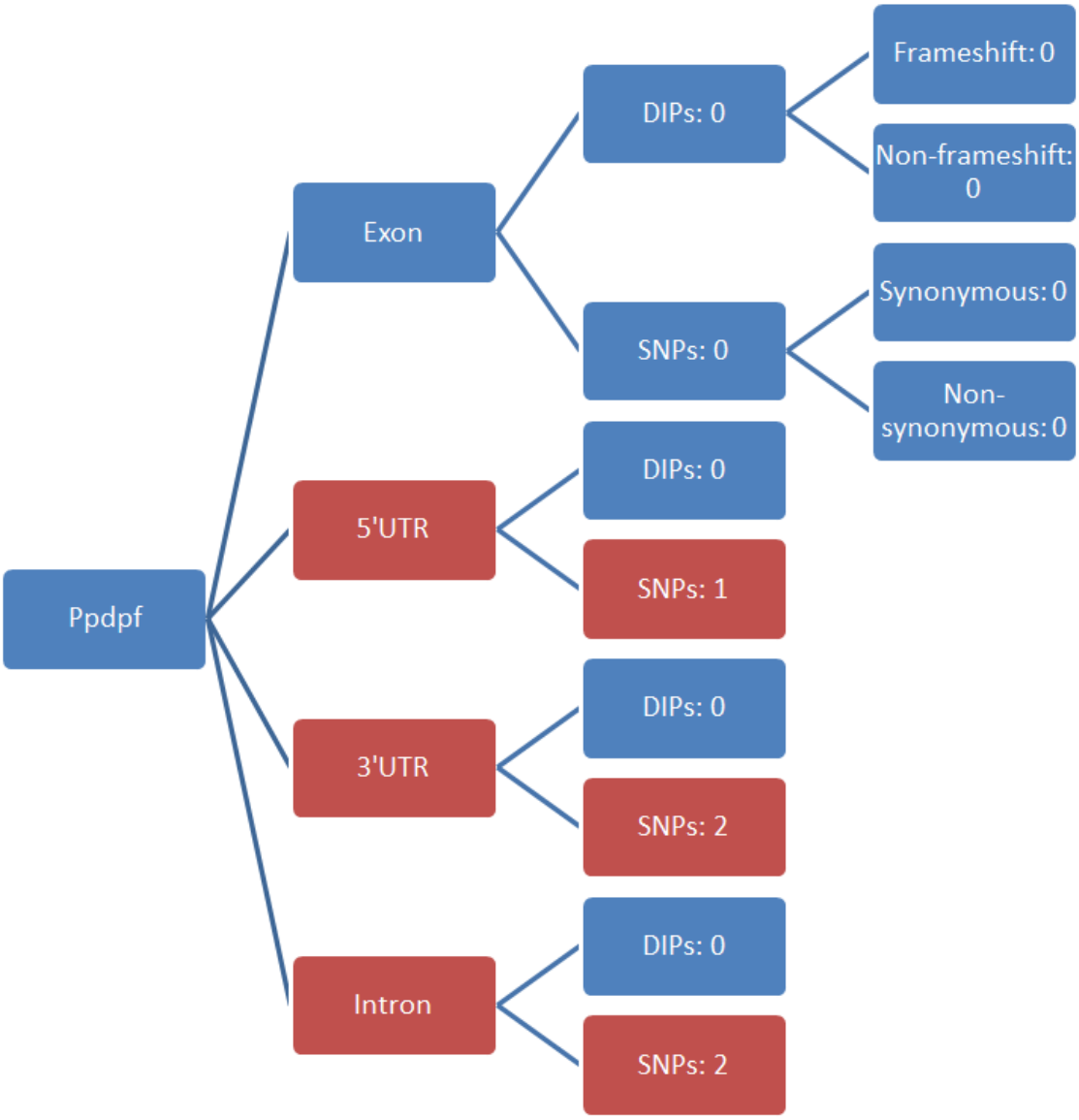
Ppdpf
Exon
DIPs: 0
Frameshift: 0
Non-frameshift: 0
SNPs: 0
Synonymous: 0
Non-synonymous: 0
5'UTR
DIPs: 0
SNPs: 1
3'UTR
DIPs: 0
SNPs: 2
Intron
DIPs: 0
SNPs: 2

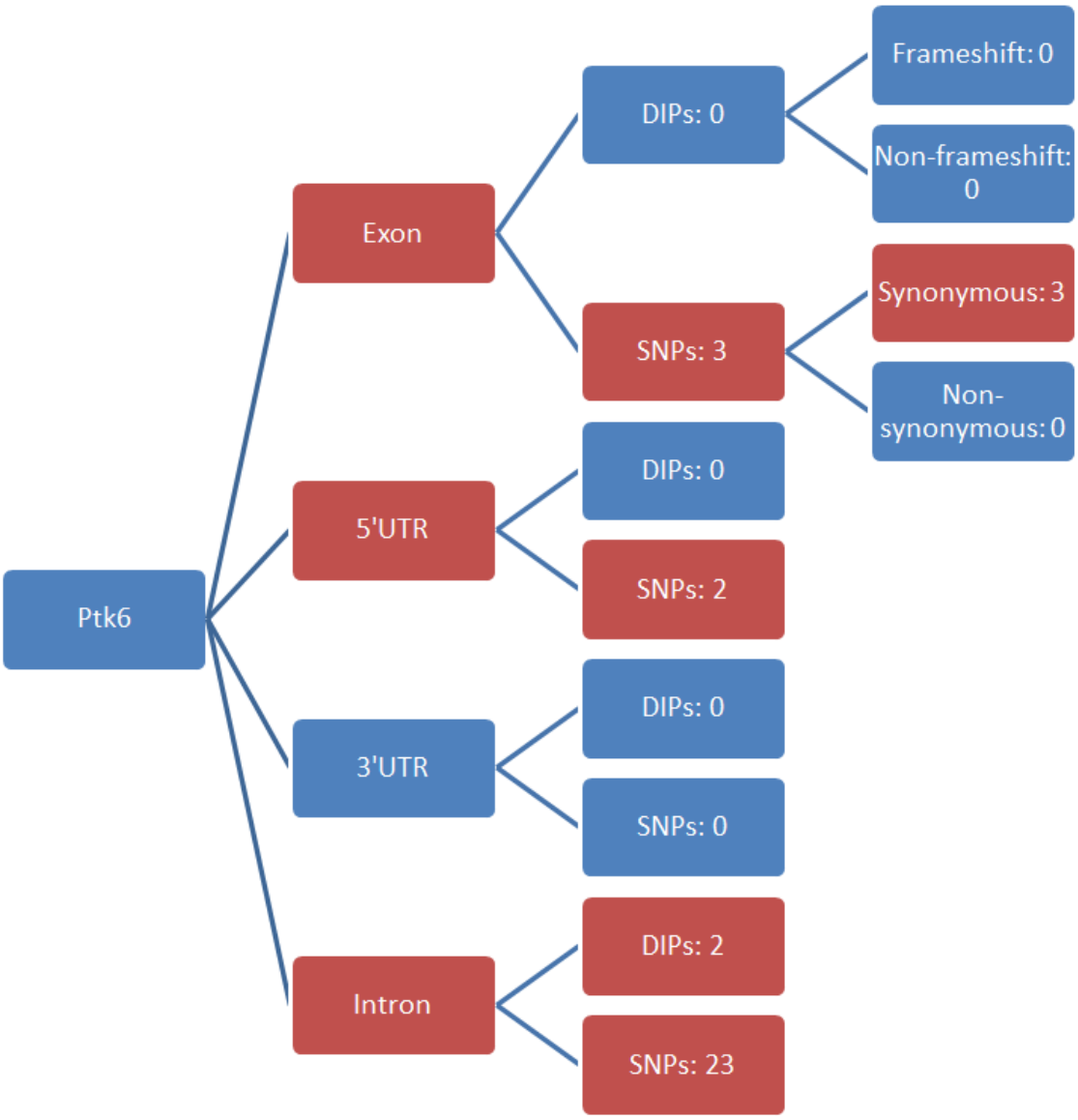
Ptk6
Exon
DIPs: 0
Frameshift: 0
Non-frameshift: 0
SNPs: 3
Synonymous: 3
Non-synonymous: 0
5'UTR
DIPs: 0
SNPs: 2
3'UTR
DIPs: 0
SNPs: 0
Intron
DIPs: 2
SNPs: 23

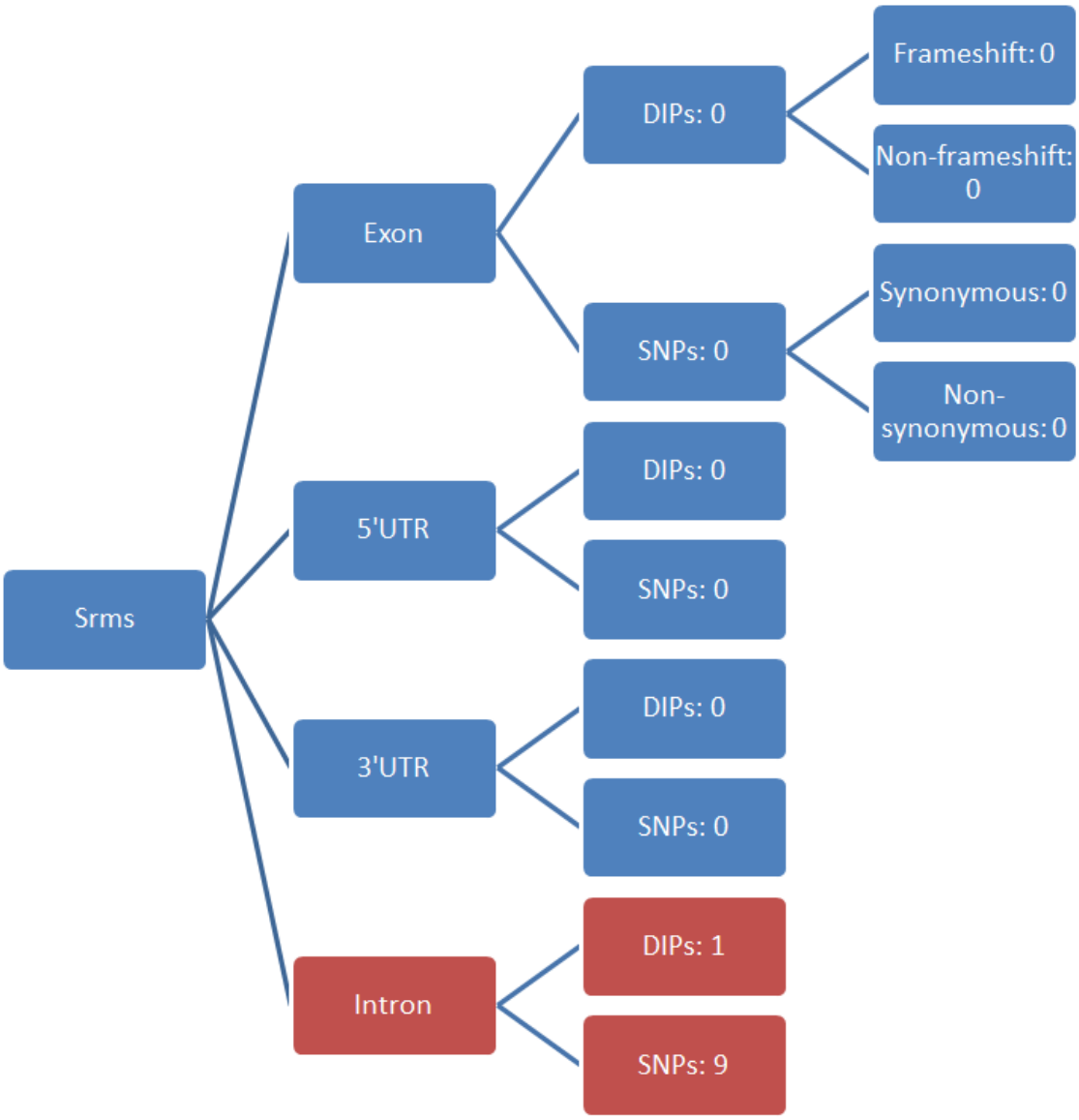
Srms
Exon
DIPs: 0
Frameshift: 0
Non-frameshift: 0
SNPs: 0
Synonymous: 0
Non-synonymous: 0
5'UTR
DIPs: 0
SNPs: 0
3'UTR
DIPs: 0
SNPs: 0
Intron
DIPs: 1
SNPs: 9

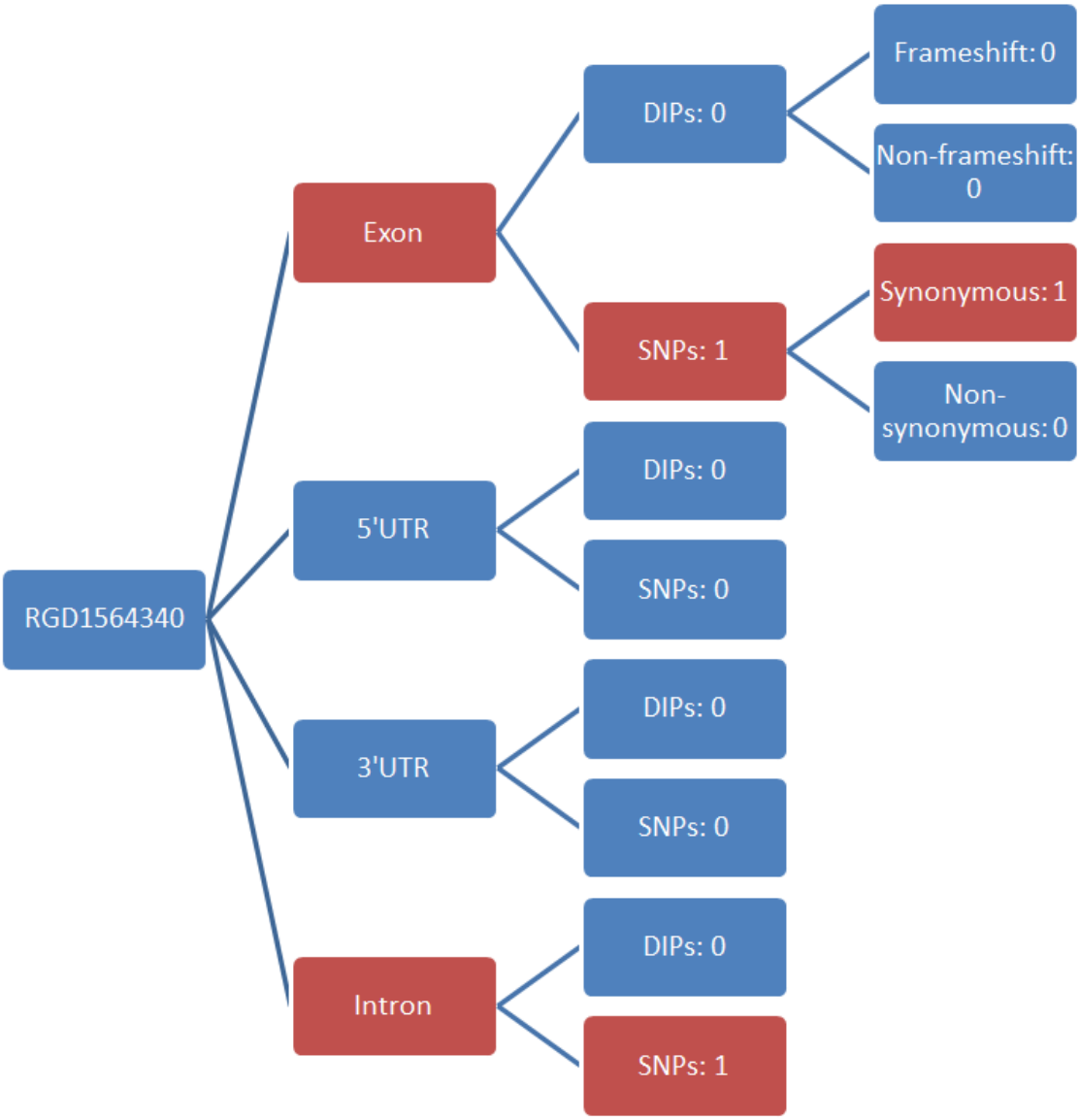
RGD1564340
Exon
DIPs: 0
Frameshift: 0
Non-frameshift: 0
SNPs: 1
Synonymous: 1
Non-synonymous: 0
5'UTR
DIPs: 0
SNPs: 0
3'UTR
DIPs: 0
SNPs: 0
Intron
DIPs: 0
SNPs: 1

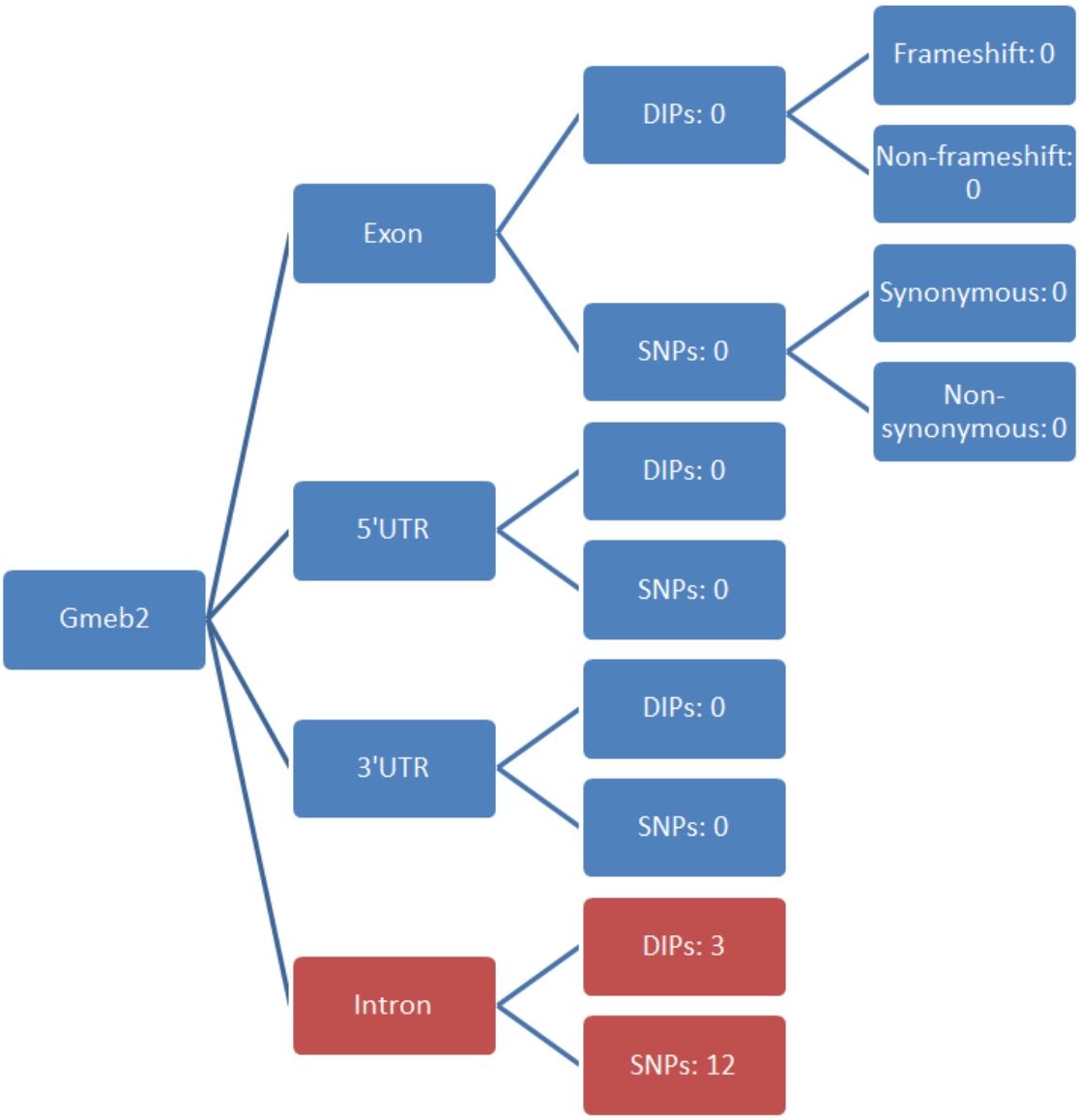
Gmeb2
Exon
DIPs: 0
Frameshift: 0
Non-frameshift: 0
SNPs: 0
Synonymous: 0
Non-synonymous: 0
5'UTR
DIPs: 0
SNPs: 0
3'UTR
DIPs: 0
SNPs: 0
Intron
DIPs: 3
SNPs: 12

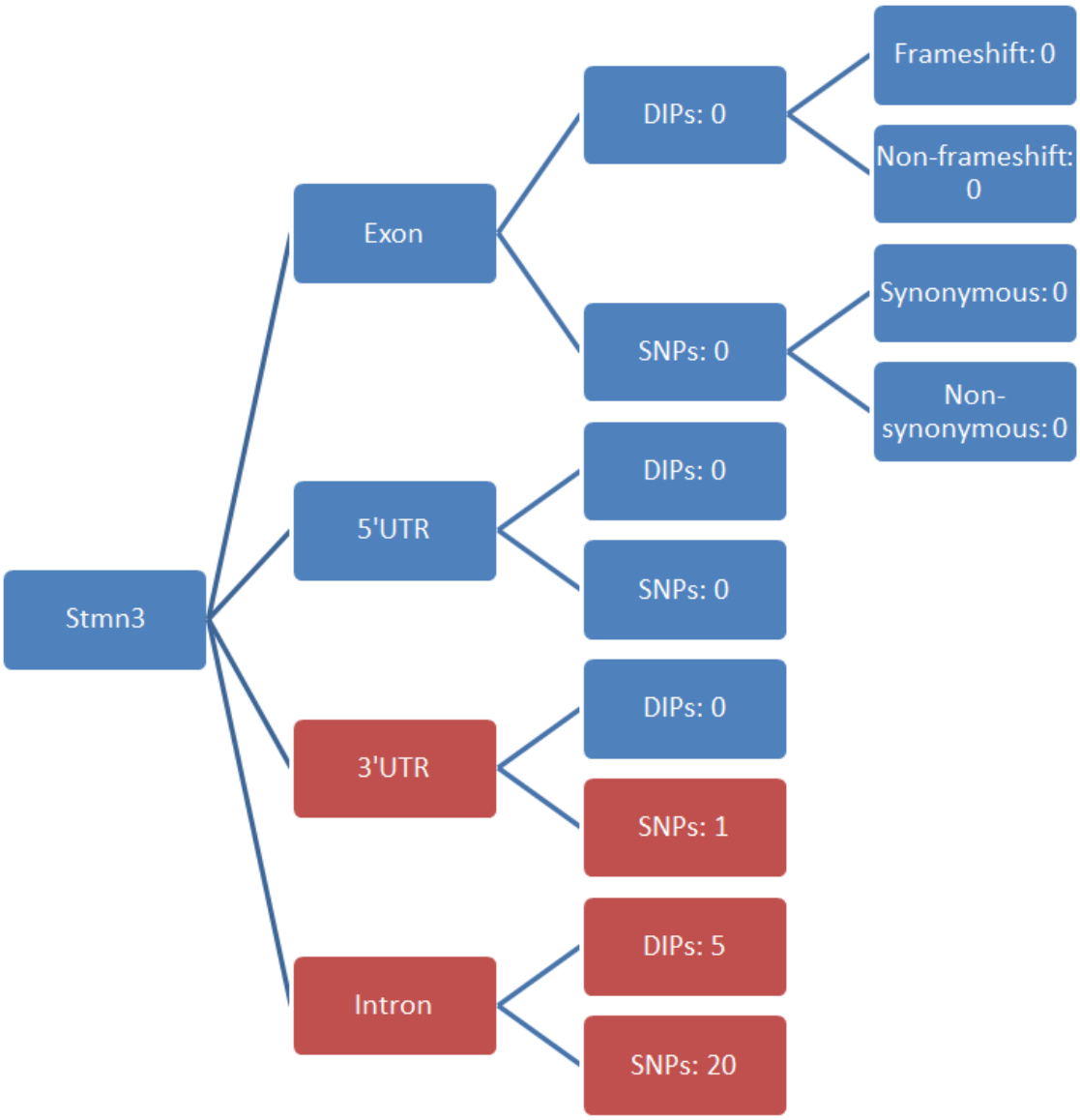
Stmn3
Exon
DIPs: 0
Frameshift: 0
Non-frameshift: 0
SNPs: 0
Synonymous: 0
Non-synonymous: 0
5'UTR
DIPs: 0
SNPs: 0
3'UTR
DIPs: 0
SNPs: 1
Intron
DIPs: 5
SNPs: 20

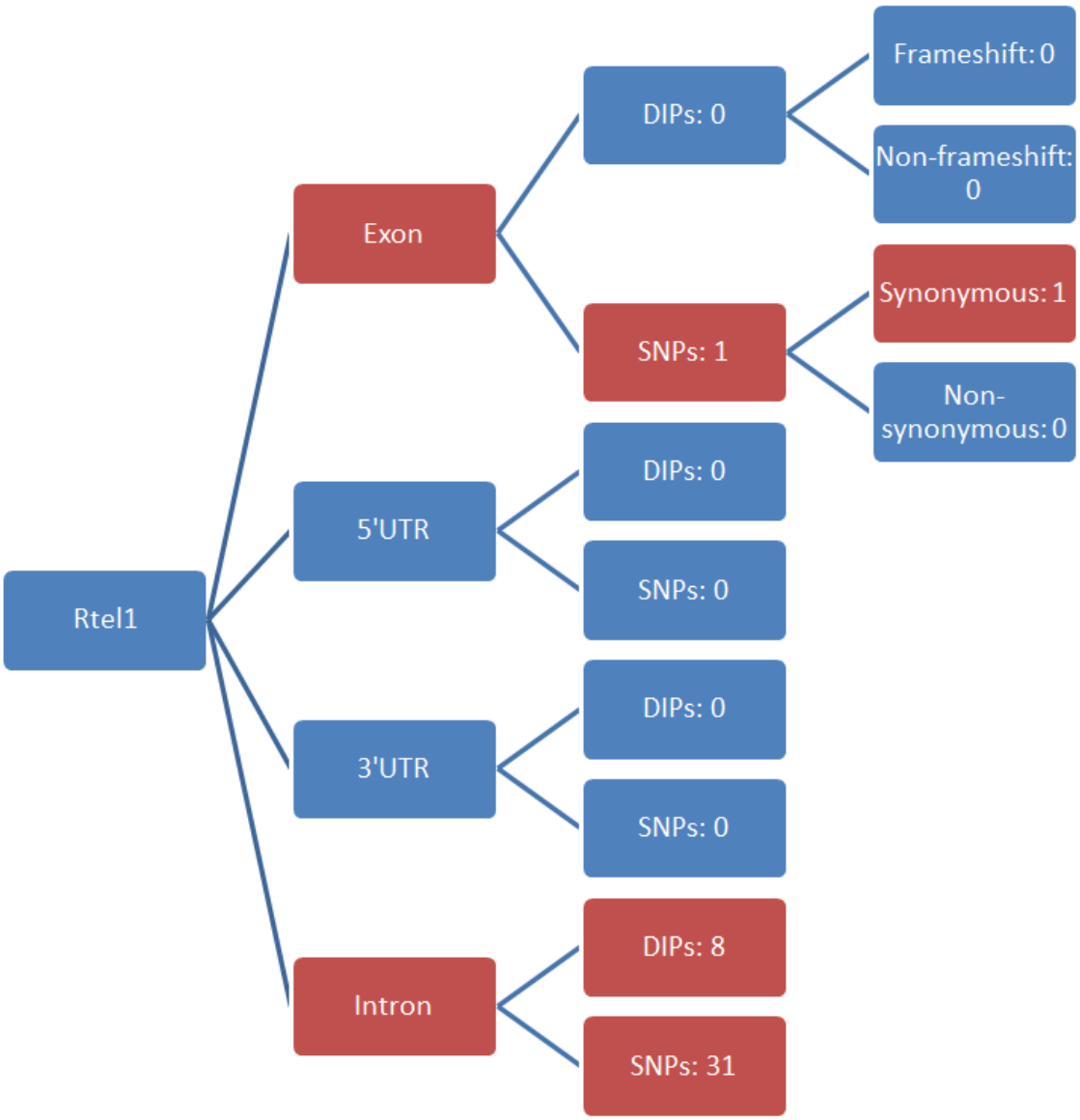
Rtel1
Exon
DIPs: 0
Frameshift: 0
Non-frameshift: 0
SNPs: 1
Synonymous: 1
Non-synonymous: 0
5'UTR
DIPs: 0
SNPs: 0
3'UTR
DIPs: 0
SNPs: 0
Intron
DIPs: 8
SNPs: 31

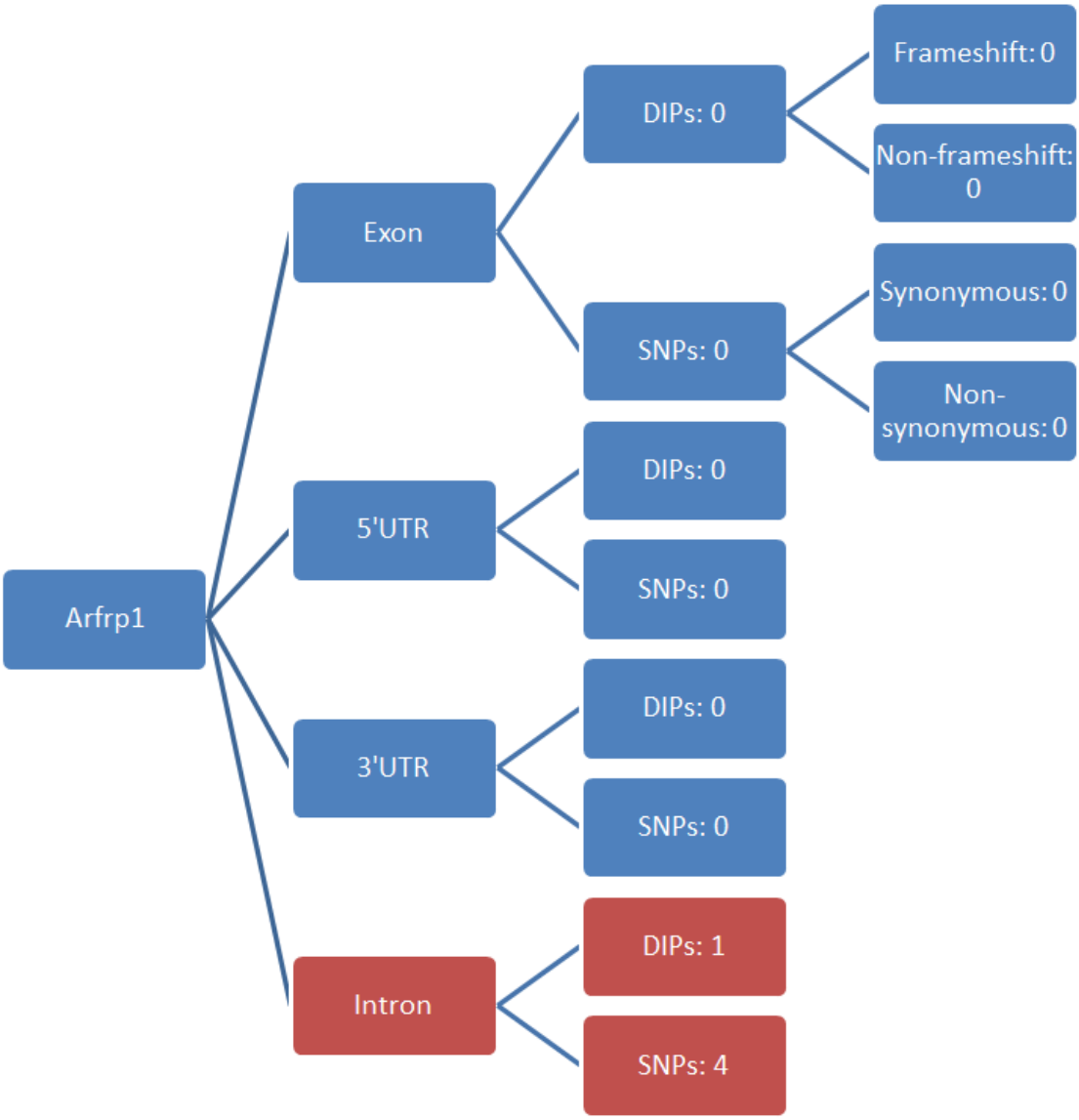
Arfrp1
Exon
DIPs: 0
Frameshift: 0
Non-frameshift: 0
SNPs: 0
Synonymous: 0
Non-synonymous: 0
5'UTR
DIPs: 0
SNPs: 0
3'UTR
DIPs: 0
SNPs: 0
Intron
DIPs: 1
SNPs: 4

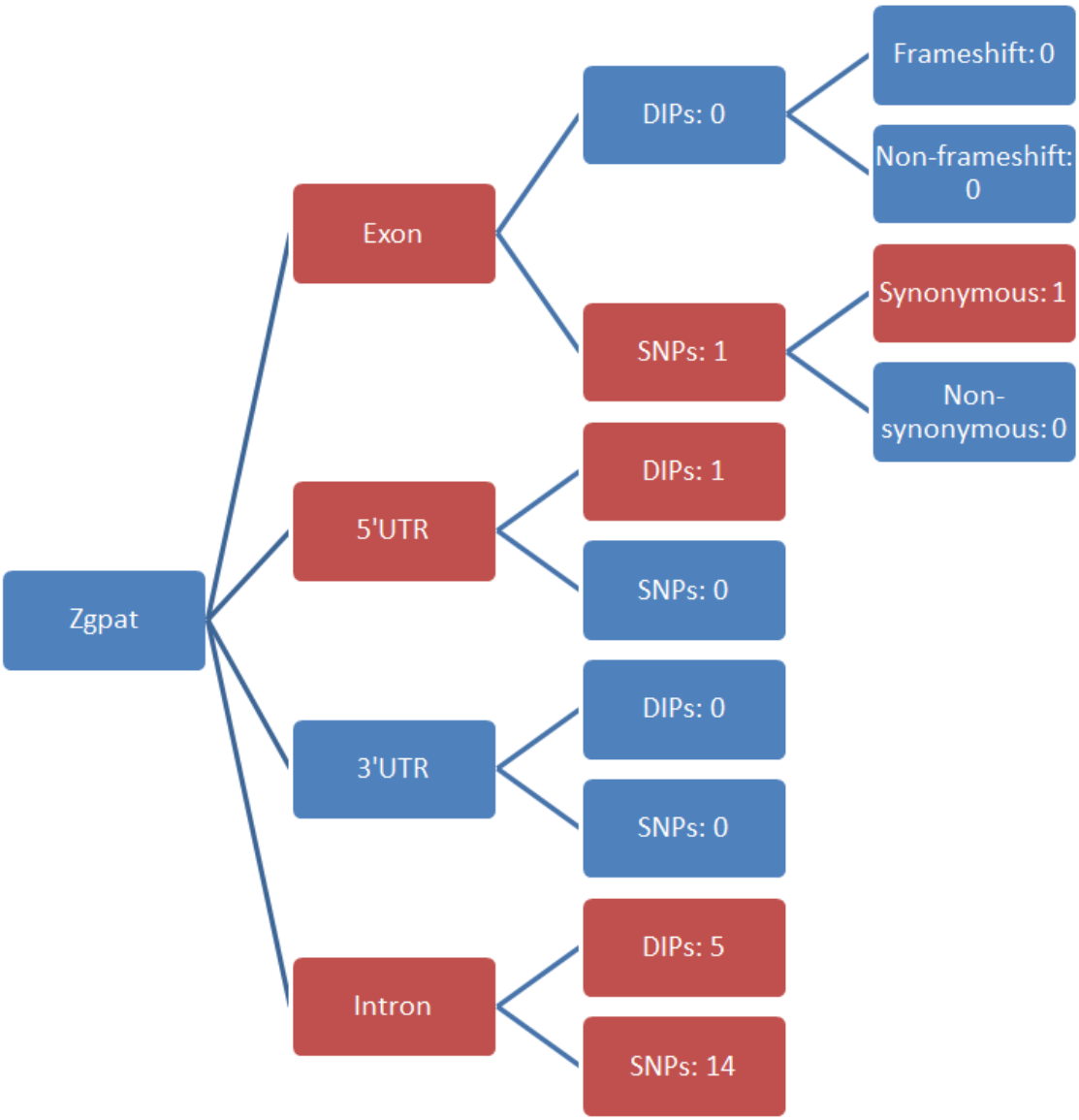
Zgpat
Exon
5'UTR
3'UTR
Intron
DIPs: 0
SNPs: 1
DIPs: 1
SNPs: 0
DIPs: 0
SNPs: 0
DIPs: 5
SNPs: 14
Frameshift: 0
Non-frameshift: 0
Synonymous: 1
Non-synonymous: 0

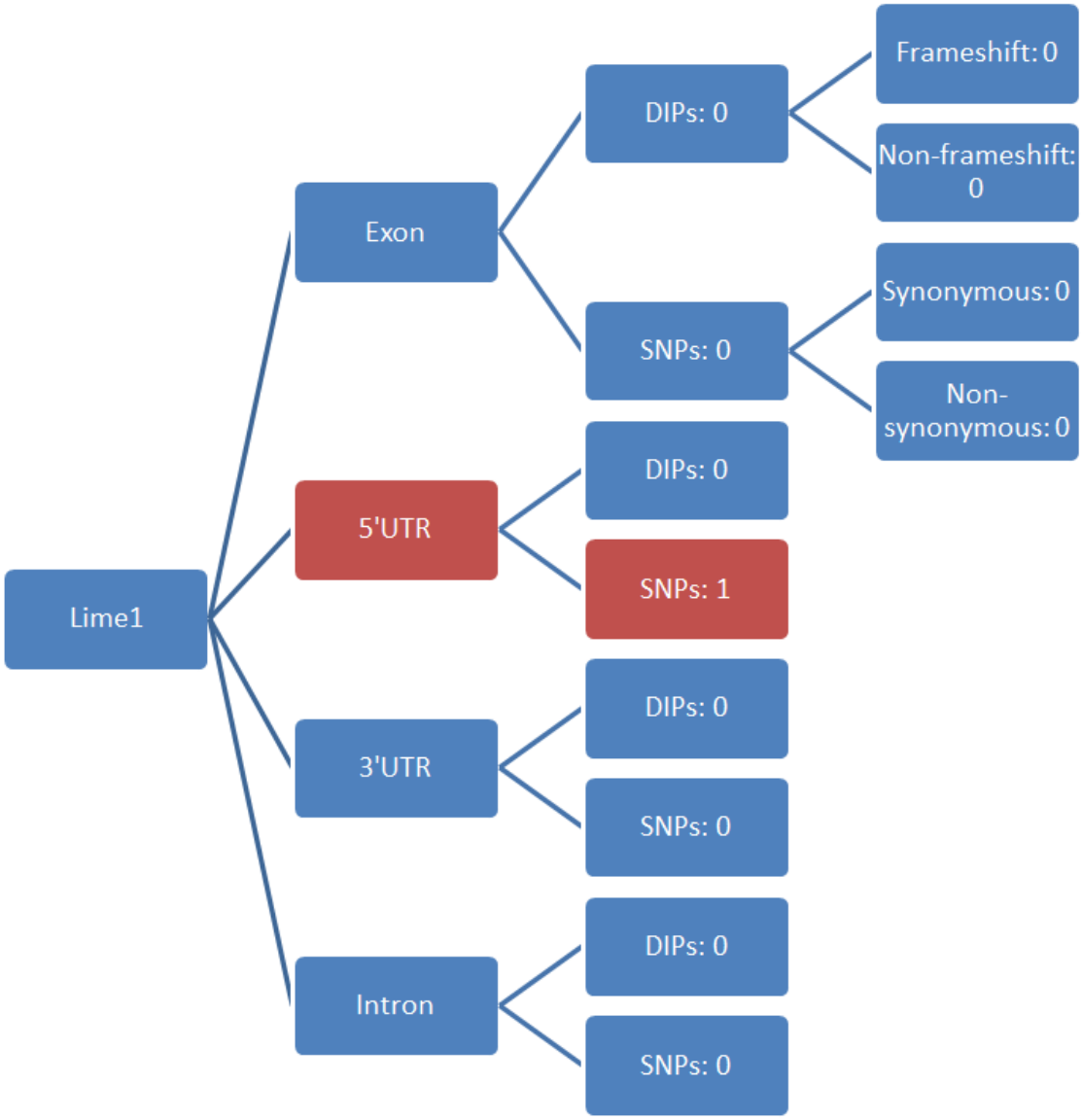
Lime1
Exon
DIPs: 0
Frameshift: 0
Non-frameshift: 0
SNPs: 0
Synonymous: 0
Non-synonymous: 0
5'UTR
DIPs: 0
SNPs: 1
3'UTR
DIPs: 0
SNPs: 0
Intron
DIPs: 0
SNPs: 0

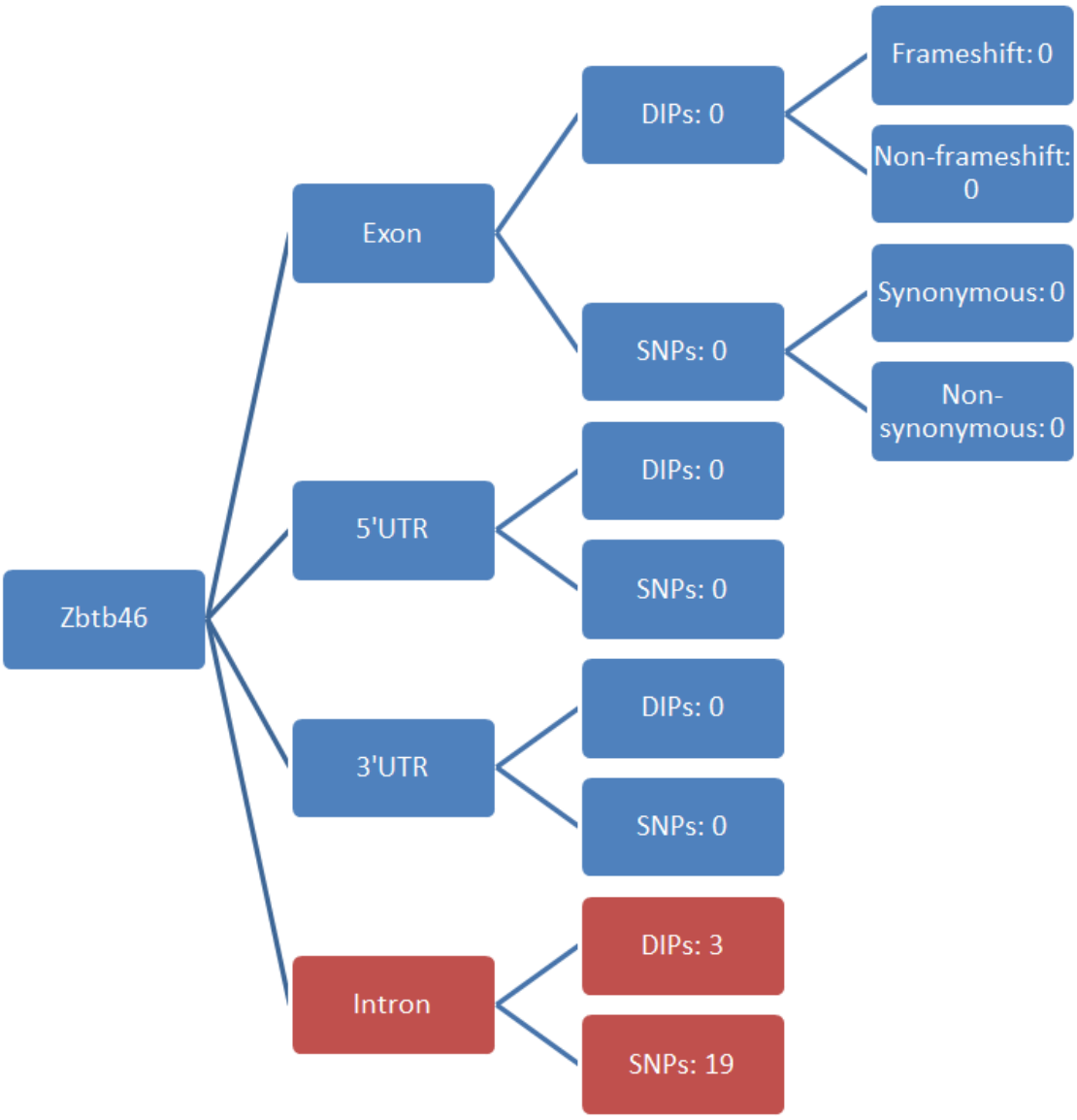
Zbtb46
Exon
DIPs: 0
Frameshift: 0
Non-frameshift: 0
SNPs: 0
Synonymous: 0
Non-synonymous: 0
5'UTR
DIPs: 0
SNPs: 0
3'UTR
DIPs: 0
SNPs: 0
Intron
DIPs: 3
SNPs: 19

APPENDIX D

ROI SNP AND DIP POSITIONS BY GENE

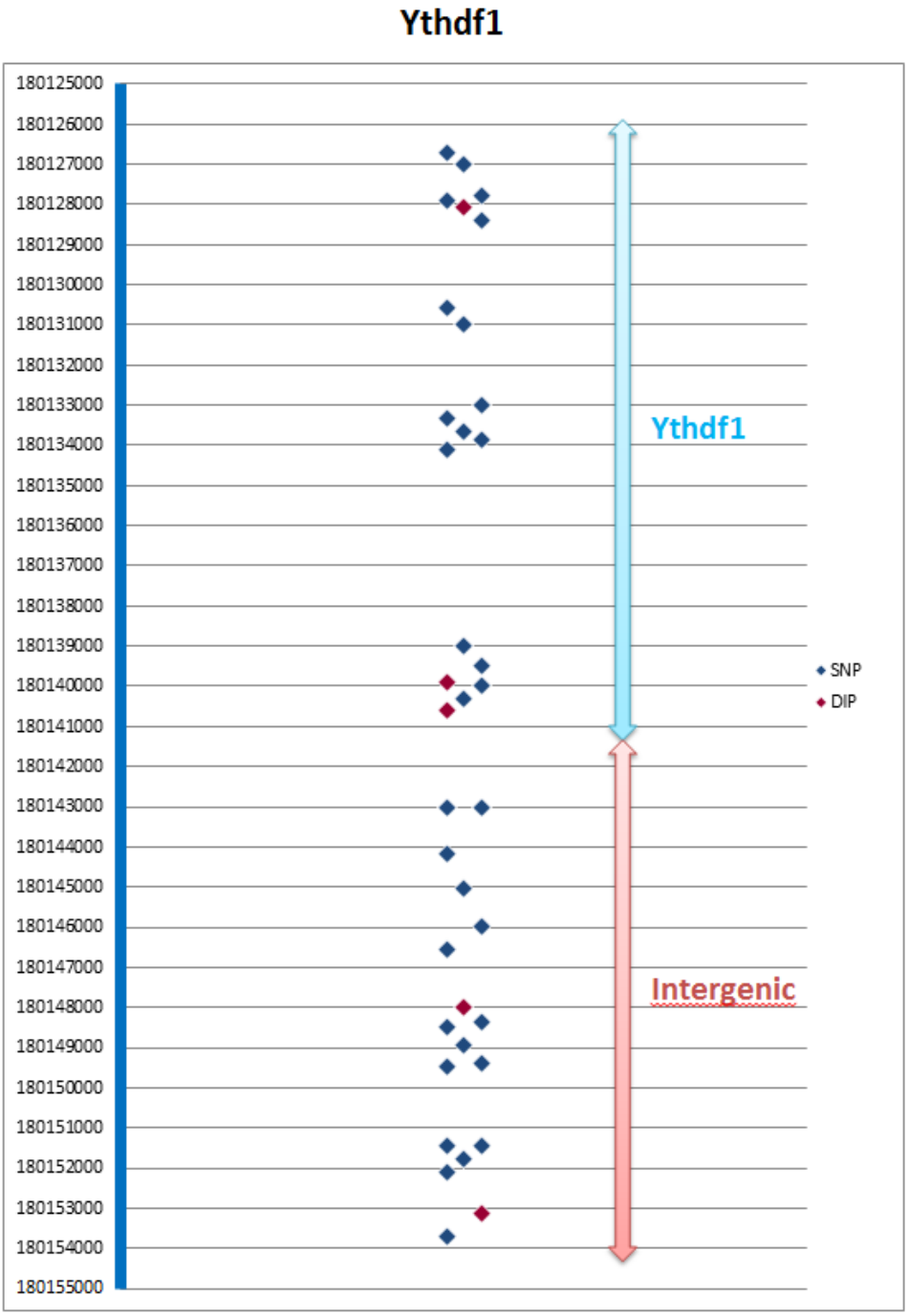

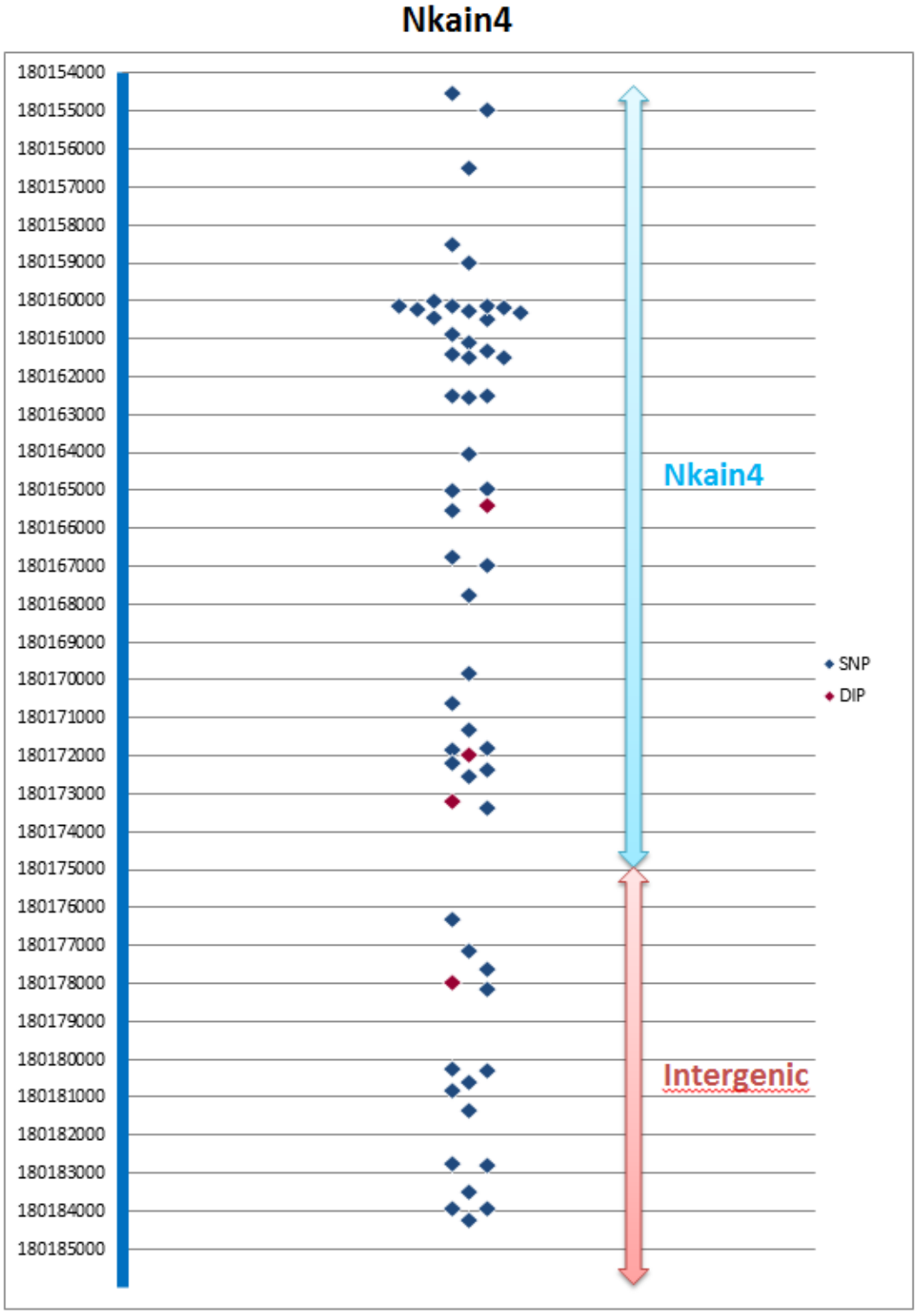
Nkain4
180154000
180155000
180156000
180157000
180158000
180159000
180160000
180161000
180162000
180163000
180164000
180165000
180166000
180167000
180168000
180169000
180170000
180171000
180172000
180173000
180174000
180175000
180176000
180177000
180178000
180179000
180180000
180181000
180182000
180183000
180184000
180185000
Nkain4
Intergenic
SNP
DIP

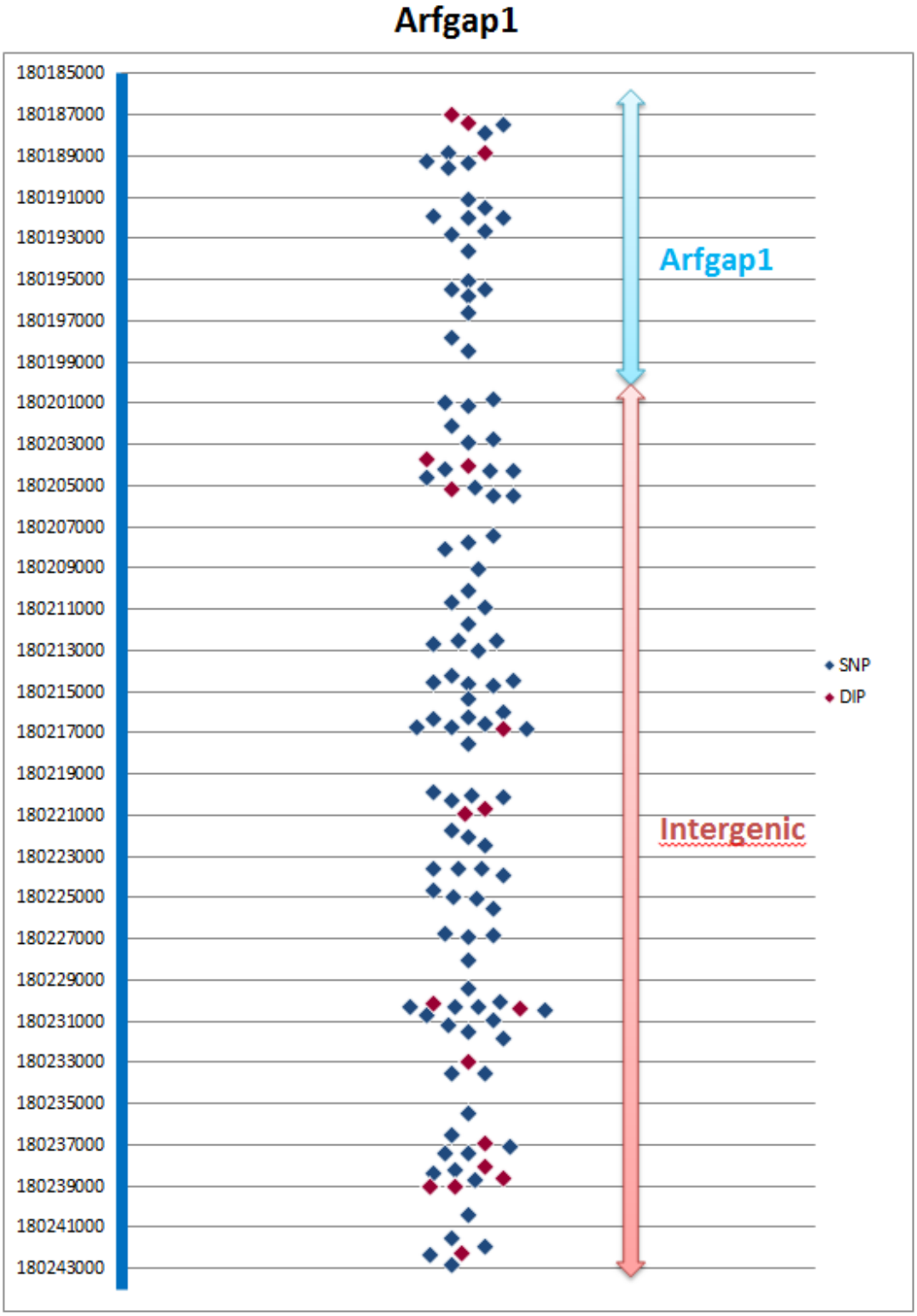
Arfgap1
180185000
180187000
180189000
180191000
180193000
180195000
180197000
180199000
180201000
180203000
180205000
180207000
180209000
180211000
180213000
180215000
180217000
180219000
180221000
180223000
180225000
180227000
180229000
180231000
180233000
180235000
180237000
180239000
180241000
180243000
Arfgap1
Intergenic
SNP
DIP

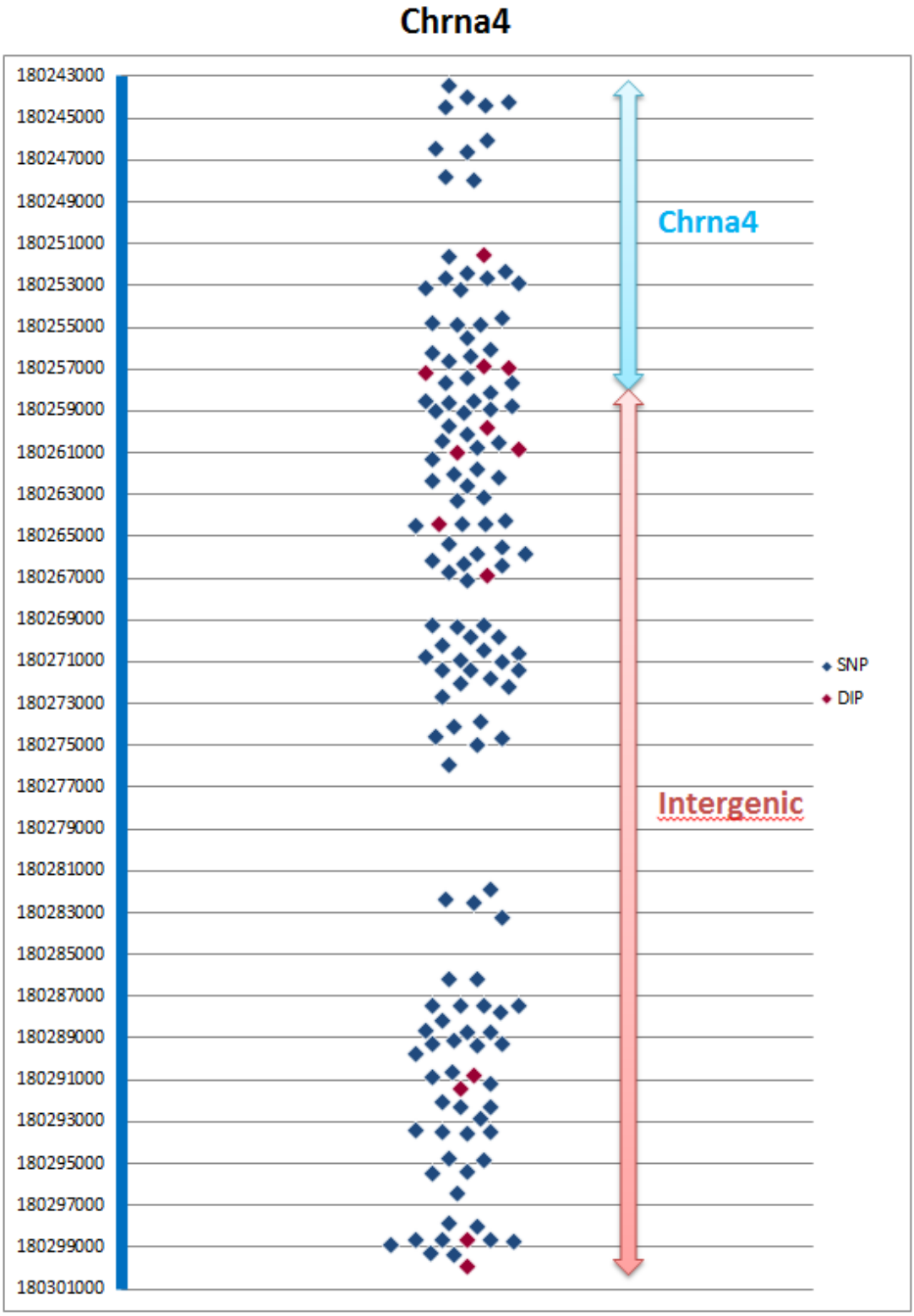
Chrna4
180243000
180245000
180247000
180249000
180251000
180253000
180255000
180257000
180259000
180261000
180263000
180265000
180267000
180269000
180271000
180273000
180275000
180277000
180279000
180281000
180283000
180285000
180287000
180289000
180291000
180293000
180295000
180297000
180299000
180301000
Chrna4
Intergenic
SNP
DIP

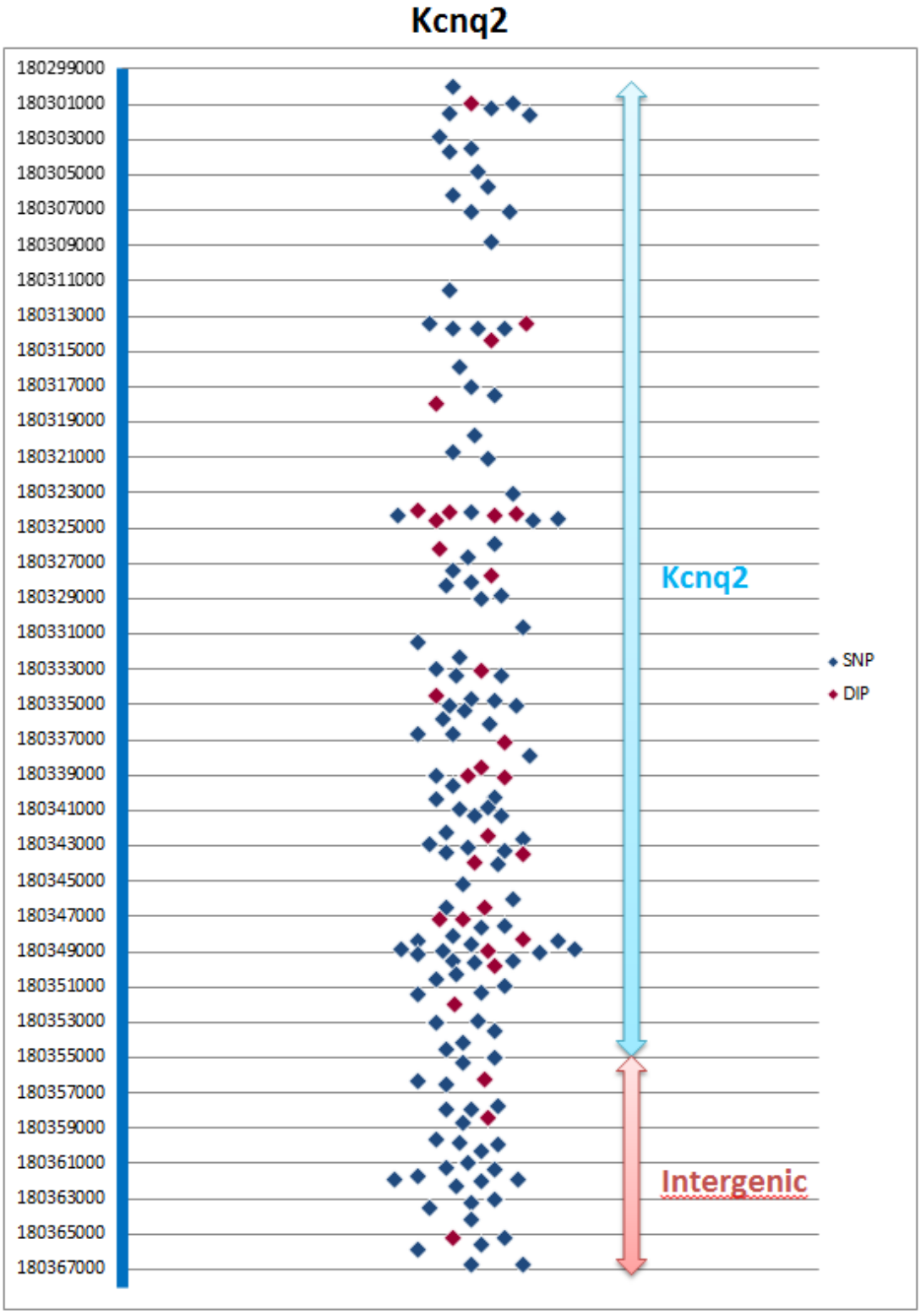
Kcnq2
180299000
180301000
180303000
180305000
180307000
180309000
180311000
180313000
180315000
180317000
180319000
180321000
180323000
180325000
180327000
180329000
180331000
180333000
180335000
180337000
180339000
180341000
180343000
180345000
180347000
180349000
180351000
180353000
180355000
180357000
180359000
180361000
180363000
180365000
180367000
Kcnq2
Intergenic
SNP
DIP

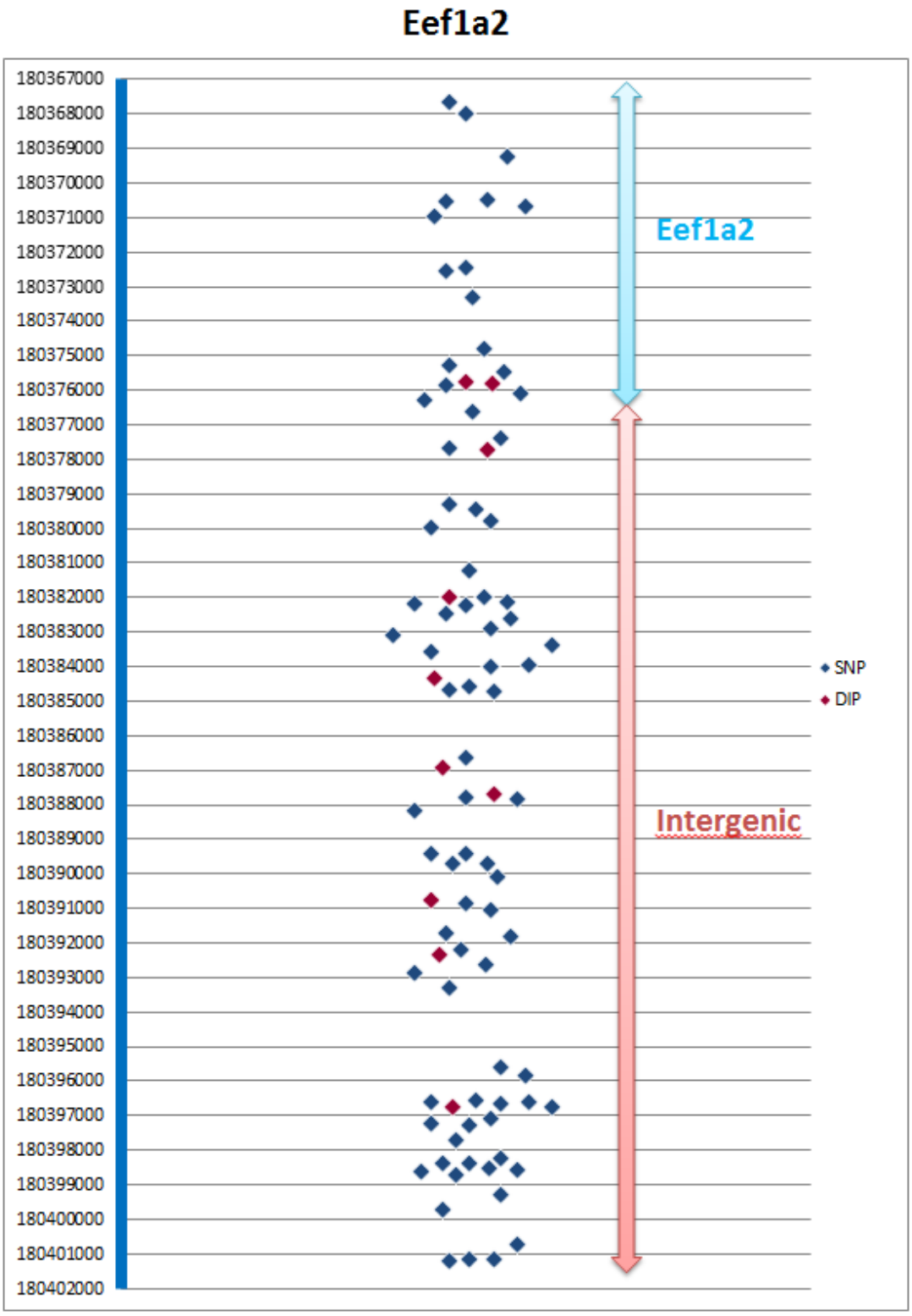
Eef1a2
180367000
180368000
180369000
180370000
180371000
180372000
180373000
180374000
180375000
180376000
180377000
180378000
180379000
180380000
180381000
180382000
180383000
180384000
180385000
180386000
180387000
180388000
180389000
180390000
180391000
180392000
180393000
180394000
180395000
180396000
180397000
180398000
180399000
180400000
180401000
180402000
Eef1a2
Intergenic
SNP
DIP

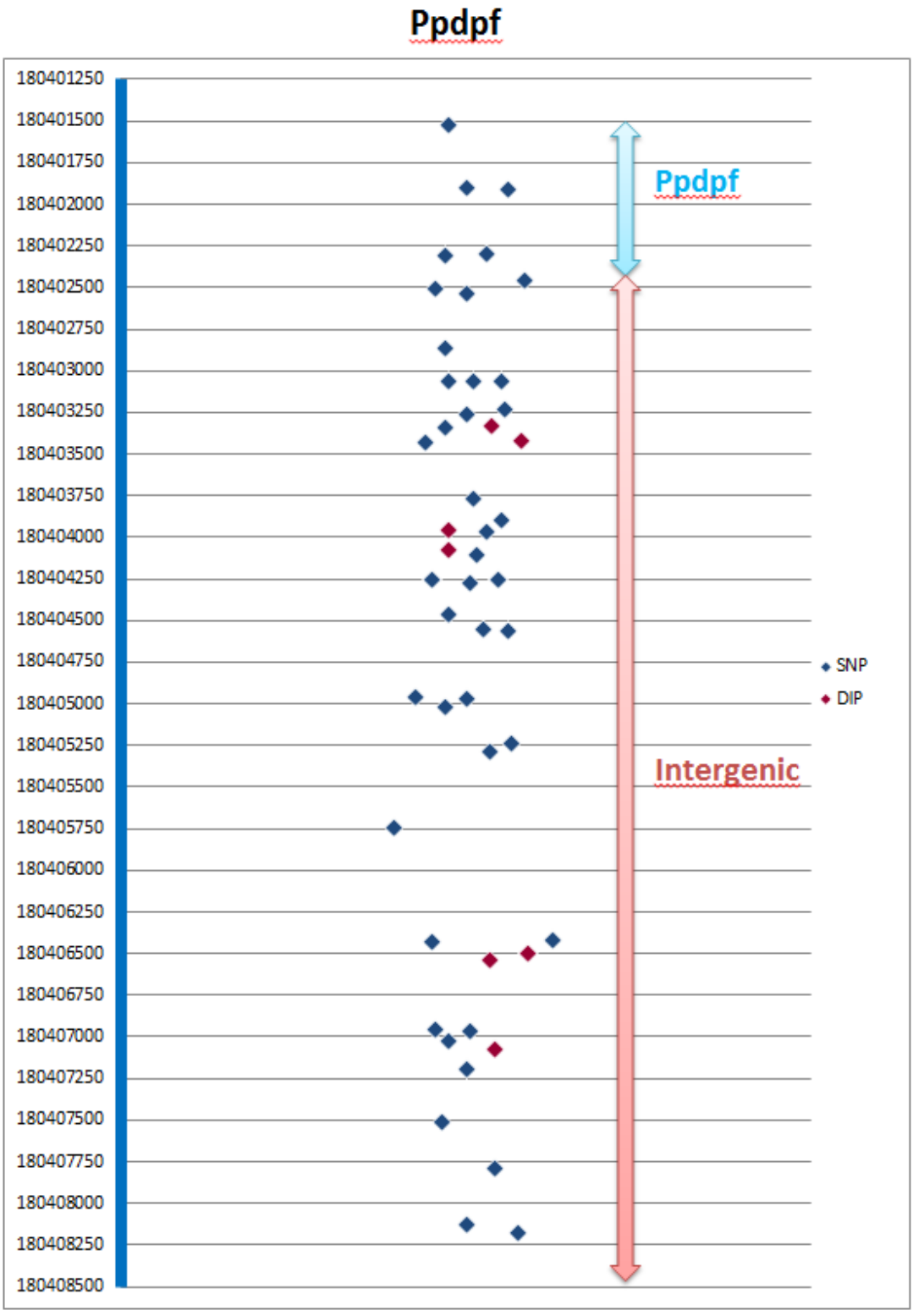
Ppdpf
180401250
180401500
180401750
180402000
180402250
180402500
180402750
180403000
180403250
180403500
180403750
180404000
180404250
180404500
180404750
180405000
180405250
180405500
180405750
180406000
180406250
180406500
180406750
180407000
180407250
180407500
180407750
180408000
180408250
180408500
Ppdpf
Intergenic
SNP
DIP

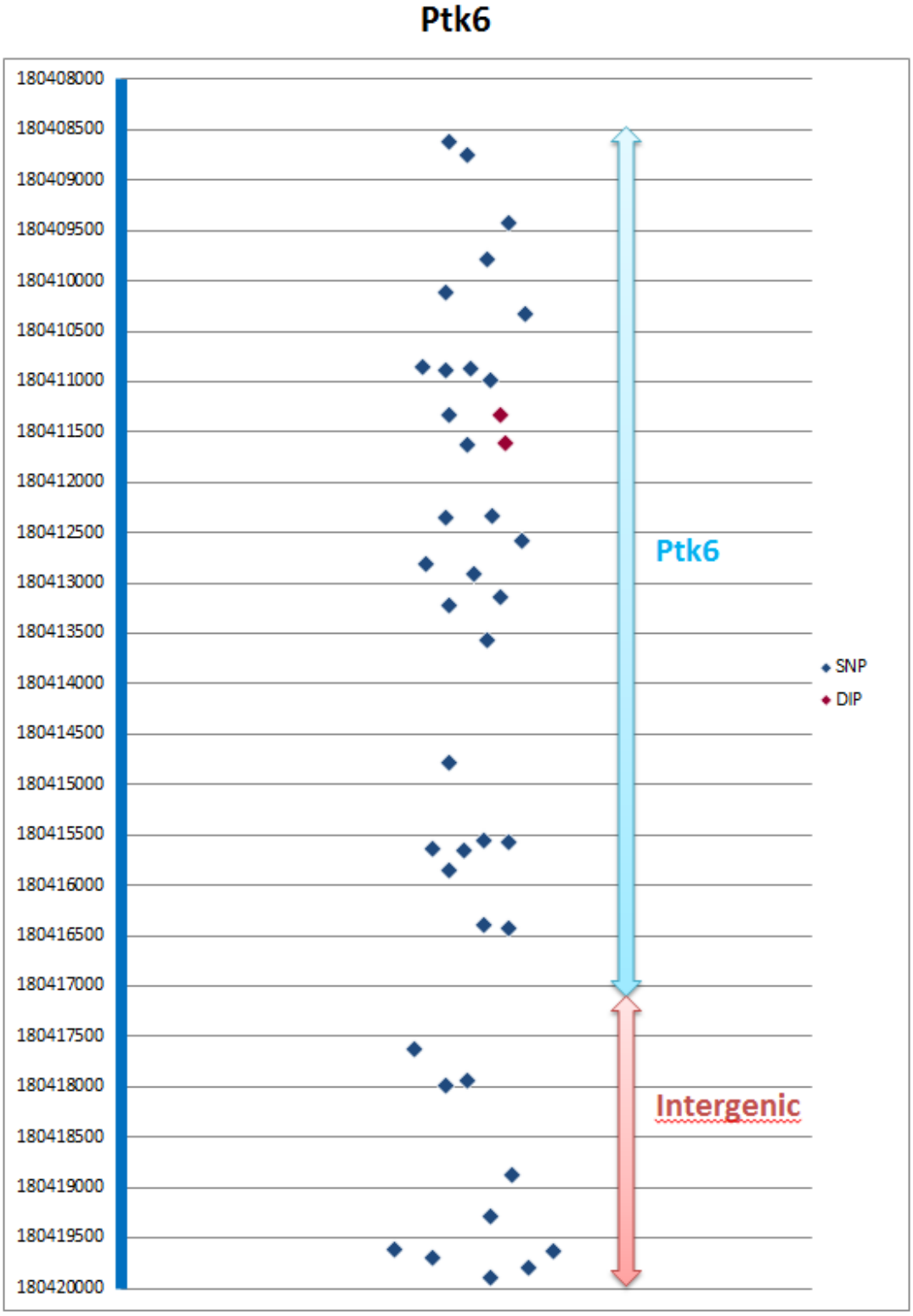
Ptk6
180408000
180408500
180409000
180409500
180410000
180410500
180411000
180411500
180412000
180412500
180413000
180413500
180414000
180414500
180415000
180415500
180416000
180416500
180417000
180417500
180418000
180418500
180419000
180419500
180420000
Ptk6
Intergenic
SNP
DIP

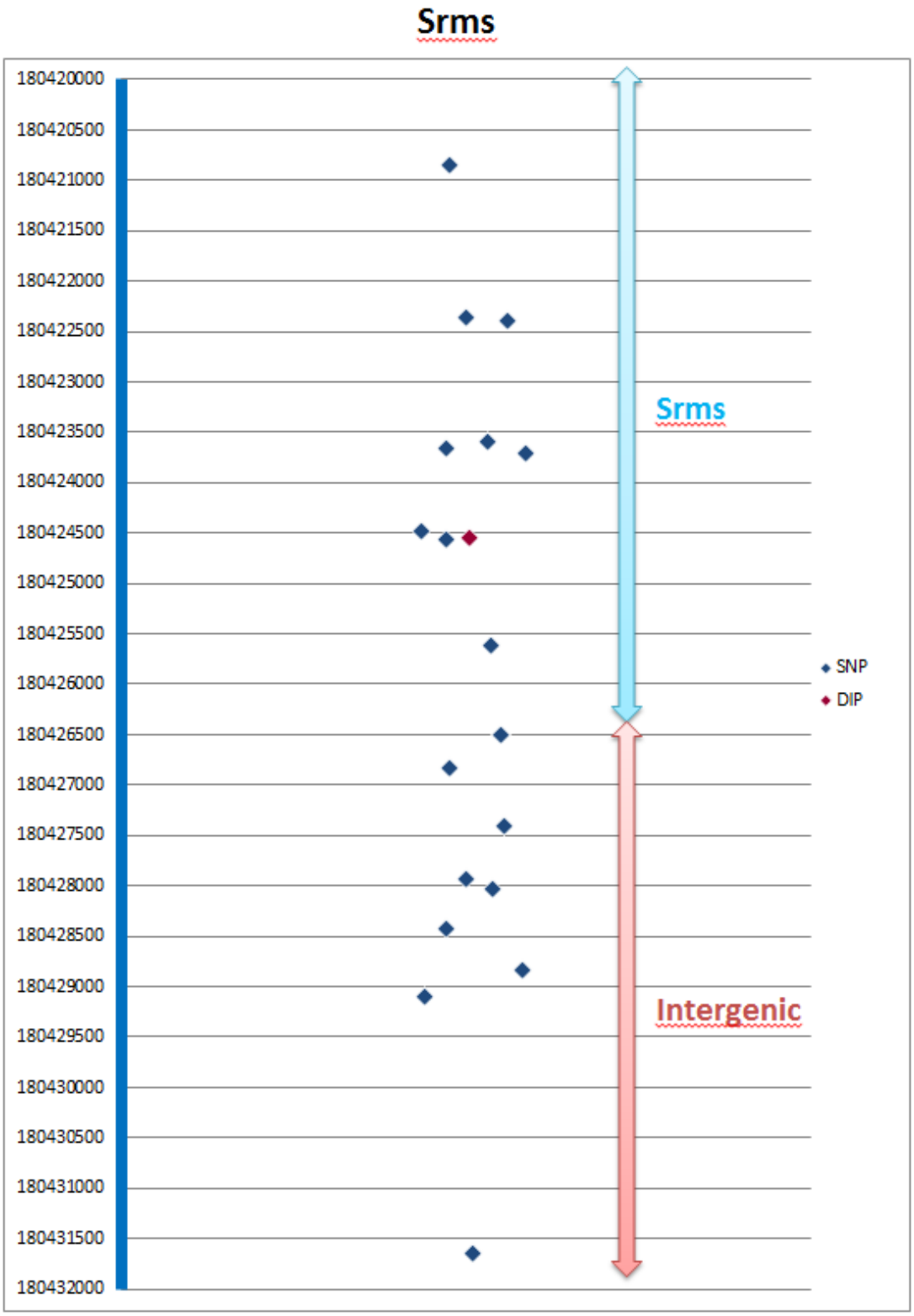
Srms
180420000
180420500
180421000
180421500
180422000
180422500
180423000
180423500
180424000
180424500
180425000
180425500
180426000
180426500
180427000
180427500
180428000
180428500
180429000
180429500
180430000
180430500
180431000
180431500
180432000
Srms
Intergenic
SNP
DIP

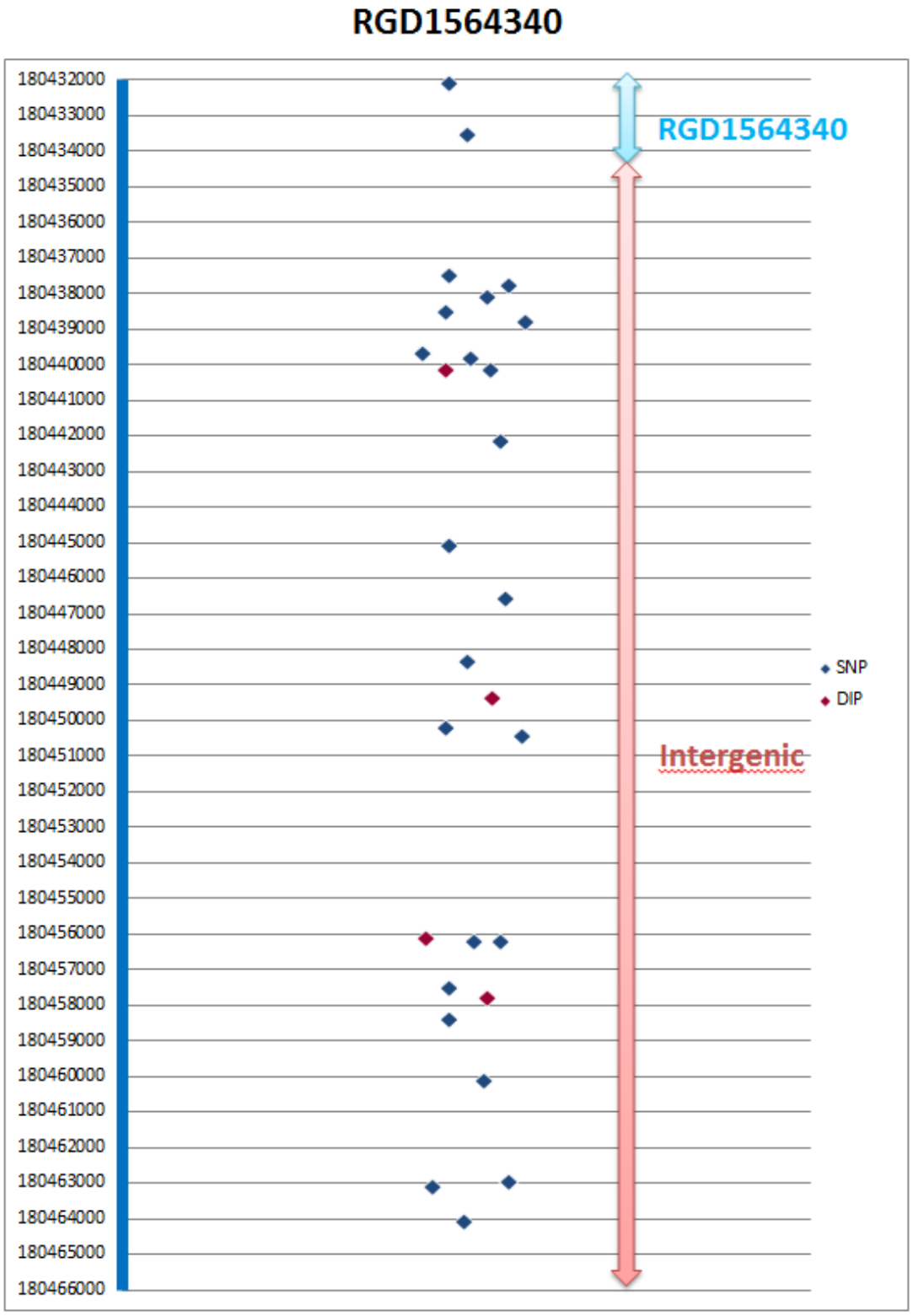
RGD1564340
180432000
180433000
180434000
180435000
180436000
180437000
180438000
180439000
180440000
180441000
180442000
180443000
180444000
180445000
180446000
180447000
180448000
180449000
180450000
180451000
180452000
180453000
180454000
180455000
180456000
180457000
180458000
180459000
180460000
180461000
180462000
180463000
180464000
180465000
180466000
RGD1564340
Intergenic
SNP
DIP

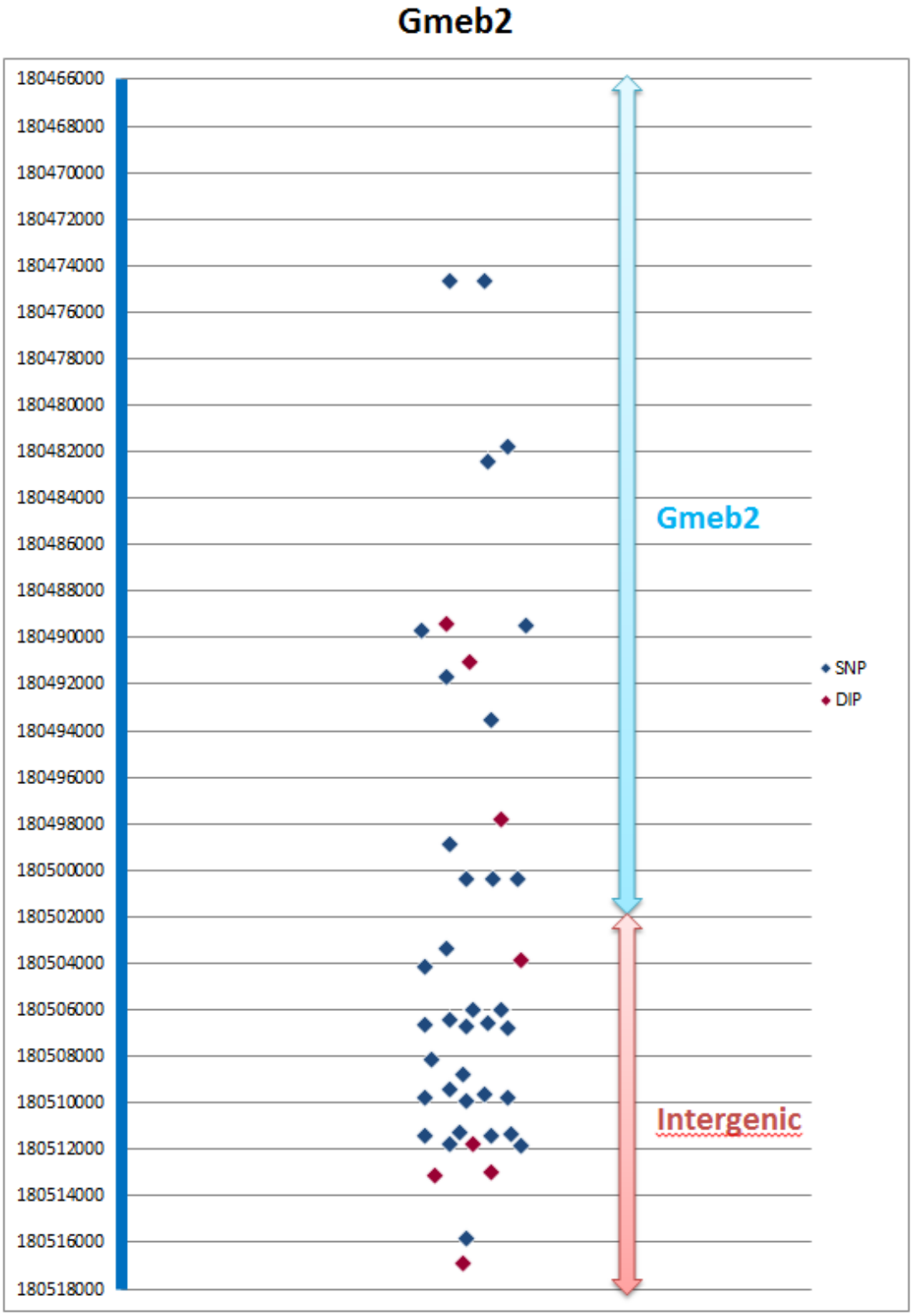
Gmeb2
180466000
180468000
180470000
180472000
180474000
180476000
180478000
180480000
180482000
180484000
180486000
180488000
180490000
180492000
180494000
180496000
180498000
180500000
180502000
180504000
180506000
180508000
180510000
180512000
180514000
180516000
180518000
Gmeb2
Intergenic
SNP
DIP

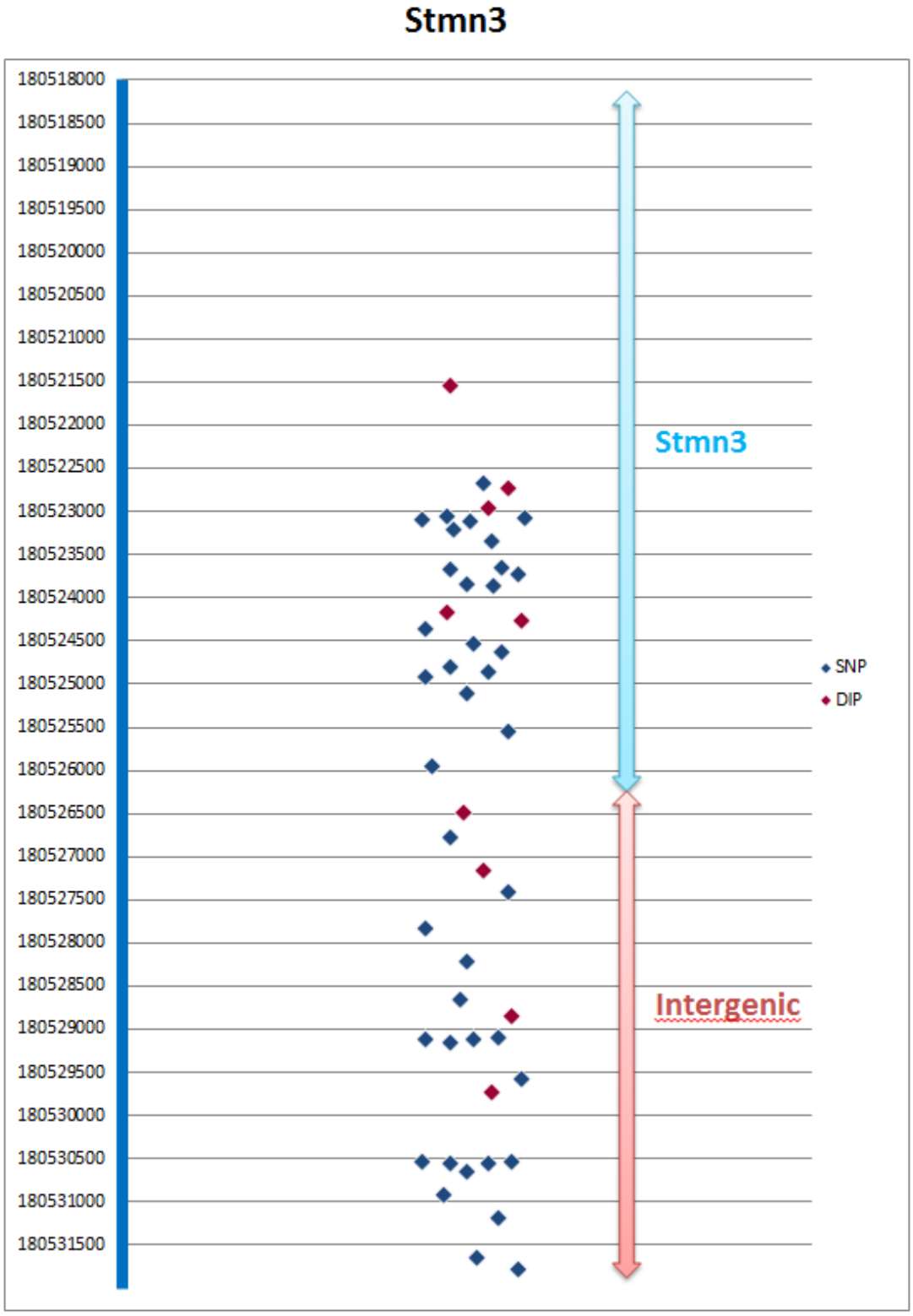
Stmn3
180518000
180518500
180519000
180519500
180520000
180520500
180521000
180521500
180522000
180522500
180523000
180523500
180524000
180524500
180525000
180525500
180526000
180526500
180527000
180527500
180528000
180528500
180529000
180529500
180530000
180530500
180531000
180531500
Stmn3
Intergenic
SNP
DIP

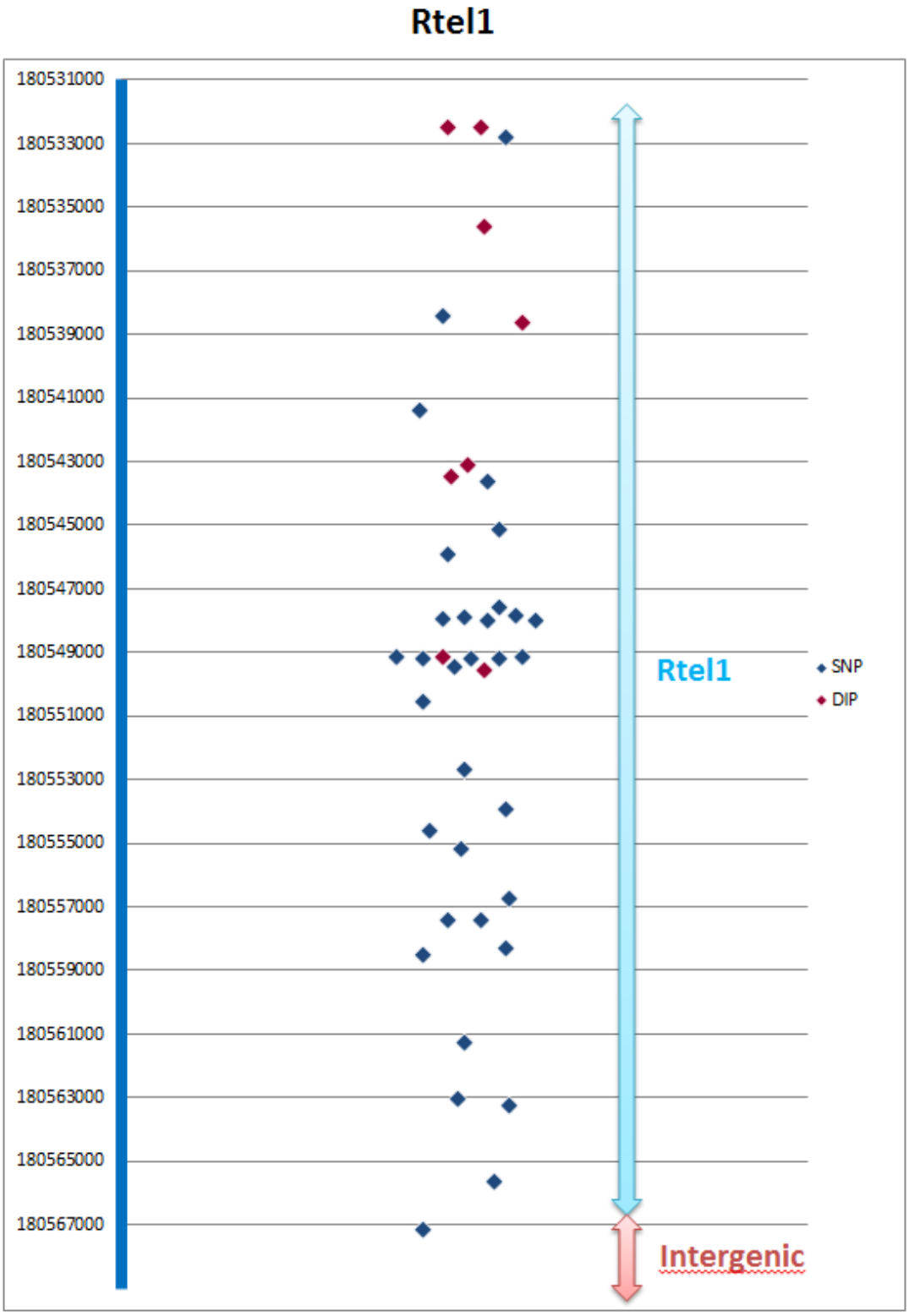
Rtel1
180531000
180533000
180535000
180537000
180539000
180541000
180543000
180545000
180547000
180549000
180551000
180553000
180555000
180557000
180559000
180561000
180563000
180565000
180567000
Rtel1
Intergenic
SNP
DIP

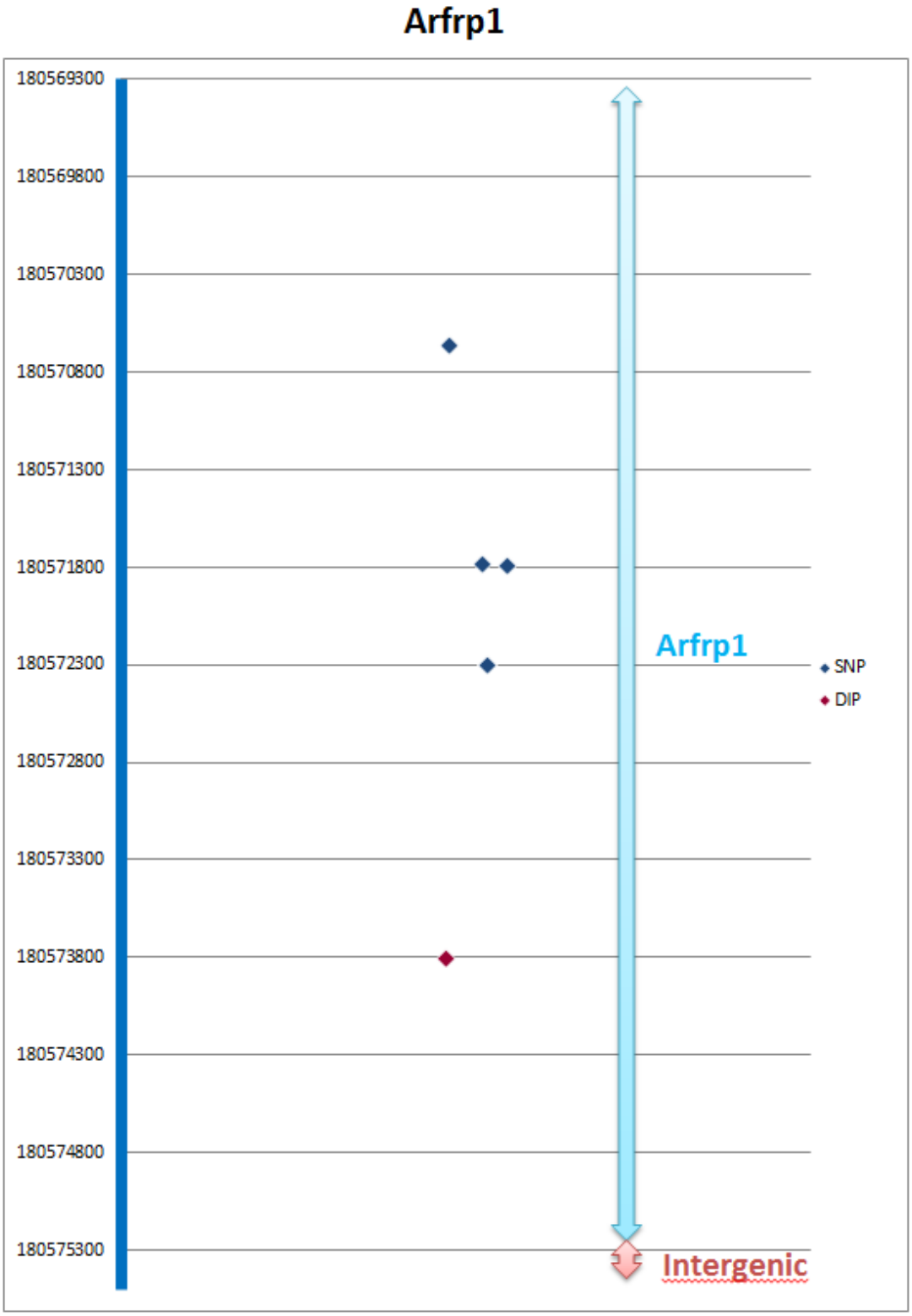
Arfrp1
180569300
180569800
180570300
180570800
180571300
180571800
180572300
180572800
180573300
180573800
180574300
180574800
180575300
Arfrp1
Intergenic
SNP
DIP

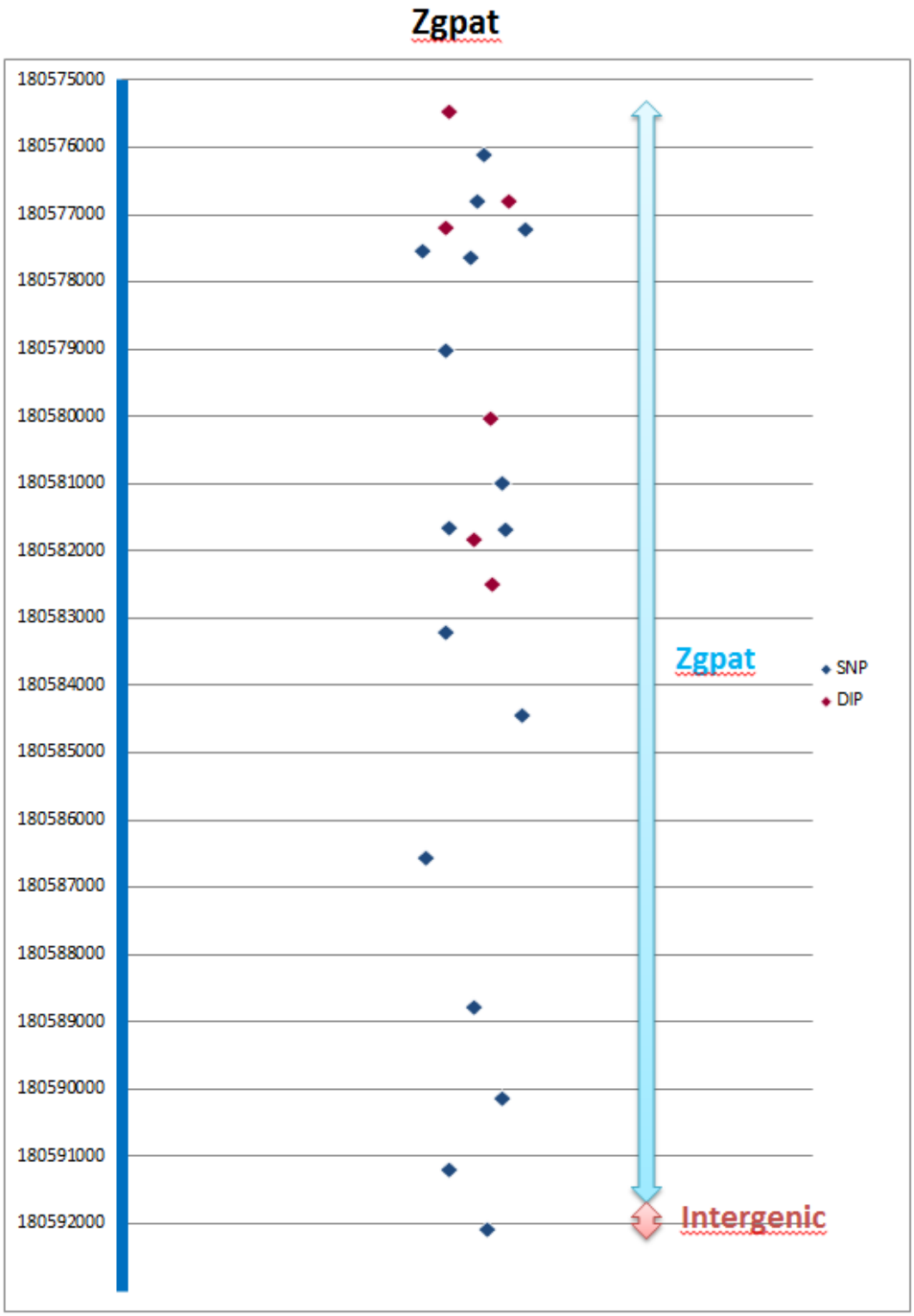
Zgpat
180575000
180576000
180577000
180578000
180579000
180580000
180581000
180582000
180583000
180584000
180585000
180586000
180587000
180588000
180589000
180590000
180591000
180592000
Zgpat
SNP
DIP
Intergenic

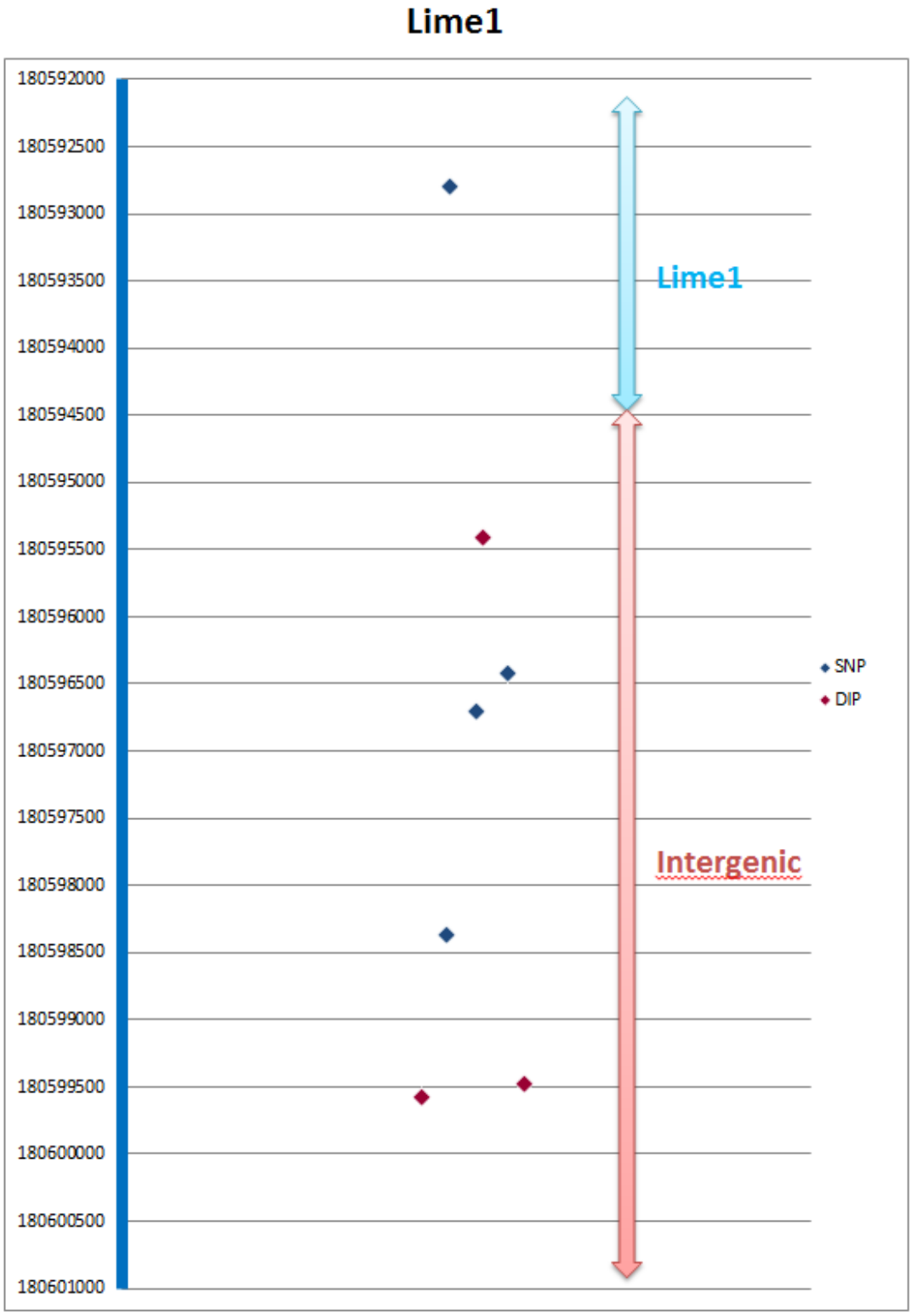
Lime1
180592000
180592500
180593000
180593500
180594000
180594500
180595000
180595500
180596000
180596500
180597000
180597500
180598000
180598500
180599000
180599500
180600000
180600500
180601000
Lime1
Intergenic
SNP
DIP

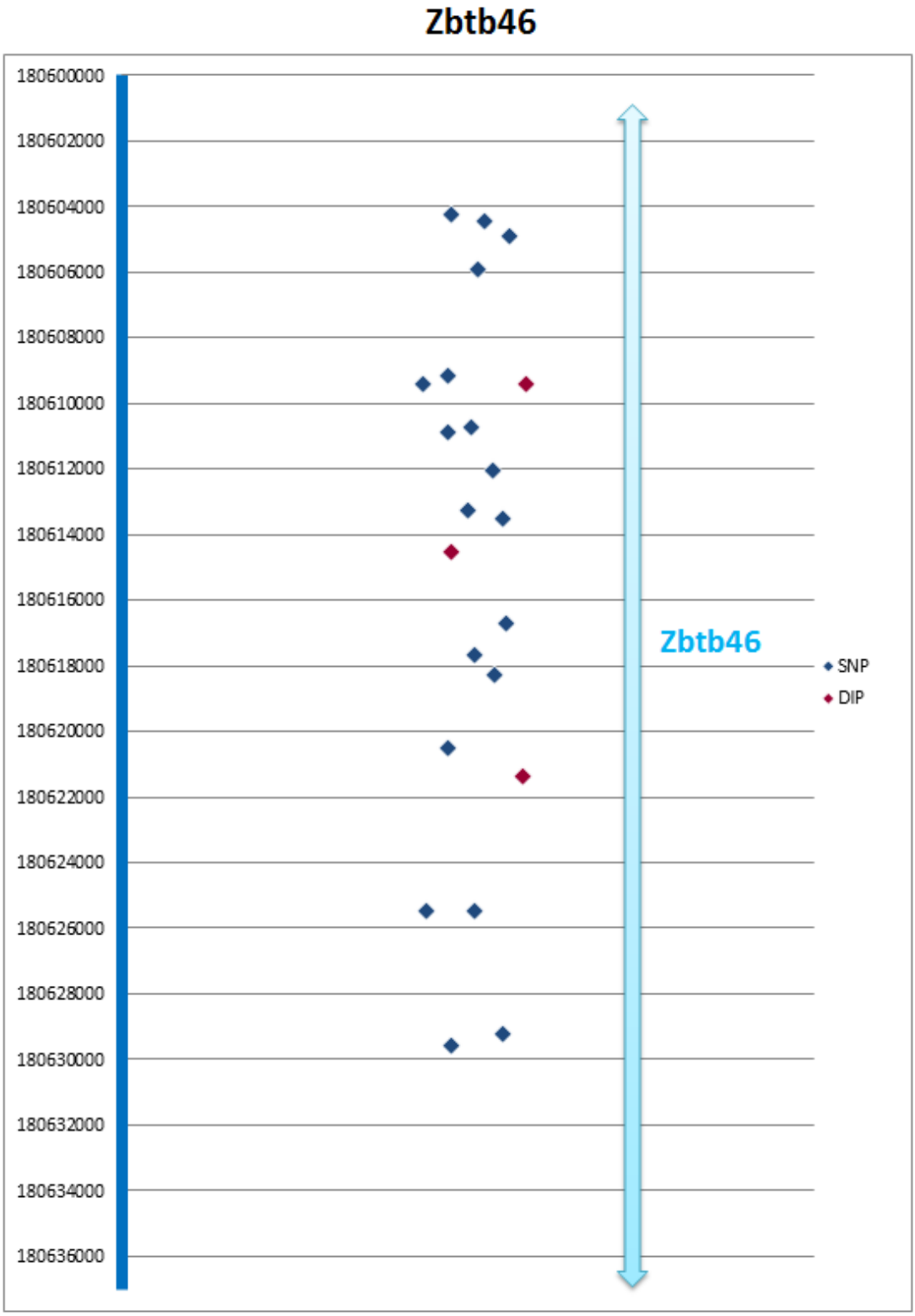
Zbtb46
180600000
180602000
180604000
180606000
180608000
180610000
180612000
180614000
180616000
180618000
180620000
180622000
180624000
180626000
180628000
180630000
180632000
180634000
180636000
Zbtb46
SNP
DIP